ROLE OF THE NLR GENE FAMILY MEMBERS IN NEUROINFLAMMATION AND DEMYELINATION IN THE CNS

SUSHMITA JHA

A dissertation submitted to the faculty of the University of North Carolina at Chapel Hill in partial fulfillment of the requirements for the degree of Doctor of Philosophy in the Department of Cell and Molecular Physiology, School of medicine

Chapel Hill

2009

Approved by:

Jenny P.-Y Ting

P Kay Lund

Manzoor A. Bhat

Glenn K. Matsushima

Scott H. Randell

Mohanish Deshmukh

ABSTRACT

SUSHMITA JHA: Role of NLRs in neuroinflammation, demyelination and remyelination in the CNS
(Under the direction of Dr Jenny P-Y Ting)

Sterile inflammation in the brain is recognized as a key component of many neurological diseases including multiple sclerosis (MS), amyotrophic lateral sclerosis, Parkinson's disease, and Alzheimer's disease. An understanding of the mechanisms by which neuroinflammation occurs and the molecular mediators involved in this process is necessary for identification of potential therapeutic targets. The NLR gene family members have emerged as important regulators of immunity and inflammation due to their genetic linkage to several human immunologic diseases. In this study, our goal was to ascertain the role of NLR dependent cellular pathways in neuroinflammation, demyelination and remyelination. An *in vivo* cuprizone-induced mouse model of demyelination and remyelination along with *ex vivo* primary cell culture assays were utilized. Mice deficient in NLRP3 (*Nlrp3*$^{-/-}$), IL-1β (*IL-1β*$^{-/-}$), caspase-1 (*casp1*$^{-/-}$), P2X$_7$R (*P2X$_7$R*$^{-/-}$), IL-18 (*IL-18*$^{-/-}$) and NLRC4 (*Nlrc4*$^{-/-}$) were used for these studies.

ACKNOWLEDGEMENTS

First and foremost, I would like to thank my advisor Dr. Jenny P.-Y Ting for mentoring me. This project would not have reached completion without her continued guidance and incessant support.

I am grateful to my committee members, Drs. Kay Lund, Manzoor Bhat, Glenn Matsushima, Scott Randell and Mohanish Deshmukh for their guidance and constructive evaluation of my work. Their insightful questions and suggestions have helped hone my critical thinking and helped me grow as a scientist.

My heartfelt thanks to members of the department of Cell and Molecular Physiology, especially, Drs. James Anderson and Jim Faber for their guidance throughout my graduate school career. Much thanks to Jan McCormick and Adriana Tavernise for their warmth and incredible technical support.

I would like to thank all my friends in the indian community at chapel hill who over the years have helped make Chapel Hill home for me. I would also like to thank my lab members and friends, Erin McElvania Tekippe and Eda Holl for their support and encouragement through all the tough times.

Finally, I would like to thank my family, my grandmother for inspiring me with her strength, my father for instilling in me the values of hard work and perseverance, my mother for her love and support, and my brother for his optimism. Siddharth Srivastava, my husband, has

been my pillar of support through all the ups and downs of graduate school. His unconditional love and optimism have given me the strength to stretch beyond my mental boundaries. I would also like to thank my father and mother-in-law for their continued unconditional support of my personal and academic decisions.

This thesis would not be possible without the spiritual guidance of my guru Swami Pranavananda Saraswati.

TABLE OF CONTENTS

LIST OF TABLES

Table

LIST OF FIGURES

LIST OF ABBREVIATIONS

ASC	Apoptosis-associated speck-like protein containing a CARD
BIR	Baculovirus inhibitor of apoptosis repeat
BMDM	Bone marrow derive macrophages
BrdU	Bromo deoxy uridine
CAPS	Cryopyrin-associated Periodic Syndromes
CARD	Caspase recruitment domain
CC	Corpus callosum
CIITA	Class II transactivator
CNS	Central nervous system
CR-3	Complement receptor-3
CSF	Cerebrospinal fluid
DAMP	Danger associated molecular patterns
DiI	1, 1'-dioctadecyl-3, 3, 3', 3'-tetramethylindocarbocyanine
EAE	Experimental autoimmune encephalomyelitis
FcγR	Fc gamma receptor
GFAP	Glial fibrillary acidic protein
GSTπ	Glutathione S transferase pi subunit
ICAM-1	Intercellular adhesion molecule-1
IFN-γ	Interferon gamma
IGF-1	Insulin-like growth factor-1

IHC	Immunohistochemistry
IL-18	Interleukin-18
IL-1β	Interleukin-1β
Kb	Kilo base
kD	Kilo dalton
LFB/PAS	Luxol fast blue/ Periodic acid schiff's staining
LRR	Leucine rich repeats
MAG	Myelin associated glycoprotein
MBP	Myelin basic protein
min	minutes
MS	Multiple sclerosis
NBD	Nucleotide binding domain
NF	Neurofilament
NLR	Nucleotide-binding, leucine rich repeat
NLRC4	NLR family, Caspase Recruitment domain containing 4
NLRP1	NLR family, Pyrin-domain containing 1
NLRP3	NLR family, Pyrin-domain containing 3
ODG	Oligodendrocyte
ORO	Oil red O
PAMP	Pathogen associated molecular patterns
PBS	Phosphate buffered saline
PFA	Paraformaldehyde
PI3K	Phosphoinositide 3-kinase

PLCγ	Phospholipase C gamma
RCA	Ricinus communis agglutinin
SRA-I/II	Scavenger receptors I and II
TNF- α	Tumor necrosis factor- alpha
TUNEL	Terminal deoxynucleotidyl transferase dUTP nick end labeling
WB	Western blot
WT	Wild- type

CHAPTER I

1.1 ABSTRACT

The nucleotide-binding, leucine rich repeat (NLR) proteins are a recently discovered family of intracellular pathogen and danger signal sensors. NLRs have emerged as important contributors to innate immunity in animals. Although the physiological relevance of these genes remains elusive, gene mutations in some of the family members leads to several autoinflammatory diseases. The association of mutations in NLR genes to autoinflammatory diseases indicates an important function of these genes in inflammation *in vivo*. This chapter reviews the NLR gene family, the NLR inflammasomes, role of inflammasome forming NLR proteins in inflammatory diseases and the possible use of some of these NLRs as pharmacological targets.

1.2 THE NLR GENE FAMILY

The nucleotide-binding, leucine rich repeat (NLR) gene family is an evolutionarily conserved family of genes, important for immune function in animals (1). There are more than 20 NLR genes in humans.

The NLR gene family members were discovered by their structural similarity to the MHC class II gene master regulator, the class II transactivator (CIITA) (2). NLR genes encode cytoplasmic proteins with a tripartite domain structure that is conserved with a subclass of plant disease resistance genes. This tripartite structure consists of a variable N terminal effector domain, a central nucleotide binding domain (NBD) and a variable number of C terminal leucine rich repeats (LRRs). Figure 1.1 provides the domain organization of some of the NLRs.

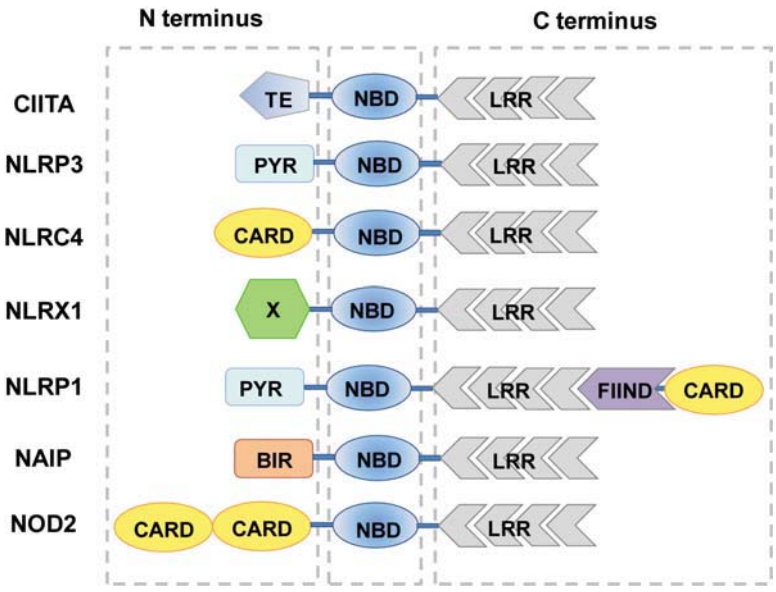

FIGURE 1.1 Domain Organization of NLRs.
NLR proteins have a conserved tripartite structure consisting of an N-terminal effector domain, a central nucleotide binding domain (NBD) and a variable number of C-terminal leucine rich repeats (LRRs). The following abbreviations have been used here: PYR, pyrin domain; CARD, caspase activating and recruitment domain; BIR, baculovirus inhibitor of apoptosis repeat; TE, transcription enhancer and FIIND, function to find domain.

The NLRs are responsible for rapid sensing of pathogen-associated molecular patterns (PAMPs) such as bacterial cell wall components; lipopolysaccaride (LPS), lipoproteins and flagellin (3-7), and bacterial and viral nucleic acids(3, 8). In addition, NLRs also sense danger associated molecular patterns (DAMPs) such as ATP (9), uric acid (10, 11), amyloid -β (12), hyaluronan and heparan sulfate (13). Recognition of PAMPs and DAMPs by NLR proteins can result in assembly of a caspase-1 activating multi-protein complex referred to as the "inflammasome" (14). This is similar to the cytoplasmic multi-protein complexes assembled for activation of caspase-9 and caspase-8 referred to as the apoptosome (containing Apaf-1) and the death-inducing signaling complex (Fas/CD95-DISC) respectively (15-17). The protein components of the caspase activating platforms are present as inactive monomers that oligomerize on exposure to the activating PAMP or DAMP signal. Inflammasome formation results in cleavage of caspase-1 from its inactive pro protein form to its active mature form. This active caspase-1 then processes the cleavage of pro-IL-1β and pro-IL-18 to IL-1β and IL-18, respectively. While IL-1β and IL-18 are the most widely studied targets of caspase-1 two recent studies have identified more than 70 new targets of caspase-1 ranging from chaperones, cytoskeletal and translation machinery, glycolysis and immune proteins (18, 19). Both IL-1β and IL-18 are proinflammatory cytokines. Release of proinflammatory cytokines and chemokines recruits immune cells (such as macrophages/microglia, B cells and T cells) to the site of infection or injury leading to phagocytosis of the pathogen or removal of danger signal, release of antimicrobial compounds and inflammation, resulting in resolution of infection and/or cell death. The three well known inflammasomes, the NLRP1, NLRP3 and NLRC4 inflammasome complexes and

their key component proteins will be discussed in some detail here. Figure 1.2 depicts the triggering PAMPs and DAMPs and key component proteins of the four inflammasomes discussed here.

1.3 THE NLR INFLAMMASOMES

The NLRP3 inflammasome: One of the NLR genes, NLR family, Pyrin-domain containing 3 (*NLRP3*, also Cryopyrin, Nalp3, PYPAF1, CIAS1) is critical for processing of caspase-1 and consequently the proinflammatory cytokines interleukin-1beta (IL-1β) and interleukin-18 (IL-18) from their inactive pro- forms to their mature active form (20). In the presence of bacterial products such as bacterial RNA (8, 21), certain toxins such as; nigericin (*Streptomyces hygroscopicus*) and maitotoxin (marine dinoflagellates), cellular danger signals such as ATP (9), uric acid crystals (10), hyaluronan and heparan sulfate (13, 22) and amyloid- β (12), environmental danger signals such as asbestos and silica (23, 24) and alum and its adjuvants (23, 25) NLRP3 forms a multi-protein complex with the adaptor protein apoptosis-associated speck-like protein containing a CARD (*ASC*) (20) and pro-caspase-1 referred to as the NLRP3 inflammasome. Association of NLRP3 with ASC is required for recruitment of pro-caspase-1 (26). The CARD domain of ASC is utilized to recruit pro-caspase-1by CARD-CARD interactions, thus leading to processing of pro-caspase1 to active caspase-1. Caspase-1 is in turn critical for processing and release of IL-1β and IL-18 (27).

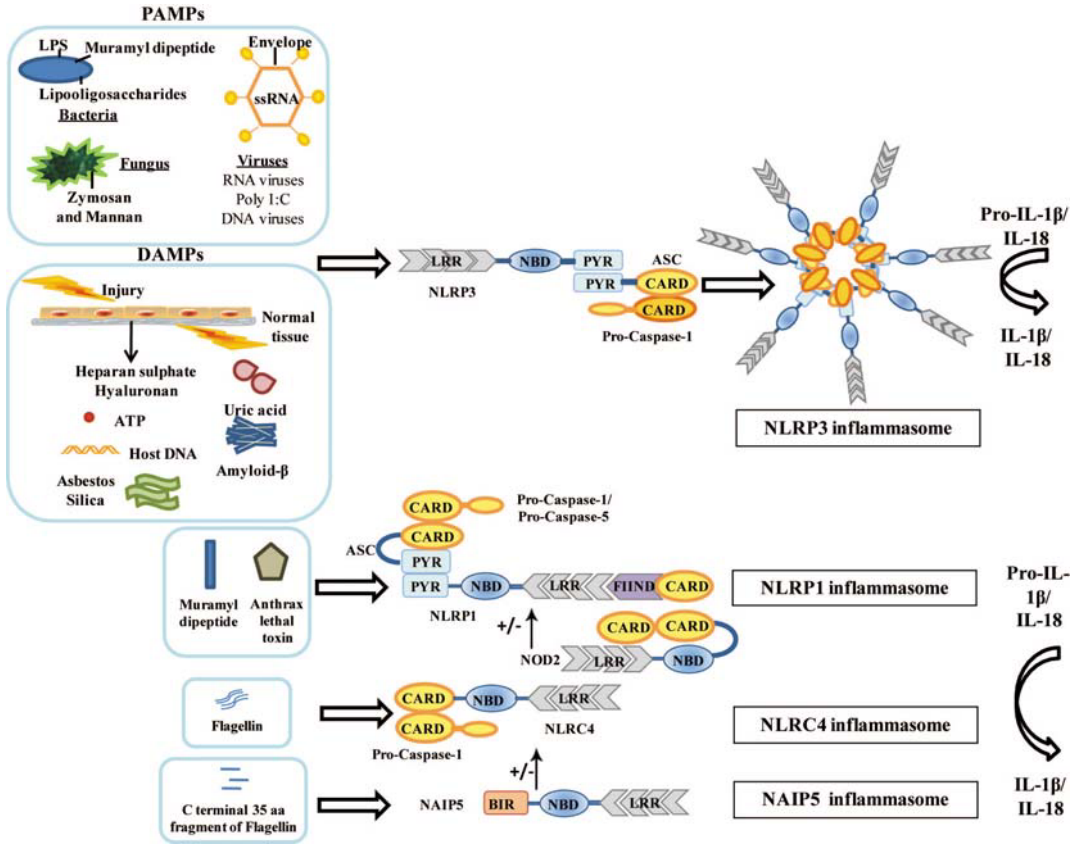

FIGURE 1.2 The NLR Inflammasomes.

In response to pathogen-associated molecular patterns (PAMPs) or damage-associated molecular patterns (DAMPs) the NLRs are activated to form multi-protein caspase activating platforms referred to as inflammasomes. The NLRP1 inflammasome when activated by muramyl dipeptide or anthrax lethal toxin can recruit pro-caspase-1 via direct CARD-CARD interactions and cause its autocatalytic cleavage to mature caspase-1. The activated caspase-1 can then process IL-1β and IL-18 from their inactive pro-protein to mature active forms. The NLRP3 inflammasome is activated in response to several PAMPs and DAMPs including but not restricted to nucleic acids (8, 21, 28, 29), LPS (8), lipooligosaccharide (30), muramyl dipeptide (31), ATP (9), uric acid crystals (10), hyaluronan and heparan sulfate (22) and amyloid-β (12), asbestos and silica (23, 24). NLRP3 forms a multi-protein inflammasome complex with the adaptor protein apoptosis-associated speck-like protein containing a CARD (ASC) and pro-caspase-1. Association of NLRP3 with ASC is required for recruitment of pro-caspase-1. The CARD domain of ASC is utilized to recruit pro-caspase-1 by CARD-CARD interactions, thus leading to processing of pro-caspase-1 to active caspase-1. Caspase-1 is in turn critical for processing and release of IL-1β and IL-18. The NLRC4 inflammasome is a cytosolic sensor of flagellin and pathogens such as *Salmonella typhimurium, Shigella flexneri* and *Legionella pneumophila* (3-7, 26, 32). NLRC4 forms a homo-oligomeric inflammasome with caspase-1. The C-terminal 35 amino acid fragment of flagellin is sensed by NAIP5 leading to a NAIP5 dependent cell death while full length flagellin induces NAIP5 independent but NLRC4 dependent cell death and IL-1β release (33).

The NLRP1 inflammasome: The human NLR family, Pyrin-domain containing 1 (*NLRP1*, also NALP1, CARD7, DEFCAP, CLR17.1) inflammasome was the first caspase-1 activating inflammasome to be identified (34). There is only 1 NLRP1 gene in humans in contrast to 3 paralogs in mice; *Nlrp1a, Nlrp1b, Nlrp1c* (35). The NLRP1 protein in humans

consists of an N terminal pyrin domain, central; NBD, NBD associated domain (NAD), LRR, and function to find (FIIND) domains, and a C terminal CARD domain. The mouse counterparts vary in structure from the human protein; *Nlrp1a* lacks the N terminal pyrin domain, *Nlrp1b* lacks both the pyrin and NAD domains and *Nlrp1c* lacks all but the NBD and LRR domains. Initial studies on NLRP1 using cell extracts suggested that the NLRP1 inflammasome in humans consisted of NLRP1, caspase-1, caspase-5 (not present in mice) and ASC (36, 37). Further studies revealed that even though the presence of ASC is not required for processing of caspase-1 by the NLRP1 inflammasome it does augment this function (38). The mouse *Nlrp1b* inflammasome is activated in response to *Bacillus anthracis* (39) and this activation is attributable to the anthrax lethal toxin. Faustin *et al.* utilized a cell-free system with recombinant NLRP1 inflammasome components to show a two step mechanism of inflammasome assembly and caspase-1 activation in response to the peptidoglycan component muramyl dipeptide (MDP) (38). Subsequently, Hsu *et al.* showed that MDP stimulation of macrophages leads to association of NLRP1 with NOD2 (39). Gel filtration experiments revealed a complex consisting of NLRP1, NOD2 and caspase-1. Moreover, *Bacillus anthracis* infection also induces NOD2 and caspase-1 dependent IL-1β secretion. These results suggest the existence of a NLRP1 and NOD2 containing inflammasome, and the potential for MDP to activate both NLRP1 and NOD2. However there is no data to show that MDP binds to either NLRP1 or NOD2, thus how MDP activates this pathway is unclear.

The NLRC4 inflammasome: NLR family, Caspase Recruitment domain containing 4 (*NLRC4*, also IPAF, CLAN, CARD12) is a cytosolic sensor of flagellin and flagellated pathogens such as *Salmonella typhimurium* (5, 26) and *Legionella pneumophila* (3) and non-

flagellated pathogens such as *Shigella flexneri* (7) and *Pseudomonas aeruginosa* (32). NLRC4 forms a homo-oligomeric inflammasome with caspase-1 (26). NLRC4 was shown to be highly expressed in human brain, bone marrow and the human monocytic cell line THP-1 by RT-PCR (40). Initial characterization of NLRC4 in human tissues and cell lines demonstrated its direct association with the CARD domain of procaspase-1 through CARD-CARD interactions (40, 41). This interaction can cause autocatalytic processing of procaspase-1 to Caspase-1 (40). A constitutively active NLRC4 could cause autocatalytic processing of procaspase-1 leading to caspase-1 dependent apoptosis in transfected cells (40). In macrophages, activation of the NLRC4 inflammasome by cytoplasmic flagellin leads to caspase-1 activation and IL-1β release (4, 5, 26). NLRC4 can interact directly with procaspase-1 through CARD-CARD interaction, however direct interaction of ASC with NLRC4 has not been demonstrated. Nonetheless, ASC-deficient macrophages show defective caspase-1 activation and IL-1β release in response to *Salmonella*, *Shigella* and *Pseudomonas* infection indicating that the function of NLRC4 is ASC-dependent (7, 26, 32).

The NAIP5 inflammasome: NLR apoptosis-inhibitory protein 5 (NAIP5 also BIRC1, NLRB1) is also a cytosolic sensor of flagellin. While the human genome has one *Naip5* gene, there are 7 paralogs of NAIP, *Naip1-7*, in mice (42). Based on co-immunoprecipitation studies utilizing over-expressed Myc-tagged NAIP and HA- tagged NLRC4 in HEK293 cells, these two proteins can co-associate, suggesting that they can be part of the same caspase-1 activating inflammasome (43). Recently, Lightfield *et al.* reported a novel role of NAIP5 in inflammasome activation in response to the C-terminus of flagellin and *Legionella pneumophila* infection (33). Interestingly, while transduction of macrophages with a C-terminal 35 amino acid fragment of flagellin led to NAIP5-dependent cell death,

full length flagellin induced NAIP5 independent but NLRC4 dependent cell death and IL-1β release. Moreover, since NLRC4 can sense some non-flagellated bacteria (7, 32) this might point to a mechanism for differential sensing of bacteria via regulation of inflammasome components. However, NAIP5 has no caspase domain, and it needs NLRC4 to activate pro-caspase 1. Thus NAIP5 appears to possess NLRC4 dependent and independent functions.

1.4 THE NLR INFLAMMASOME END PRODUCTS

Caspase-1, IL-1β and IL-18: Activation of the NLRP1, NLRP3 and NLRC4 inflammasomes leads to processing of inactive pro-caspase-1 to active caspase-1. Caspase-1 is an inflammatory caspase whose activation by the inflammasomes leads to its processing of the proinflammatory cytokines IL-1β and IL-18. Caspase-1 levels are significantly increased in peripheral blood mononuclear cells from MS patients (44). Moreover, caspase-1 is known to contribute to the pathology of EAE (45, 46).

IL-1β (Interleukin-1β) is a 17kDa proinflammatory cytokine that is essential for innate immune responses. IL-1β is released primarily by microglia and macrophages in the central nervous system (CNS). IL-1β promotes leukocyte infiltration by inducing expression of many cytokines, chemokines and adhesion molecules. The release of IL-1β also mobilizes neutrophils and other immune cells to help resolve infections and promote wound healing. Chronic release of IL-1β however, can be detrimental and cause skin rashes, inflammatory arthritis, and systemic fever. It is for this reason that IL-1β production is very tightly regulated at the levels of transcription, translation and release. IL-1β is produced as an inactive precursor that has to be cleaved by caspase-1 to generate the mature active form.

IL-18 (Interleukin-18) is an 18kDa member of the IL-1 family of cytokines. IL-18 is produced by several immune and non-immune cells including monocytes, macrophages, splenocytes, keratinocytes, microglia, macrophages and astrocytes (47-49). In the CNS, IL-18 induces microglial production of proinflammatory cytokines such as IL-1β, TNFα and matrix metalloproteinases (MMPs). Extravasation of polymorphonuclear leukocytes (PMNs) and monocytes/macrophages is amplified by IL-18 dependent upregulation of intercellular adhesion molecule-1 (ICAM-1) on endothelial cells.

1 .5 INFLAMMASOME NLRS AND INFLAMMATORY DISEASE:

It has been recently proposed that NLR related inflammatory diseases can be classified into 3 categories based on mutations of core components of the inflammasome complexes (intrinsic inflammasomopathies), accessory or regulatory proteins upstream or downstream of the inflammasome complex (extrinsic inflammasomopathies) and disease resulting from aberrant activation of the inflammasome complex (acquired or complex inflammasomopathies) (50, 51). Table 1.2 provides a list of the disease associated mutations discussed in this section.

Intrinsic inflammasomopathies:

Cryopyrin-associated Periodic Syndromes (CAPS or cryopyrinpathies)- Autosomal dominant mutations in *NLRP3* in humans leads to three autoinflammatory syndromes collectively referred to as Cryopyrin-associated Periodic Syndromes (CAPS or cryopyrinpathies) (52, 53 , 54-56). Gain of function mutations of *NLRP3*, cause a lowered activation threshold which leads to IL-1β secretion even in the absence of a stimulus *in vitro* (34, 57). All CAPS are characterized by increased levels of IL-1β in the absence of infection. CAPS consist of a spectrum of diseases ranging from the mild such as Familial Cold

Autoinflammatory Syndrome (FCAS), to the intermediate such as Muckle Wells Syndrome (MWS) and the severe such as Chronic Infantile Neurological, Cutaneous and Articular syndrome (CINCA) also known as Neonatal-Onset Multisystem Inflammatory Disease (NOMID). All three syndromes present with fever, urticaria-like rash and varying degrees of arthropathy and neurological manifestations (1, 58-60). Of the 3 CAPS, FCAS consists of the mildest symptoms including cold-induced urticaria and mild arthralgia. MWS is intermediate with spontaneous urticaria (not cold-induced), sensorineural hearing loss, arthralgia and in some cases renal amyloidosis. CINCA is the most severe with spontaneous urticaria, deforming arthropathy, sensorineural hearing loss, and chronic aseptic meningitis.

In 2001 Hoffman et al, sequenced regions of chromosome 1q44, this region was known to contain mutations that lead to FCAS and MWS (61). This screening approach led to the discovery of 4 distinct mutations in exon 3 of a 9 exon gene that segregated with the disorder in 3 families with FCAS and 1 family with MWS. This gene is now referred to as *NLRP3*. NLRP3 is a cytoplasmic protein that is expressed in monocytes, macrophages, granulocytes, dendritic cells, non-keratinized epithelial cells, osteoblasts, uroepithelial cells, and T and B cells (62, 63). NLRP3 is composed of 3 distinct domains the N terminal pyrin domain (PYD), the central nucleotide binding domain (NBD), and the C terminal leucine-rich repeats (LRRs). All 84 of the disease associated mutations lie within exon 3 which encodes the central NBD of NLRP3 (64). The PYD of NLRP3 is essential for homotypic interactions with PYD domain of other proteins. The NBD is thought to be involved in oligomerization of NLRP3 to form the inflammasome complex. The LRR domain is suggested to mediate interaction with intracellular or extracellular PAMPs or DAMPs albeit no evidence has been reported. Several studies reported the role of NLRP3 in response to

bacterial RNA, dsRNA, viral RNA, uric acid crystals, TLR ligands and ATP in *Nlrp3*-deficient mice (8-10, 20, 21). Recently, the Strober and Hoffman labs separately generated mice expressing mutations corresponding to human FCAS or MWS mutations (65, 66). Meng *et al.* generated a mouse expressing the R258W mutation corresponding to the human R260W substitution (66). Brydges *et al.* generated two lines of mice carrying the A350V and L351P mutations corresponding to the human A352V and L353P mutations downstream of a LoxP –flanked Neomycin resistance cassette in reverse orientation (65). When these mice were crossed with Cre recombinase expressing mice they would express the mutated NLRP3 protein in all tissues (CreZ), in myeloid cells only (CreL), or after exposure to tamoxifen (CreT). The mice generated by both studies developed severe cutaneous lesions associated with inflammatory cell infiltrates, recapitulating some of the urticaria-like skin lesions in MWS patients. Interestingly, both studies could recapitulate human disease by either expressing mutant NLRP3 only in myeloid cells (65) or by generation of bone marrow chimeras with the mutant R258W protein in bone marrow cells (66). Moreover, both groups found that the disease phenotype was only partially dependent on IL-1β and was dependent on the expression of mutated NLRP3 in antigen presenting cells and not in T cells.

Vitiligo – This is an autoimmune disease resulting from destruction of melanocytes causing patches of depigmented skin in patients. Vitiligo patients are at a higher risk for development of other autoimmune diseases such as rheumatoid arthritis, diabetes, lupus and thyroid disease. Fine scale association analyses of patients with vitiligo identified *Nlrp1* variants that are associated with development of vitiligo alone (67). The mechanism by which NLRP1 leads to skin hypopigmentation in vitiligo remains unknown.

NLR	Mutation(s) (Amino acid change)	Disease association	Reference
NLRP3	A439V, V198M, E627G, A352V	FCAS and MWS	(61)
	R260W, D303N, T348M, A439T, and G569R	FCAS and MWS	(58)
	F575S, Q306L, T436N, H358R, M662T, D303N, F309S	CINCA	(62)
	L264H, D303N, A374N, Y570C, F523L	CINCA	(59)
	L353P	FCAS	(60)
	T348M, E354D, L632N,R260L, R260P, D303N, D303G, F309S, T405P, T436I, Y570C	CINCA	(56)
NLRP1	L155H	Vitiligo	(67)
NLRP12	R284X, V635T	Guadeloupe Variant Periodic Fever Syndrome	(68)

TABLE 1.1 Disease associated mutations in inflammasome forming NLRs

Extrinsic inflammasomopathies:

Extrinsic inflammasomopathies are diseases arising from defects in NLR proteins that are not part of an inflammasome complex or from defects in NLR protein associated proteins.

Familial Mediterranean fever (FMF) **-** FMF is one of the most common autoinflammatory diseases. It affects individuals of Mediterranean ancestry and the carrier rates can be as high as 1 in 3 (69). FMF is characterized by acute attacks of fever and inflammation of the joints (arthritis), skin (pustular skin disease), pleura (pleuritis) or peritoneum (peritonitis) (70). These episodes may last 12-72 hours to days. FMF is clinically divided into 2 sub types: type 1 is characterized by short episodes of peritonitis, synovitis, pleuritis, pericarditis and meningitis while type 2 is characterized by amyloidosis. Before the development of therapy, amyloidosis frequently led to renal failure by age 40.

Segregation analyses of families manifesting FMF symptoms led to the discovery that FMF is a single-gene recessive disorder with incomplete penetrance (51). Further linkage studies established the FMF susceptibility locus to the short arm of chromosome 16.

All genes within the 200-kb region were screened for disease associated mutations which led to the discovery of the Mediterranean fever (*MEFV*) gene. *MEFV* consists of 10 exons covering 15kb of DNA which encodes a 781 amino acid protein called pyrin.

Pyrin is expressed in peritoneal and synovial fibroblasts, granulocytes, dendritic cells and monocytes (71, 72). Pyrin is composed of four domains: the N terminal pyrin domain and 3 C terminal domains including- a B box zinc finger domain (B-box), an α helical coiled coil domain (CC) and a B30.2 (PRYSRPY) domain. The B-box domain is necessary and sufficient for interactions with the proline serine threonine phosphatase interacting protein (PSTPIP1) (73). The B-box can also act as an intramolecular inhibitor by binding to the PYD domain and thus inhibiting pyrin interactions with ASC which occur via PYD-PYD interactions (74). The CC domain is required for homotrimer formation during the ASC pyroptosome formation (74). The B30.2 domain plays a role in interaction with the NBD of NLRP3 (75). Pyrin can also bind to caspase-1 via its B30.2 domain thus reducing caspase-1 activation (75, 76).

Mice expressing a truncated form of pyrin produce increased amounts of caspase-1 and IL-1β in response to stimuli such as a LPS and IL-4 (77). Most mutations associated with FMF in humans affect the B30.2 domain however; the contributions of these to the clinical disease remain uncertain (75).

Recent studies utilizing the human monocytic cell line, THP1, have suggested that PSTPIP1 interaction with pyrin can induce pyrin interaction with ASC leading to formation of a pyroptosome complex which can cause procaspase-1 cleavage to active caspase-1 (74, 78).

Crohn's disease and Ulcerative colitis- Crohn's disease (CD) and ulcerative colitis (UC) are collectively referred to as inflammatory bowel disease (IBD). IBD constitutes chronic disease of the gastrointestinal tract with unknown etiology. The prevalence of UC and CD are between 150-200 per 100,000 in western countries (79). Though the etiology remains unknown both genetic predisposition and intestinal microflora are known to contribute to the pathology.

UC is characterized primarily by pathology of the colon, though the rectum is involved in 95% of the patients. Inflammation is limited to the mucosa and consists of continuous but variable severity of ulceration, edema and hemorrhage along the length of the colon. Acute and chronic inflammation is characterized by infiltration of PMNs and mononuclear cells, crypt abscesses, distortion of the mucosal glands and goblet cell depletion.

In contrast to UC, CD can affect any part of the gastrointestinal tract from the oropharynx to the perianal area. The common locations in decreasing order are the ileocecal region, followed by the terminal ileum, diffuse small bowel and colon. The pathology consists of small superficial ulcers over a Peyer's patch and focal chronic inflammation that can extend to the submucosa and can lead to granuloma formation.

Even though, mononuclear cells from the lamina propria of UC and CD patients show enhanced TNF, IL-6 and IL-1 secretion (80), no NLR gene has been implicated in the pathology of UC yet. Inheritance of CD was known to be linked to chromosome 16. Using linkage and genetic association analyses two groups simultaneously discovered that mutations in NOD2 gene showed strongest linkage to CD (81, 82).

NOD2 is expressed primarily by myeloid lineage cells. The NOD2 protein has two N-terminal CARD domains , a central NBD domain and 10 C terminal LRRs. NOD2 interacts with RICK/RIP2, via CARD-CARD interactions, to activate the NF-κβ and mitogen-activated protein (MAP) kinase signaling pathways (83-86). The NBD domain has ATP-binding activity and the LRRs mediate intracellular recognition of bacterial cell wall component MDP by an unknown mechanism (87). While most CD mutations are found in the NOD2 gene, three mutations in the C-terminal account for 80% of the NOD2 associated CD patients.

The mechanisms by which CD mutations lead to inflammatory bowel disease remain largely unknown. Thus far, the results obtained from animal studies vary with the cell types under study. BMDMs from mice with a CD associated NOD2 mutation exhibit increased NF-κβ activity and IL-1β in response to MDP (86). This is consistent with increased NF-κβ activation in lamina propria of CD patients (88) however, PBMCs from these patients show decreased activation in response to MDP (89, 90). Another study utilizing MDP activation of NOD2 showed a down regulation of multiple TLR induced responses (91). This may provide a possible mechanism for increased susceptibility to intestinal inflammation following exposure to gut microflora.

NOD2 is not the only gene involved in innate immunity that is also involved with CD. More than 30 genetic disease susceptibility factors associated with CD have been identified in humans such as several autophagy related genes such as ATG16L1 and *Irgm*. Mice deficient in Atg16L1 exhibit abnormalities in granule exocytosis from their Paneth cells, similar to that seen in CD patients (92). Moreover these mice are also more susceptible to chemical-induced colitis in an IL-1β dependent manner (93). *Irgm* deficient mice have a

defective capacity to clear intracellular pathogens (94, 95). These findings suggest a complex interplay between NOD2, autophagy genes and other immunity genes that could affect susceptibility to CD.

Blau syndrome- Blau syndrome is characterized by granulomatous uveitis, arthritis, and skin rashes with camptodactyly (flexion contractures of the fingers and toes) (96). Blau syndrome is caused by mutations in the NOD2 gene. In contrast to CD mutations that target the LRR, in Blau syndrome the mutations target the NBD of NOD2.

Pyogenic Arthritis Pyoderma Gangrenosum and Acne syndrome (PAPA) **–** Patients with PAPA syndrome manifest episodic destructive arthritis that may lead to periosteal proliferation and ankylosis. Skin manifestations range from severe cystic acne on the face, chest or back to pyoderma gangrenosum, an ulcerating skin condition that can be triggered by minor trauma. Linkage studies in patients with PAPA lead to chromosome 15q (97). Further studies lead to the discovery of two mutations within the gene encoding PSTPIP1.

PSTPIP1 is expressed in hematopoietic tissues including spleen and peripheral blood leukocytes (73). The PSTPIP1 protein contains a CIP4 domain, CC domain and a SH3 domain. The CC and SH3 domains are utilized for interaction with the B-box domain of pyrin (73). Mutations in PSTPIP1 lead to its hyperphosphorylation which increases its avidity for pyrin (73, 74). Cell lines co-transfected with PAPA-associated PSTPIP1 mutants and pyrin show increased IL-1β production (73).

Complex or acquired inflammasomopathies:

Complex or acquired inflammasomopathies arise from aberrant inflammasome activation by environmental or endogenous stimuli.

Gout/ Pseudogout – Gout and pseudogout are rheumatic diseases caused by deposition of monosodium urate (MSU) and calcium pyrophosphate dihydrate (CPPD) crystals respectively, in joints and periarticular tissues. This deposition can lead to acute or chronic inflammation of the joints. MSU and CPPD crystals increase caspase-1 activation and IL-1β release from murine macrophages in an NLRP3 and ASC dependent manner (10). The importance of IL-1β in gout studied in mice was further supported by the resistance of mice deficient in the IL-1 and TLR signaling adaptor protein MyD88 to MSU induced inflammation (98). While TLR deficient mice still showed inflammation, the IL-1β receptor deficient mice did not thus indicating a specific role for IL-1 signaling in the pathology. Finally, bone marrow reconstitution experiments established that IL-1 receptor expression in non-hematopoietic cells and hematopoietic cells is required for initiation of inflammation upon MSU stimulation indicating IL-1β engagement to its receptor in this model.

Alzheimer's disease- Alzheimer's disease (AD) is a neurodegenerative disease that affects more than 20 million individuals worldwide and approximately 4.5 million Americans (99). Amyloid-β oligomers lead to the pathogenic lesions in AD. Amyloid-β oligomers and fibrils have been shown to signal via the TLRs leading to inflammatory responses (100). However, TLR signaling can also be neuroprotective since it aids in recruitment of T cells and enhances phagocytosis and clearance of amyloid β by microglia (101). NLR inflammasomes are known to trigger release of IL-1β and IL-18. These cytokines are upregulated in both brain and plasma of patients with AD (102-104). Amyloid β oligomers are known to be more potent inducers of IL-1β release than fibrillar amyloid β. Moreover, transgenic Alzheimer's mice express increased IL-1β staining in reactive astrocytes that surround the amyloid β plaques. Human brain autopsy studies from AD patients show

increased release of IL-1β from microglia in AD brain than normal brain after amyloid β peptide stimulation (105).

Halle *et al.,* recently showed that, amyloid β protein when phagocytosed by human microglia could activate the Nlrp3 inflammasome and cause IL-1β release (12). Amyloid-β phagocytosis induces lysosomal destabilization and subsequent release of cathepsin B which leads to NLRP3 inflammasome activation.

Asbestosis and Silicosis- Prolonged inhalation of asbestos and silica lead to two environmentally induced forms of pulmonary fibrosis referred to as asbestosis and silicosis respectively. Alveolar macrophages from individuals with prolonged exposure to asbestos exhibit enhanced IL-1β release (106). Moreover, *Nlrp3*-deficient mice show decreased IL-1β release in response to asbestos and silica (23, 24) indicating a role for NLRP3 in the immune response to asbestos and silica. Silica crystals once phagocytosed cause lysosomal damage leading to release of the lysosomal protease cathepsin B which can activate the cytoplasmic NLRP3 inflammasome. Inhibition of phagosomal acidification or cathepsin B impairs NLRP3 inflammasome activation (23). In the bleomycin (BLM)-induced lung injury model of fibrosis, the NLRP3 inflammasome is triggered by local uric acid release in response to DNA damage and degradation after BLM injury suggesting that uric acid may be one of triggering DAMPs in lung fibrosis and disease (107).

Guadeloupe Variant Periodic Fever Syndrome (FCAS2) - This syndrome was first reported in two families in Guadeloupe and thus named Guadeloupe Variant Periodic Fever Syndrome (68). Based on the similarities in symptoms to FCAS this syndrome is also referred to as FCAS2. Individuals with this syndrome present with cold-induced

heterogeneous symptoms including fever, arthralgia, myalgia, sensorineural hearing loss, aphthous ulcers and lymphadenopathy.

Genetic studies in patients with Guadeloupe Variant Periodic Fever Syndrome revealed 2 missense mutations, 1 nonsense mutation and 1 deletion mutation, in the *Nlrp12* gene. The nonsense mutation caused a truncation within the NBD domain of the protein while the splice mutation caused a deletion of the C-terminal LRRs. NLRP12 was recognized as one of the few NLR proteins that can suppress NF-κβ signaling (108, 109). Both the missense mutations in *Nlrp12* caused a reduction in the suppression of NF-κβ signaling by NLRP12, while the NBD mutation caused a more significant impact on normal NLRP12 induced NF-κβ signaling as compared to the LRR mutation.

1. 6 NLRS IN THE BRAIN

The initial characterization of NLRs lead to the belief that they were expressed in cells that contributed to innate immunity such as monocytes, macrophages and dendritic cells. However, recent research has confirmed that they are almost ubiquitously expressed throughout the human body. Interestingly, different inflammasome components show distinct, non-overlapping tissue and cellular distribution suggesting different roles in different cell types (110). Even though, the expression of the activating surface receptors upstream of the inflammasome (such as TLRs and purinergic receptors such as $P2X_7R$) and downstream signaling molecules of inflammasome activation (such as IL-1β, IL-18 and caspase-1) is well characterized in the normal and diseased CNS, the expression of NLRs in the CNS remains largely uncharacterized. Some NLRs such as, NLRP2 (111), NLRP10 (112), NLRX1 (113) and NAIP4 (113, 114) have been shown to be expressed in brain tissue

by RT-PCR however, their cellular localization remains undetermined. Here we present some recently published findings regarding the expression of NLRs in the brain. A summary of the findings is reported in Table1.2.

Microglia:

Historically, the CNS was thought to be an immunologically privileged site because it lacks lymphatic drainage and is physically separated from the rest of the body by a blood brain barrier. However it is well established now that there is an intact immune surveillance of the CNS. Microglia are hematopoietic-derived, resident immune cells of the CNS. Microglia constitute approximately 10% of the cells in the CNS. During development microglia function to structure neuronal architecture while in adults they remain dormant until challenged. Once activated microglia perform several functions. They phagocytose microbes, apoptotic cells and debris, present antigens to T cells and release several cytokines and chemokines including but not restricted to IL-1β, TNF-α, IL-18 and IL-6. Several NLRs have been reported to be expressed in microglia including the MHC class II transactivator (CIITA) (115, 116), NOD2 and NLRP3. The NLR adaptor protein ASC is also expressed by microglia (117).

Astrocytes:

Astrocytes perform several diverse roles in the CNS. Astrocytes are essential to neuronal survival and maintaining the blood brain barrier. They provide nutrients such as glucose to neurons and play a key role in the repair and scarring process in the brain. Astrocytes have their foot processes in close contact with endothelial cells and therefore encounter T cells first. Astrocytes can act as APCs since IL-1 detected in the supernatants of cultured astrocytes is capable of T cell activation. Moreover, APCs express MHC class II

antigens and astrocytes can be made to express these by the T cell-derived factor IFN-γ. Similar to microglia, astrocytes express a wide variety of NLRs including the MHC class II transactivator (CIITA) (116, 118), NOD1 and NOD2.The adaptor protein ASC is also expressed by astrocytes (117).

Neurons:

Even though most NLR proteins are expressed by cells that come in contact with antigens such as microglia, macrophages and astrocytes, recent research has shown that several NLR family members are expressed in neurons. Kummer *et al.* showed that NLRP1 is expressed by pyramidal neurons (110). Shortly after this discovery, a NLRP1 inflammasome consisting of NALP1, ASC, caspase-1, caspase-11 (the rodent ortholog of human caspase-5) and the X-linked inhibitor of apoptosis protein (XIAP) was shown to be present in rat spinal cord motor neurons, utilizing protein co-immunoprecipitation and immunofluorescence experiments (117). NAIP1, an NLR involved in inhibition of cell death, is known to be predominantly expressed in neurons, macrophages and/or dendritic cells (119-122).

Mature Oligodendrocytes:

Oligodendrocytes are the myelin-producing cells of the CNS. ODG progenitors give rise to mature myelinating oligodendrocytes. Very little is known about the expression of NLR proteins in oligodendrocytes or their progenitors. The NLR adaptor protein ASC is known to be expressed by mature oligodendrocytes (117). NLRP1 was recently shown to be expressed by oligodendrocytes in the mouse cerebral cortex by immunohistochemistry (110). These authors also found a nuclear expression of NLRP1 in their study.

NLR (HUGO nomenclature)	Alternative or previous name(s)	Expression	References
Apaf1		Brain	{Yoshida, 1998 #233}
CIIta	MHC2TA, C2TA	Microglia, Astrocytes	{Stuve, 2002 #238}, {O'Keefe, 1999 #237}
Naip1		Spinal Motor neurons	{Holcik, 2000 #232} {Pari, 2000 #257}
Naip4		Brain and Spinal cord (by RT-PCR)	{Gotz, 2000 #256} {Pari, 2000 #257}
NLRC3	Nod3, CLR16.2		{Conti, 2005 #24}
NLRC4	IPAF, Card12	Brain Cellular localization unknown	{Poyet, 2001 #128}
NLRP1	NALP1,CARD7, DEFCAP,CLR17.1	Pyramidal neurons, oligodendrocytes	{de Rivero Vaccari, 2008 #234}
NLRP10	NALP10,NOD8, PYNOD,CLR11.1	Brain (by RT-PCR)	{Wang, 2004 #258}
NLRP12	Monarch1,PYPAF7,CLR19.3		
NLRP2	NALP2, PYPAF2,CLR19.9	Brain (by RT-PCR)	{Kinoshita, 2005 #235}
NLRP3	CIAS1, Cryopyrin, Pyrin 1,	Microglia, macrophages (by RT-PCR)	
NLRX1	Nod9, CLR11.3	Brain (by RT-PCR) Cellular localization unknown	{Tattoli, 2008 #249}
NOD1	CARD4, CLR7.1	Astrocytes	{Sterka, 2006 #254} {Rodriguez-Martinez, 2005 #251}
NOD2		Astrocytes, microglia	{Rodriguez-Martinez, 2005 #251; Chen, 2008 #252; Guo, 2006 #253; Sterka, 2006 #254}
ASC (NLR Adaptor protein)		Astrocytes, ODGs, microglia	{de Rivero Vaccari, 2008 #234}

Table 1.2: Nomenclature and expression of NLR family members in the CNS

1. 6 ENDOGENOUS INITIATORS OF INFLAMMASOME ACTIVATION IN THE BRAIN

The NLR genes, particularly those associated with the inflammasome function, have gained much interest as sensors of pathogen associated molecular patterns (PAMPs) as well as damage-associated molecular patterns (DAMPs), however their roles in inflammatory disorders of the brain have not been extensively studied. This section lists the known and possible endogenous activation stimuli in the brain for the NLRP1, NLRP3 and NLRC4 inflammasomes.

ATP and K^+ efflux:

Extracellular ATP availability in the CNS is a balance of release and enzymatic degradation. Pathological events such as mechanical or metabolic stress, inflammation, cellular injury, or changes in ionic environment can stimulate ATP release leading to widespread increase in ATP concentrations that can activate $P2X_7$Rs on microglia and astrocytes. $P2X_7$Rs are ATP gated ion channels that are activated at ATP concentrations of ≥1mM whereas other P2X receptors are activated at concentrations of ≤ 100μM. $P2X_7$Rs are expressed on monocytes, macrophages, microglia, astrocytes, dendritic cells, mast cells and lymphocyte populations (123-127). Continuous ligation of $P2X_7$Rs causes their transformation into pores as large as 900 Da and consequently to cell death (128). Recent research utilizing macrophages from *Nlrp3* $^{-/-}$ and C57Bl/6 mice has shown that pannexin-1 is critical for caspase-1 activation and IL-1β secretion in LPS-stimulated macrophages pulsed with ATP (9, 129). The role of $P2X_7$Rs during inflammation in experimental autoimmune encephalomyelitis (EAE) remains controversial, one study utilizing the MOG_{35-55} model of EAE on *P2X7R* $^{-/-}$ mice showed delayed EAE (130) while another study utilizing the same

model and bone marrow chimera studies suggested exacerbated EAE in *$P2X_7R^{-/-}$* mice (131) and in chimeras transplanted with *$P2X_7R^{-/-}$* mice bone marrow.

ATP and K^+ efflux have also been shown to be involved in cerebral injury. Intracellular K^+ is known to decrease during hypoxic and ischemic injury. Decrease in intracellular K^+ activates the NLRP3 and NLRP1 but not the NLRC4 inflammasome(s) (132). K^+ efflux is also involved in activation of NLRP1 inflammasome and release of IL-1β from cultured spinal motor neurons (117).

Myelin:

Myelin is a lipid rich membranous insulation of axons in the CNS and PNS that is critical for neuronal conduction. The protein content and structure of myelin varies between the CNS and PNS (133). Axonal damage, mature oligodendrocyte or Schwann cell death, leads to demyelination and accumulation of myelin debris. Clearance of myelin debris by macrophages and microglia is central to the repair mechanisms during demyelination in both central and peripheral nervous system diseases (134). Removal of myelin debris is critical for resolution of inflammation, further death of oligodendrocytes and differentiation of ODG progenitors for remyelination (135). Myelin phagocytosis is an important feature of EAE as well as autoimmune diseases such as multiple sclerosis. Both CNS and PNS myelin proteins can cause murine macrophages to release proinflammatory cytokines such as TNF-α, IL-12, and angiotensin converting enzyme (ACE) (136). Proinflammatory cytokines, such as TNF-α and IL-1β are known to induce mature oligodendrocyte death *in vitro* and *in vivo* leading to a vicious cycle of neuroinflammation. Myelin basic protein (MBP) is a protein common to both CNS and PNS myelin. Treatment of cultured oligodendrocytes with exogenous MBP causes a rapid and dose dependent death caused by rapid and sustained increase in

intracellular calcium (137). However, treatment of cultured oligodendrocytes with MBP peptides does not lead to their death, suggesting that the degradation of MBP during demyelination may prevent further cell death (137). Myelin debris can activate the complement system to form membrane attack complexes that disintegrate intact myelin (138, 139). Moreover, myelin debris impairs remyelination in the adult rat CNS by inhibiting oligodendrocyte precursor cell differentiation (135, 140). There are several receptor complexes that are involved in myelin phagocytosis including scavenger receptors I and II (SR-A I/II), complement receptor 3 (CR-3), Galectin-3 and the Fc gamma receptor (FcγR) (141-145). It is possible that following myelin phagocytosis the NLRP3 inflammasome is activated and results in modulating phagocytosis by affecting expression or signal transduction of some of the receptors required for myelin phagocytosis.

1. 7 NLRS IN NEUROINFLAMMATION

Neuroinflammation is a key component of many neurological diseases including multiple sclerosis (MS), amyotrophic lateral sclerosis, Parkinson's disease and Alzheimer's disease (AD). An understanding of the mechanisms by which neuroinflammation occurs, and the molecular mediators involved in this process, is necessary for identification of potential therapeutic targets.

Role of NLRs in multiple sclerosis (MS): MS is an inflammatory neurodegenerative disease, that affects more than 2.5 million individuals worldwide (146). The severely debilitating symptoms of MS, including sensory and motor dysfunctions, and reduced cognitive function, result from demyelination and neuroinflammation of the central nervous system (CNS) (147-152). There are three different categories of experimental CNS demyelination- i) Toxin-induced (cuprizone, ethidium bromide and lysolecithin, ii)

autoimmune-induced (experimental autoimmune encephalomyelitis (EAE) and iii) virus-induced (theiler's murine encephalomyelitis virus (TMEV), Semliki forest virus (SFV)). The cuprizone induced and the EAE models will be discussed in detail here since this forms the basis of my thesis project.

A. The cuprizone model of CNS demyelination and remyelination Copper is an essential trace element that is required for a number of enzymes involved in the electron transport chain (cytochrome oxidase), skin and hair pigmentation (Tyrosinase), skeletal development (ascorbate oxidase), elastin and collagen cross linking (lysyl oxidase), and breakdown of dopamine, norepinephrine and epinephrine (monoamine oxidase). Inability to absorb copper in the hereditary disease, Menkes kinky hair syndrome, leads to skin, hair and connective tissue disturbances and progressive neurological deficits leading to lethality by age 3 (153, 154). Cuprizone (bis-cyclohexanone-oxaldihydrazone) is a copper chelator that when fed in the diet leads to copper deficiency and predictable CNS demyelination. Oligodendrocytes are particularly sensitive to low concentrations of cuprizone that leaves other cells unaffected (155, 156). The mechanism of cuprizone-induced demyelination remains unknown however, it has been hypothesized that cuprizone-induced disturbance in mitochondrial function and energy metabolism in oligodendrocytes leads to demyelination (156). Cuprizone causes disruption in formation of myelin by causing a reduction in myelin basic protein (MBP) and myelin-associated glycoproteins (MAG) (157).

Dr. Glenn K. Matsushima established the cuprizone-induced model of demyelination and remyelination in the C57Bl/6 strain to take advantage of the many

transgenic and knockout mice available on this genetic background. In this model mice are fed ground chow containing 0.2% cuprizone *ad libidum* for 6 weeks. At this low concentration cuprizone fed in the diet manifests CNS demyelination without systemic toxicity, as measured by gross liver histology and liver function tests for aspartate aminotransferase (AST), alanine aminotransferase (ALT), bilirubin, alkaline phosphatase and albumin (156, 158). During cuprizone treatment mice show lethargic movement, approximately 10% weight loss and altered gait (159). Demyelination and immune cell recruitment are monitored at the mid-line corpus callosum, at the fornix region. At the end of 5 weeks of cuprizone diet demyelination is complete but mice are fed cuprizone for one more week to ensure complete demyelination in all mice. After 6 weeks the mice are returned to normal chow to allow for remyelination. There is an increase in ODG progenitors during demyelination with maximum infiltration after 5 weeks of cuprizone treatment and by the end of 9 weeks of start of treatment remyelination is complete. Untreated control mice were maintained on a diet of normal pellet chow.

There are several **advantages of the cuprizone model: 1)** It exhibits type III and IV MS neuropathology characterized by microglial infiltration and astrogliosis in the absence of T cell infiltrates thus allowing for study of the role of the innate immune system of the CNS in neuroinflammation **2)** Both demyelination and remyelination follow a predictable time course **3)** Cuprizone-induced demyelination occurs at major nerve tracts such as the corpus callosum and cerebellar peduncles that can be located easily and studied reproducibly. **4)** Cuprizone can be easily administered through ground chow.

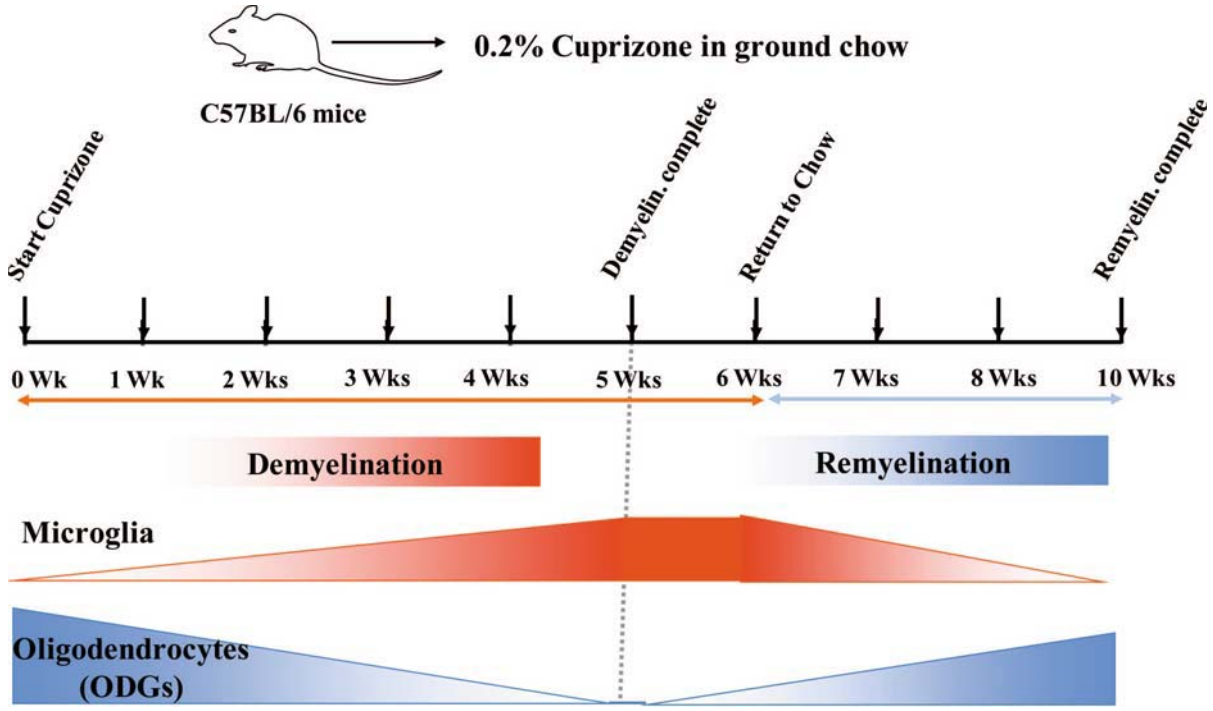

Figure 1.3. Schematic of cuprizone-induced model of CNS demyelination
Our laboratory uses cuprizone to induce demyelination in the brain of C57Bl/6 mice as a model for MS. Mice are fed 0.2 % cuprizone mixed in ground chow *ad libidum* for 6 weeks after which they are returned to normal chow to allow for remyelination. Demyelination is maximal at 5 weeks of cuprizone treatment and remyelination is complete 10 weeks after starting treatment (4 weeks after cuprizone withdrawal).

B. Experimental Autoimmune Encephalomyelitis (EAE) is a widely used model of MS. EAE is induced in mice by active priming with whole myelin proteins or specific myelin peptide epitopes in adjuvant. EAE can also be induced by adoptive transfer of myelin-specific CD4+ T cells. The symptoms of EAE are varied and can mimic different clinical manifestations of human MS. Unlike the cuprizone model, in EAE, the blood brain barrier is breached and myelin damage is T-cell mediated.

During MS an autoimmune attack is triggered against myelin. This is characterized by recruitment and proliferation of microglia and astrocytes, release of pro-inflammatory cytokines such as IL-1β, IL-18 and TNFα, demyelination, death of the myelin-producing ODG cells and axonal loss. IL-1β levels in the cerebrospinal fluid (CSF) of MS patients

correlates with disease susceptibility, severity and progression (160, 161). IL-1β immunoreactivity has been shown in activated microglia and macrophages during EAE in rats (162). Treatment with either soluble IL-1 receptor (sIL-1R) or IL-1 receptor antagonist (IL-1Ra) reduced clinical signs of EAE in rats (162, 163). IL-1β is cytotoxic to mature oligodendrocytes both *in vivo* and *in vitro* and causes proliferation of both microglia and astrocytes. Moreover, IL-18 levels are elevated in demyelinating cerebral lesions of MS patients and mice with a deletion of IL-18 (IL-$18^{-/-}$) are resistant to EAE. Expression of IL-18 and its receptor on oligodendrocytes is greater in brain tissue from patients with active MS than in patients with silent MS or from neuropathologically normal subjects.

Role of NLRs in other diseases of the CNS:

As described previously in this section mutations in *NLRP3* in humans leads to three autoinflammatory syndromes - FCAS, MWS and CINCA that are collectively referred to as CAPS(52-56). All CAPS are characterized by increased levels of IL-1β in the absence of infection. CINCA patients often display chronic aseptic meningitis which is reversed after treatment with the IL-1β receptor antagonist Anakinra (164). This is indicative of a role for NLRP3 in neuroinflammation.

1.8 NLRS IN REMYELINATION

Regulation of oligodendrogenesis by progenitors is a potential therapeutic intervention for functional loss after demyelination in MS. Previous studies have shown that remyelination is dramatically reduced in IL-$1\beta^{-/-}$ mice in the cuprizone model (158). This reduction in remyelination was attributed to defect in generation of mature $GSTpi^{+}$ mature ODG cells in spite of normal accumulation of $NG2^{+}$ ODG progenitor cells (158). It was proposed that IL-1β regulates remyelination via regulation of IGF-1 which is critical for

conversion of ODG progenitors to mature oligodendrocytes (165). Subsequent studies with transgenic mice that expressed IGF-1 constitutively, confirmed the role of IGF-1 in inhibition of mature ODG death by apoptosis (166, 167). Thus, it is possible that NLRs via their regulation of IL-1β and IL-18 processing and consequently IGF-1 can regulate oligodendrogenesis and remyelination.

1. 9 NLRS AS POTENTIAL PHARMACOLOGICAL TARGETS IN NEURODEGENERATIVE DISEASES

Activation of the various inflammasome complexes discussed here leads to activation of caspase-1 and subsequent production of the proinflammatory cytokines IL-1β and IL-18. While specific drugs interfering with inflammasome components are under development, there have been several clinical studies exploring the modification of the IL-1β pathway owing to its central role in several diseases. Modulation of IL-1β function has been approached at 3 levels: firstly, the release of IL-1β can be blocked by inhibition of upstream pathways (168, 169), secondly, the released cytokine can be neutralized or its receptor blocked to prevent downstream signaling (168, 170), and finally, the signaling mechanisms in the target cells can be blocked by disrupting further downstream signaling pathways (171-176). A detailed list of the available drugs targeting the above mentioned steps of regulation for the IL-1β pathway along with their mechanism of action is provided in Table 1.2. There are some caveats in the use of some of the inhibitors since they can inhibit not only the IL-1β but also the IL-18 pathways. A better understanding of the underlying mechanism for each disease would provide more accurate targets. Target specificity would also enable a more accurate control of pathology. CAPS symptoms remain the gold standard, which can be reversed by treatments of the IL-1 receptor antagonist Kineret®. While some of these drugs

are efficacious in relieving symptoms (170, 172-176), several others are in clinical trials or remain to be tested in humans awaiting further studies of their mode of action and/or effects in animal models of disease (168, 169).

Action	Target	Drug (Company)	Description	Reference
Suppression of IL-1β production:				
Caspase-1 inhibition	Caspase-1	Pranalcasan (Aventis/Vertex)	VX-740; VX-765	(168)
IL-1β posttranslational processing	Unknown	CP424174, CP412245 (Pfizer)	Diarylsulphonyl urea	(168)
IL-1β production inhibitor	Unknown	CJ14877, CJ14897 (Pfizer)	Pyridine-2-carboxylates	(168)
	Unknown	LL-Z1217a (Pfizer)	Terpenoid lactone	(168)
Suppression of IL-1β release:				
IL-1β release inhibitors	Unknown	CP424174 (Pfizer)	Diarylsulphonyl urea	(168))
Neutralization of secreted IL-1β:				
	IL-1	Anakinra (Kineret, Amgen)	rhuIL-1Ra	(168)
	IL-1	IL-1trap (Regeneron/Novartis)	Human IL-1R1:IgG1 protein	(168)
	IL-1	CDP-484 (Celltech)	PEGylated Antibody	(168)
Inhibition of IL-1R signal transduction:				
MyD88 inhibitors	MyD88	† hydrocinnamoyl-l-valyl pyrrolidine	MyD88 mimic	(70, 73)
		† ST2825 (Sigma-Tau)	Peptidomimetic	(172)
IRAK-4 inhibitors	IRAK-4	† Names unavailable	Amides, imidazo[1,2-*a*]pyridine compounds	(76-78)

† May also inhibit IL-18R and TLR signal transduction

TABLE 1.3 Pharmacological inhibitors targeting IL-1β production, release or action

1. 10 CONCLUDING REMARKS

The association of the NLRs with several immunological diseases suggests a role for these proteins in both innate and adaptive immunity. Recent studies are beginning to unfold the role of this family in immune regulation and dysregulation however, a plethora of

questions remain unanswered. Firstly how is the diversity of PAMPs and DAMPs sensed and differentiated from self molecules? Secondly how does such a wide range of symptoms in CAPS arise from mutations that are relatively clustered in the NBD of NLRP3? Thirdly is there a cross talk between the different inflammasome pathways and do they compensate for each other? Finally what are the DAMPs and PAMPs that might activate the inflammasome pathways in complex immune diseases such as type II diabetes, multiple sclerosis and atherosclerosis? Considering the vibrant research in this field, significant progress is likely to resolve several of these issues.

CHAPTER II

NLRP3 REGULATES NEUROINFLAMMATION AND THE CLEARANCE OF MYELIN DEBRIS IN THE CNS

2.1 ABSTRACT

Sterile inflammation is increasingly recognized as an important contributor to a host of CNS disorders however its regulation in the brain remains poorly understood. NLRP3 is a key component of the inflammasome complex which also includes ASC and procaspase-1. In the immune system, inflammasome formation is primarily triggered by membrane $P2X_7R$ engagement leading to cleavage-induced maturation of caspase-1 and IL-1β/IL-18. This work shows that expression of the *Nlrp3* gene was increased over 100 fold in a neurotoxin (cuprizone)-induced demyelination and neuroinflammation model. Mice lacking the *Nlrp3* gene exhibited reduced neuroinflammation, demyelination and oligodendrocyte loss in this model. This outcome is also observed for mice lacking caspase-1, while mice lacking IL-1β were indistinguishable from wild-type controls indicating that the *Nlrp3*-mediated function is independent of IL-1β. The absence of $P2X_7R$ reduced neuroinflammation but not demyelination suggesting that this pathway does not affect the latter. Further analyses revealed that macrophages from *Nlrp3*$^{-/-}$ and *casp1*$^{-/-}$ mice but not controls exhibited augmented capacity to phagocytize myelin and clear myelin debris. This difference did not extend to latex beads or bacteria which agrees with the differential regulation of distinct phagocytosis pathways. These results suggest that NLRP3 plays an important role in a neurologic disease model by exacerbating CNS inflammation but also by a novel function evoking myelin clearance. Thus the therapeutic inhibition of NLRP3 might not only reduce sterile CNS inflammation but also enhance the clearance of CNS debris which has broad implications for resolving other CNS diseases.

2.2 INTRODUCTION

Sterile inflammation refers to inflammation that is not caused by microbial pathogens, and is recognized as a key component of many neurological diseases including multiple sclerosis (MS), Parkinson's disease, and Alzheimer's disease. MS results from neuroinflammation characterized by infiltration of microglia and astrocytes, enhanced expression of cytokines/chemokines, demyelination and axonal loss (148, 149). An understanding of the mechanisms by which neuroinflammation affects demyelination is necessary to identify potential therapeutic targets.

Several families of innate immune receptors or sensors have been identified, with the NLR genes receiving significant attention due to their genetic linkage to human immunologic diseases and their role in immune regulation (1, 2). Among NLRs, NLRP3 represents a core component of a caspase-1-activating inflammasome complex, comprised of an NLR protein, the adaptor molecule ASC (Apoptosis associated Speck-like protein containing a CARD) and procaspase-1 (20, 177). Activated caspase-1 in turn cleaves and activates over seventy substrates including the proinflammatory cytokines interleukin-1beta (IL-1β) and IL-18 (18, 19). NLRP3 forms an inflammasome in response to bacterial RNA and toxins (8, 21), ATP (9), uric acid (10), hyaluronan (22), amyloid-β (12), asbestos, silica (23, 24) and alum (23, 25). Mutations in the human *NLRP3* gene have been identified in dominantly-inherited autoinflammatory syndromes collectively referred to as CAPS (Cryopyrin-associated Periodic Syndromes) (56, 122) characterized by hyperactivation of the inflammasome complex and increased IL-1β (56, 164). CAPS symptoms have been reversed by treatments with the IL-1 receptor antagonist Kineret® (178). Although the role of NLRP3 in CAPS is

well known, its role in other inflammatory diseases, including CNS inflammation, is less understood.

In this study we utilized the cuprizone-induced mouse model of demyelination to evaluate the role of NLRP3 in sterile CNS inflammation. This model has several advantages: 1) It exhibits type III and IV MS neuropathology characterized by microglial infiltration and astrogliosis in the absence of T cell infiltrates (147); 2) it is easily induced by administering cuprizone through the chow; 3) the disease course follows a predictable time course, and 4) demyelination has a reproducible pathology involving major nerve tracts such as the corpus callosum and cerebellar peduncles that are easily located (156). Using the cuprizone model, we studied mice deficient in genes encoding NLRP3 (*Nlrp3*$^{-/-}$), caspase-1 (*casp1*$^{-/-}$), IL-1β (*IL-1β*$^{-/-}$), IL-18 (*IL-18*$^{-/-}$), and P2X$_7$R (*P2X$_7$R*$^{-/-}$) as a way to examine the role of the NLRP3 inflammasome complex in neuroinflammation and demyelination *in vivo*. We found a significant role for the NLRP3 inflammasome pathway in the activation of neuroinflammation, but we also found an additional function for this pathway in the clearance of myelin debris.

2.3 MATERIALS AND METHODS

Mice.

Nlrp3 $^{-/-}$ mice were provided by Millennium pharmaceuticals through Drs. Fayaz Sutterwala and Richard Flavell (Yale University), and were further backcrossed to C57BL/6 mice for a total of nine generations. *Casp1*$^{-/-}$ were provided by Dr. Richard Flavell. *P2X*$_7$*R*$^{-/-}$ were obtained from Beverly Koller (UNC-CH). C57BL/6 mice (WT) were purchased from the National Cancer Institute (Bethesda, MD) and Jackson Research Labs (Bar Harbor, ME). All mice were 8-10 weeks old prior to the start of treatment. All animal procedures conducted were approved by the Institutional Animal Care and Use Committee of UNC at Chapel Hill. *IL-1β*$^{-/-}$ mice were kindly provided by Dr. David Chaplin (University of Alabama, Birmingham) (179). Breeder pairs for *IL-18*$^{-/-}$ mice were purchased from Jackson laboratories (Bar Harbor, ME) and bred in house to generate mice needed for our studies.

Cuprizone treatment.

8-10 weeks old male mice were fed 0.2% cuprizone [oxalic bis(cyclohexylidenehydrazide)] (Aldrich, St. Louis, MI) mixed into ground chow *ad libidum* for 6 weeks to induce progressive demyelination. Untreated control mice were maintained on a diet of normal pellet chow. During cuprizone treatment mice showed lethargic movement, weight loss (Fig 2.10), ruffled hair and altered gait as described earlier (158, 159)

Tissue preparation.

Mice were deeply anesthetized and intra-cardially perfused with phosphate-buffered saline (PBS) followed by 4% paraformaldehyde (PFA). Brains were removed, post-fixed in PFA, and embedded in paraffin. 5-µm coronal sections were cut at the fornix region of the corpus callosum. For frozen sections, mice were perfused and post-fixed as described earlier.

Brains were allowed to sink in 30% sucrose in PBS and snap frozen on dry ice in OCT. 5µm and 20µm coronal sections were cut at the fornix region of the corpus callosum for immunohistochemistry (IHC) and *in situ* hybridization respectively. All analyses were restricted to the mid-line corpus callosum as described previously (158, 180, 181).

Staining.

To examine demyelination, paraffin sections were rehydrated through a graded series of alcohol washes and stained with Luxol fast blue-periodic acid-Schiff's base (LFB-PAS; Sigma, St. Louis, MI) as described previously (158, 180, 181). Sections were read by three double-blinded readers and graded on a scale from 0 (complete myelination) to 3 (complete demyelination). Higher scores indicate greater pathology. For the detection of microglia/macrophages, tissue sections were rehydrated and permeabilized with 0.1% Triton/PBS for 20 min at room temperature and then incubated with *Ricinus communis* agglutinin-1 (RCA-1) lectin (1:500, Vector, Burlingame, CA) at 37 °C for 1hr. Only RCA-1^{+} cells with observable 4', 6'-diamidino-2-phenylindole (DAPI) stained nucleus were included in the quantification.

Immunohistochemistry (IHC).

IHC was performed on 5-µm paraffin embedded sections that were deparaffinized and rehydrated through alcohols as described earlier. For the detection of mature oligodendrocytes, the sections were processed by boiling in antigen unmasking solution (1:100, Vector, Burlingame, CA) for 13 min in a microwave. These sections were permeabilized with 0.1% Triton/PBS for 20 min and incubated with 2% normal goat serum in 0.1% triton-PBS for 20 min at room temperature. Subsequently, the sections were incubated with rabbit anti mouse polyclonal antibody anti- GSTπ (1:500, Stressgen, Ann

Arbor, MI) at 4°C overnight. Sections were then washed in PBS and incubated with the appropriate biotinylated antibody against primary antibody (1:100, Vector, Burlingame, CA) and texas red-conjugated avidin (1:500, Vector, Burlingame, CA). The sections were washed and incubated with Alexa Fluor conjugated 594. To detect astrocytes, sections were incubated with 5% normal goat serum in 0.1% triton-PBS for 20 min at room temperature. Subsequently, the sections were washed and incubated with rabbit anti-cow monoclonal antibody (1:100, DAKO) and goat-anti-rabbit-fluorescein conjugated secondary antibody (1:100, Vector, Burlingame, CA). For the detection of myelin basic protein (MBP) sections were permeabilized with 0.1% Triton/PBS for 10 min and incubated with 5% normal goat serum in 0.1% triton-PBS for 20 min at room temperature. Subsequently, the sections were incubated with mouse monoclonal antibody anti-MBP (1:1000, Steinberger) at 4°C overnight. Sections were then washed in PBS and incubated with anti-mouse IgG conjugated with texas red (1:1000, Vector, Burlingame, CA) for 45mins at room temperature. For the detection of 2', 3'-cyclic nucleotide phosphodiesterase (CNPase), the sections were processed by boiling in antigen unmasking solution (1:100, Vector, Burlingame, CA) for 13 min in a microwave. These sections were permeabilized with 0.1% Triton/PBS for 20 min and incubated with 5% normal goat serum (NGS) in 0.1% Triton-PBS for 20 min at RT. Subsequently, the sections were incubated with chicken polyclonal antibody to CNPase (1:500, chemicon, Billerica, MA) at RT for 1h. Sections were then washed in PBS and incubated with rabbit polyclonal to chicken IgY biotin (1:500, Abcam, Cambridge, MA) for 1h at RT. After PBS washes the sections were incubated with Alexa 594-conjugated avidin (1:500, Invitrogen) for 1h at RT.

Immunopositive cells with an observable DAPI stained nucleus were counted blindly twice. Cell counts are averages of at least 9 and up to 14 mice per time point.

Imaging.

All cell counts are within the mid line of the corpus callosum, confined to an area of 0.033 mm^2. An Olympus BX-40 microscope with camera (optronics engineering) and Scion image acquisition software was used for taking images.

Reverse transcription-PCR and quantitative real-time reverse transcription-PCR.

Total RNA was isolated from a dissected region of the brain containing the corpus callosum of wild-type and *Nlrp3* $^{-/-}$ mice at several points during and after cuprizone treatment. RNA isolation was performed using Trizol reagent (Ambion) under RNase-free conditions (158).

***In situ* Hybridization.**

3 mice per time point were perfused with PBS followed by a solution of 4% PFA. 20-µm OCT embedded frozen sections were cut at the fornix region of the corpus callosum. These sections were processed for *in situ* hybridization at the UNC neuroscience center *in situ* hybridization core.

Primary cell culture.

Bone marrow derived macrophages were extracted from femurs of WT, *Nlrp3* $^{-/-}$ and *casp1*$^{-/-}$ mice. The cells were cultured as described previously (182).

Phagocytosis Assays.

A schematic for all the phagocytosis assays is provided in figure 2.7 a. For phagocytosis of fluorescent beads, 0.25×10^6 cells per well were incubated with 0.25×10^8 beads for 0, 30, 60 and 120 minutes at 37°C. Each experimental set consisted of an untreated

control and a negative control for phagocytosis, treated with 10μM cytochalasin D a known inhibitor of phagocytosis. For myelin phagocytosis experiments, myelin was extracted from adult C57BL/6 mouse brains as described previously. A schematic of myelin extraction from adult mouse brain is provided in figure 2.7b. Myelin was labeled with the lipophilic dye 1, 1'-dioctadecyl-3, 3, 3', 3'-tetramethylindocarbocyanine perchlorate (DiI; Molecular probes: SKU# D-282) as described previously. 0.25×10^6 cells/well in 24-well culture dish was incubated with 20μg labeled myelin for 0, 30, 60 and 120 minutes at 37°C. After phagocytosis non- ingested myelin was removed by washing the cells twice with media and once with PBS. For Escherichia coli (*E. coli*) phagocytosis experiments, *E. coli* strain O114:B4 (ATCC) transformed with the pEGFP plasmid (Clontech), to express GFP were kindly provided by our collaborator Dr. Glenn Matsushima. *E. coli* were cultured to log phase in Luria broth (LB) containing ampicillin. 0.25×10^6 cells/well in 24-well culture dish were incubated with 0.25×10^8 *E. coli* for 0, 30, 60 and 120 minutes at 37°C. After phagocytosis non-ingested *E. coli* were removed by washing the cells twice with media and once with PBS.

The internalization of myelin beads or *E. coli* was quantified by measuring the mean cellular fluorescent intensity by flow cytometry. A Beckman coulter (Dako) CyAn ADP flow cytometer was used for all the above mentioned experiments. Experiments were repeated at least four times and the significance was determined by using student's t-test. Differences were considered statistically significant if $p < 0.05$.

Confocal microscopy was used to visualize myelin and bead phagocytosis by macrophages. For this, 0.25×10^6 cells were plated on 24 well glass bottom plates and after 2

hours of phagocytosis, the cells were washed thrice with PBS and fixed with 2% paraformaldehyde for 10 minutes. Subsequently, cells in the wells were stained with RCA as described previously in the staining section. A Zeiss LSM5 Pascal confocal laser scanning microscope was used for all the confocal microscopy.

Protein analysis.

Total protein was extracted from the forebrains of cuprizone-treated and untreated control C57BL/6 mice. Briefly, corpus callosi were homogenized on ice in 600µl of RIPA buffer containing protease inhibitors. The homogenate was centrifuged at 10000g for 15mins at 4°C. Supernatants were used for further analyses. For protein extraction from cultured cells, 0.25×10^6 cells were lysed in 0.25 ml RIPA buffer by rotating cell at 4°C for 20 minutes followed by centrifugation at 13100rpm for 20 minutes. The supernatants were used for further analyses. Protein concentrations were determined using a coomasie (Bradford) protein assay kit (Pierce). IL-1β levels were determined by ELISA (optiEIA ELISA, BD).

Transmission electron microscopy (TEM).

3 mice per time point were perfused with PBS followed by a solution of 4% PFA and 2.5% glutaraldehyde. Brains were sliced into 1-mm sections, and the section corresponding to the region of the fornix was trimmed and reoriented so that a cross-section of the corpus callosum was achieved. Thin sections were cut, stained with uranyl acetate and lead citrate and analyzed as previously described.

Statistical Analysis.

Data are expressed as mean ±s.e.m. Unpaired Student's *t* tests were used to statistically evaluate significant differences. Differences were considered statistically significant if $p < 0.05$.

2.4 RESULTS

Nlrp3 expression is increased in the cuprizone model of demyelination

Nlrp3 transcript expression in the CNS of cuprizone treated C57BL/6 mice was examined by real-time PCR amplification. It was found to increase progressively to more than 120 fold by the 4 week time point of a course of cuprizone-induced demyelination (Fig. 2.1a). This increase coincided with the peak of inflammatory cell infiltration, demyelination and mature oligodendrocyte death. Since commercial antibodies for mouse NLRP3 are of poor quality, we evaluated the production of IL-1β as a surrogate indicator of NLRP3 protein activation. Protein lysates from corpus callosi of cuprizone treated mouse brains analyzed by ELISA showed a similar increase in IL-1β protein as *Nlrp3* mRNA, supporting a functional increase in NLRP3 activity (Fig. 2.1b). Moreover, these studies corroborate results from an earlier study that quantified the number of IL-1β^+ cells during cuprizone-induced demyelination and remyelination (165). To further assess *Nlrp3* expression, we also analyzed *Nlrp3* expression in control untreated and 5 week cuprizone treated brains of C57BL/6 control and *Nlrp3* $^{-/-}$ mice as negative control by *in situ* hybridization using a digoxigenin labeled antisense probe to detect *Nlrp3*. A sense strand probe was also included as negative control. *Nlrp3* expression is evident in untreated C57BL/6 control brains (Fig. 2.1c).

Recruitment of microglia and astrocytes is delayed in Nlrp3$^{-/-}$ mice

To explore if NLRP3 has a role during cuprizone-induced sterile inflammation, we used mice lacking the *Nlrp3* gene. WT and *Nlrp3*$^{-/-}$ mice showed similar reduction in weight during the course of cuprizone treatment (Fig. 2.9). We first examined if deletion of this gene

in mice had an effect on microglial accumulation and astrogliosis (Fig. 2.1c-f). Microglia are resident immune cells of the CNS (183). Activated microglia can phagocytose myelin debris, present antigens to T cells, and release cytokines and chemokines (183, 184). Activated astrocytes and microglia perform several overlapping roles during neuroinflammation (185). Microglial and astroglial populations at the corpus callosum were identified by *Ricinus communis* agglutinin-1 (RCA-1) lectin and glial fibrillary acidic protein (GFAP) staining, respectively (Fig. 2.1d-e). Untreated, age-matched (0 Wk) *Nlrp3*$^{-/-}$ mice and C57BL/6 (WT) controls showed no difference in the quantitation of microglia and astrocytes at the corpus callosum (Fig. 2.1d-g). A histological representation of these data is shown in Figs. 2.1d-e, and quantitation is shown in Figs. 2.1f-g. At 3, 3.5 and 4 weeks of cuprizone treatment, there was a progressive and significant (P= 0.02 at 3 Wks, P= 0.05 at 3.5 Wks, P= 0.01 at 4 Wks) reduction in microglial infiltration in *Nlrp3*$^{-/-}$ mice relative to WT controls (Fig.2.1f). Similarly, there was a progressive and statistically significant reduction in astrogliosis in the *Nlrp3*$^{-/-}$ mice at weeks 3 and 4 of cuprizone treatment (Fig. 2.1g, P=0.03 at 3 Wks, P=0.001 at 4 Wks). These results indicate that NLRP3 enhances microglia accumulation and astrogliosis in the affected tissues. After 5 weeks of cuprizone treatment, microglial accumulation and astrogliosis between *Nlrp3*$^{-/-}$ and C57BL/6 control animals were similar (Fig. 2.1f-g). This is consistent with other studies of the cuprizone model wherein the removal of inflammatory genes has not affected neuropathology after this time point (158, 165).

Demyelination is delayed in cuprizone-treated Nlrp3*$^{-/-}$ *mice

A second component of the cuprizone model that is relevant to human diseases is the demyelination process. To assess if NLRP3 plays a role in demyelination and in the loss of mature oligodendrocytes, *Nlrp3*$^{-/-}$ mice along with age matched WT control mice were treated with cuprizone for 3, 3.5, 4 and 5 weeks. Representative scoring of the extent of demyelination as measured by Luxol fast blue-periodic acid Schiff (LFB-PAS) staining is shown in Fig. 2.2a. Slides were read by three blinded readers on a scale of 0 (no demyelination) to 3 (complete demyelination). WT mice showed significant demyelination initiating at the 3 week time point and continuing to the end of the study at the 5 Wk time point (Fig. 2.2b). *Nlrp3*$^{-/-}$ mice showed a significant delay in demyelination at the 3, 3.5 and 4 week time points when compared to WT controls (Fig. 2.2b). LFB is a screening assay for myelin which requires further verification with more specific stains such as glutathione S transferase pi subunit (GSTπ), a marker of the mature oligodendrocyte population. Prior to cuprizone treatment (0 Wk), *Nlrp3*$^{-/-}$ mice and WT controls showed no difference in mature oligodendrocyte populations at the corpus callosum as shown in Fig. 2.2c. After 3, 3.5 and 4 weeks of cuprizone treatment, the reduction of mature oligodendrocytes was attenuated in *Nlrp3*$^{-/-}$ mice relative to C57BL/6 controls. A quantitation of the composite data is shown in Fig. 2.2d (P=0.004 at 3 Wks, P=0.02 at 3.5 Wks and P=0.002 at 4 Wks). After 5 weeks of cuprizone treatment, *Nlrp3*$^{-/-}$ and WT control mice showed no difference in demyelination and mature oligodendrocyte death (Fig. 2.2d). Together, these data indicate that NLRP3 delays demyelination but does not obviate this process. This is consistent with studies of other inflammatory genes in the cuprizone model (158, 165, 180, 181). As an additional analysis of oligodendrocytes, a CNPase stain was performed and showed similar results (Fig. 2.2e).

Demyelination, mature oligodendrocyte death, astrogliosis and microglial infiltration during cuprizone-induced demyelination are independent of IL-1β

The above results indicate the importance of NLRP3 in pathology associated with the cuprizone model; hence we examined the role of an inflammasome end-product, i.e. IL-1β, in this model. An earlier study of *IL-1β*$^{-/-}$ mice showed delayed remyelination but no difference in demyelination in the cuprizone model, although this latter issue was only peripherally addressed in that report (165). To elaborate on these results, we performed a more extensive analysis of cuprizone-induced demyelination in *IL-1β*$^{-/-}$ mice. *IL-1β*$^{-/-}$ mice showed no difference in demyelination (Fig. 2.3a), loss of GSTπ mature oligodendrocyte (Fig. 2.3b), accumulation of microglia (Fig. 2.3c) or astrogliosis (Fig. 2.3d) during demyelination. This indicates that all of the measured neuropathology observed in the cuprizone model is IL-1β independent.

Cuprizone-induced microglial accumulation, astrogliosis and demyelination are caspase-1 dependent

NLRP3 is required for the processing of caspase-1, which in turn cleaves IL-1β and IL-18 (Sutterwala et al., 2006). To establish if NLRP3-dependent CNS inflammation and demyelination are caspase-1 dependent, we studied *casp1*$^{-/-}$ mice. *casp1*$^{-/-}$ and WT mice showed a statistically significant difference in the extent of demyelination as measured by LFB (Fig. 2.4a) and in the number of mature oligodendrocyte as detected by GSTπ immunostaining after cuprizone treatment (Fig. 2.4b). c*asp1*$^{-/-}$ mice also showed delayed microglial infiltration and astrogliosis when compared to WT controls (Fig. 2.4c and d).

These results suggest that the phenotype of *casp1*$^{-/-}$ mice is similar to mice deficient in the *Nlrp3* gene.

The role of IL-18 in demyelination and neuroinflammation

Age-matched untreated (0 Wk) *IL-18* $^{-/-}$ mice and C57BL/6 WT controls showed no difference in numbers of microglia and astrocytes at the corpus callosum (Fig 2.5c-d). At 3weeks of cuprizone treatment there was progressive and significant reduction ($p< 0.05$) in microglial infiltration in *IL-18* $^{-/-}$ mice relative to WT controls (Fig. 2.5e). Similarly, there was an overall trend of reduced astrogliosis in the *IL-18* $^{-/-}$ mice at week 3. After 4 and 5 weeks of cuprizone treatment there was no difference in microglial accumulation and astrogliosis between *IL-18* $^{-/-}$ and C57BL/6 controls (Fig. 2.5e-f). To study the role of IL-18 in demyelination we utilized staining for myelin and mature ODGs. WT mice showed significant demyelination initiating at the 3 week time point and continuing to the end of the study at the 5 week time point (Fig 2.5b). *IL-18* $^{-/-}$ mice showed a significant delay in demyelination at the 3 week time point when compared to WT controls (Fig 2.5b). Further verification with GSTπ , a marker of mature ODG population showed that prior to cuprizone treatment (0 Wk) *IL-18* $^{-/-}$ mice and C57BL/6 controls showed no difference in mature ODG populations at the corpus callosum as shown in Fig. 2.5c. At 3 weeks of cuprizone treatment, the reduction of mature ODGs was attenuated in *IL-18* $^{-/-}$ mice relative to C57BL/6 controls. A quantitation of the composite data is shown in Fig. 2.5d. After 4 and 5 weeks of cuprizone treatment, there was no difference in demyelination and mature ODG death between *IL-18* $^{-/-}$ and C57BL/6 control mice (Fig. 2.5d) indicating that IL-18 delayed demyelination but did not obviate this process.

Cuprizone-induced microglial accumulation and astrogliosis but not demyelination is dependent on P2X$_7$R

ATP mediated activation of P2X$_7$R, a membrane associated ATP-gated ion channel, has been linked to the activation of the NLRP3 inflammasome and consequently to the activation of caspase-1 and IL-1β release (9). To test if cuprizone-induced neuroinflammation is dependent on the engagement and activation of P2X$_7$R, we examined P2X$_7$R$^{-/-}$ mice (186). Demyelination, mature oligodendrocyte number, microglial infiltration and astrogliosis were studied in the cuprizone model as described earlier. *P2X$_7$R$^{-/-}$* and WT controls showed no difference in the kinetics or extent of demyelination or mature oligodendrocyte depletion (Fig. 2.6a and b). However, *P2X$_7$R$^{-/-}$* mice showed significantly reduced microglial infiltration and astrogliosis (Fig. 2.6c and d, P=0.005 and P <0.05 respectively). These results indicate that P2X$_7$R is involved in the inflammatory response observed in the cuprizone model, but not with the demyelination process.

Myelin phagocytosis is enhanced in *Nlrp3*$^{-/-}$ macrophages

The data presented thus far suggest that NLRP3, caspase-1 and P2X$_7$R all exacerbate the extent of inflammation as measured by microglial activation and astrogliosis. However, NLRP3 and caspase-1 also mediate a function that is distinguishable from IL-1β and P2X$_7$R in the eventual loss of myelin and mature oligodendrocyte numbers. Microglia/macrophages and astrocytes are active sensors of the CNS milieu where they sample their environment by highly mobile processes (such as filopodia) (183). Microglia sense their environments through surface receptors or intracellular sensors after phagocytosis. During demyelination,

microglia are responsible for several proinflammatory as well as anti-inflammatory roles, one of the most important being the removal of myelin debris by phagocytosis (184, 187). Removal of myelin debris is critical for the resolution of inflammation, death of oligodendrocytes and recruitment of oligodendrocyte progenitors for remyelination (135, 184). To investigate the role of NLRP3 in myelin phagocytosis, macrophages were isolated from WT, *Nlrp3*$^{-/-}$ and *casp1*$^{-/-}$ mice. We first established conditions for the phagocytosis of latex beads, bacteria and myelin. A schematic for the experimental design is provided in Fig 2.7. Macrophages from C57BL/6 mice readily phagocytized fluorescent latex beads (Fig. 2.8a, second row). Treatment with cytochalasin D (cytD), a known inhibitor of phagocytosis, was used as a negative control for all treatment groups (Fig. 2.8a; also Fig. 2.10c). Similarly, these cells readily phagocytized *E. coli* (Fig. 2.8a, fourth and fifth rows) and myelin (Fig. 2.8a, bottom two rows). Myelin phagocytosis was studied by incubating macrophages with myelin that was labeled with the fluorescent carbocyanine lipophilic dye 1, 1'-dioctadecyl-3, 3, 3', 3'-tetramethylindocarbocyanine perchlorate (DiI). To explore if loss of the *Nlrp3* gene affected phagocytosis, macrophages prepared from WT controls, *Nlrp3*$^{-/-}$ and *casp1*$^{-/-}$ were incubated with beads, *E. coli* or DiI-labeled myelin (Figs. 2.8b-d respectively) for 0, 30, 60 and 120 min. Internalization was measured over time by flow cytometry. *Nlrp3*$^{-/-}$, *casp1*$^{-/-}$ and WT cells phagocytized beads or bacteria to a comparable extent with similar kinetics profiles (Figs. 2.8b and c). In contrast, the internalization of DiI-labeled myelin was greatly increased in *Nlrp3*$^{-/-}$ mice at all three time points when compared to control cells (Fig. 2.8d). Myelin phagocytosis by *casp1*$^{-/-}$ macrophages was also enhanced at two time points but not at the last time point. These findings suggest that NLRP3 and caspase-1 negatively impacts myelin phagocytosis which is important for myelin clearance. An examination of *P2X*$_7$*R*$^{-/-}$

cells did not show such a decrease of myelin phagocytosis (not shown), thus providing a mechanism to explain how NLRP3 and caspase-1 but not $P2X_7R$ exacerbate CNS disease outcome via a new pathway.

Role of NLRP3 in remyelination

Regulation of oligodendrogenesis by progenitors is a potential therapeutic intervention for the functional loss after demyelination in MS. Previous studies in the cuprizone model have shown that; 1) remyelination is dramatically reduced in *IL-1β*$^{-/-}$ mice(165), 2) IL-1β regulates remyelination via regulation of IGF-1 which is critical for conversion of ODG progenitors to mature ODGs (165, 188) 3)Transgenic mice expressing IGF1 constitutively have reduced mature ODG death by apoptosis (166, 167). We hypothesized that NLRP3 via its regulation of IL-1β processing and consequently IGF-1 may regulate oligodendrogenesis and remyelination. Our data with *Nlrp3*$^{-/-}$ mice during remyelination (8, 10 and 12 week time points) indicate that remyelination remains unchanged relative to C57Bl/6 controls by GST pi and LFB/PAS staining, and TEM analysis (Fig 2.9).

2.5 DISCUSSION

The NLR genes, particularly those associated with the inflammasome function, have secured much interest as sensors of pathogen associated molecular patterns (PAMPs) as well as damage-associated molecular patterns (DAMPs); however, their roles in CNS inflammatory disorders have not been extensively studied (9, 10, 182). In this report we provide evidence that NLRP3 has a role in regulating neuroinflammation and demyelination in a mouse model of cuprizone-induced demyelination. However the outcome is much more complex than anticipated. We found that one of the end products of the inflammasome, namely IL-1β, has no role in any of the pathologic events that were investigated. Conventional inflammasome components including NLRP3, caspase-1 and $P2X_7R$ all exacerbated inflammatory readouts such as microglial accumulation and astrogliosis, but only NLRP3 and caspase-1 enhanced demyelination and accelerated the loss of mature oligodendrocytes. Additionally, a cell-based investigation indicates that NLRP3 and caspase-1 decreased the capability of macrophages to phagocytose and therefore clear myelin debris. These data reveal a novel and important role for NLRP3 that has not been appreciated previously.

NLRP3 is known for its classic role in the formation of a multi-protein complex with ASC and pro-caspase-1 that is critical for caspase-1 cleavage and maturation, which in turn is important for the processing of pro-IL-1β/IL-18 to mature IL-1β/IL-18. In the CNS, IL-1β is released primarily by microglia and macrophages (165). IL-1β promotes leukocyte infiltration by inducing expression of many cytokines, chemokines and adhesion molecules (189). The release of IL-1β also mobilizes neutrophils and other immune cells to aid in resolving infections and promoting wound healing. Chronic release of IL-1β is detrimental as

it can contribute to skin rashes, inflammatory arthritis, and systemic fever (164). For this reason, IL-1β production is tightly regulated at the levels of transcription, translation and release. Previous studies examining the role of IL-1β in neuroinflammation have not yielded consistent findings. IL-1β levels in the cerebrospinal fluid (CSF) of MS patients correlate with disease susceptibility, severity and progression (160, 161). IL-1β immunoreactivity has been found in activated microglia and macrophages during EAE in rats (162). Treatment with either soluble IL-1 receptor (sIL-1R) or IL-1 receptor antagonist (IL-1Ra) reduce clinical signs of EAE in rats (163, 190). IL-1β is cytotoxic to mature oligodendrocytes both *in vivo* and *in vitro*, while stimulating proliferation of both microglia and astrocytes (191). However, *IL-1β*$^{-/-}$ mice also display delayed remyelination indicating a reparative role of IL-1β (165). Our study of *IL-1β*$^{-/-}$ mice in the cuprizone model showed no differences in demyelination, microglial infiltration, astrogliosis or mature oligodendrocyte death after 0, 3, and 4 weeks of cuprizone treatment. This indicates that the demyelination observed in the cuprizone model is IL-1β independent even though IL-1β levels increase concurrent with inflammatory cell infiltration during demyelination (165).

Since *IL-1β*$^{-/-}$ mice did not replicate the demyelination as seen in *Nlrp3*$^{-/-}$ mice we explored the role of caspase-1 and IL-18 in demyelination. Caspase-1 has been implicated in both human and mouse neuroinflammation. Caspase-1 levels are significantly increased in peripheral blood mononuclear cells from MS patients (44). Moreover, caspase-1 is known to contribute to the pathology of EAE (45, 46). Our studies with *casp1*$^{-/-}$ mice showed delayed microglial infiltration, astrogliosis, reduction in mature oligodendrocyte depletion and a delay in demyelination.

IL-18 is an 18kDa member of the IL-1 family of cytokines. IL-18 is produced by several immune and non-immune cells including monocytes, macrophages, splenocytes, keratinocytes, microglia, macrophages and astrocytes (47-49). In the CNS, IL-18 induces microglial production of proinflammatory cytokines such as IL-1β and TNFα and matrix metalloproteinases (MMPs). Extravasation of polymorphonuclear leukocytes (PMNs) and monocytes/macrophages is amplified by IL-18 dependent upregulation of intercellular adhesion molecule-1 (ICAM-1) on endothelial cells. IL-18 levels are elevated in demyelinating cerebral lesions of MS patients (192-194). Moreover, expression of IL-18 and its receptor on oligodendrocytes is greater in brain tissue from patients with active MS than in patients with silent MS or from neuropathologically normal subjects (195). In experimental autoimmune encephalomyelitis (EAE) a murine model of MS in which the induction of myelin basic protein (MBP)-specific $CD4^+$ T cells secreting cytokines, particularly IFN-γ and TNF-α, results in limb paralysis, elevated IL-18 mRNA is seen in the CNS of EAE rats at onset and during the disease (196, 197). However, EAE studies with mice deficient in IL-18 (*IL-18*$^{-/-}$) remain controversial, while Shi *et al.*, reported that *IL-18*$^{-/-}$ mice are resistant to EAE (198), Gutcher *et al.*, reported that *IL-18*$^{-/-}$ mice are susceptible to EAE but IL-18 receptor α deficient mice (*IL-18Rα*$^{-/-}$) are resistant to EAE indicating the role of a ligand other than IL-18 acting via IL-18Rα to cause EAE (199). *IL-18*$^{-/-}$ mice replicated the data obtained with *Nlrp3*$^{-/-}$ mice at the 3 week time point of demyelination.

Several studies have shown that caspase-1 has numerous targets beside IL-1β and IL-18, with more than seventy substrates (18, 19). The above results led us to explore mechanisms mediated by NLRP3 other than those mediated by loss of IL-1β. One possible mechanism is the role of NLRP3 in myelin phagocytosis. This idea is largely stimulated by

the role reported for TLRs in phagocytosis, although we appreciate the controversy regarding those findings (200-202). Our data suggest that *Nlrp3*$^{-/-}$ and *casp1*$^{-/-}$ macrophages show an increased ability to phagocytose myelin debris, but not latex beads nor bacteria. This finding is important as it reflects a novel function for the NLRP3 protein. Myelin phagocytosis is an important component of the pathology observed in both EAE and MS patients. A prevailing model supported by data considers that clearance of myelin debris by macrophages and microglia is central to the repair mechanisms that follow demyelination in both central and peripheral nervous system diseases (136, 138, 177, 203, 204). Myelin debris can activate the complement system to form membrane attack complexes that disintegrate intact myelin (139). Moreover, myelin debris impairs remyelination in the adult rat CNS by inhibiting oligodendrocyte precursor cell differentiation (135). Therefore, myelin debris removal is critical for resolution of demyelination and for creating a pro-regenerative environment after demyelination. We provide evidence that bone marrow derived macrophages from *Nlrp3*$^{-/-}$ and *casp1*$^{-/-}$ mice have increased myelin phagocytosis as compared to WT. This corroborates our *in vivo* data with *Nlrp3*$^{-/-}$ and *casp1*$^{-/-}$ mice that showed delayed demyelination. Thus, *Nlrp3*$^{-/-}$ and *casp1*$^{-/-}$ mice show an efficient removal of myelin debris which affects demyelination, myelin regeneration and oligodendrocyte recovery. This implicates a new mechanism by which NLRP3 and caspase-1 might exacerbate neurodegeneration *in vivo*.

It remains unclear how NLRP3 exerts its effects on phagocytosis. There are several receptor complexes that are involved in myelin phagocytosis including scavenger receptors I and II (SR-A I/II) (143, 145), complement receptor 3 (CR-3), galectin-3 (144) and the Fc gamma receptor (FcγR) (205). It is possible NLRP3 affects any, some or all of these receptors by affecting their expression or signal transduction pathways required for optimal

myelin phagocytosis. It is intriguing that NLRP3 does not negatively affect the phagocytosis of bacteria or latex beads. This may have physiologic implications, since key host responses to bacterial infection are the uptake of bacteria by macrophages and the resultant production of IL-1β. Thus it would be counterproductive if NLRP3, a main route by which IL-1β maturation occurs to combat microbes, would then negate anti-bacterial responses by inhibiting bacterial phagocytosis. Instead our data show that NLRP3 only affects the phagocytosis of myelin debris but not of bacteria, consistent with the anti-bacterial role of NLRP3.

The endogenous triggers of NLRP3 activation in the CNS and in the cuprizone-induced model of demyelination remain undescribed. It is known that cell death at the site of inflammation or injury can cause increases of local ATP concentration to ranges of 1-10mM due to the release of cytoplasmic stores (123, 206). Unlike other P2X receptors, $P2X_7Rs$ are activated at concentrations of >1mM. Continuous ligation of $P2X_7R$ can lead to cell death by the formation of large pores in the cell membrane (128). These pores are formed by a $P2X_7R$ associated protein, pannexin-1. Recent research utilizing macrophages from *Nlrp3*$^{-/-}$ and C57BL/6 mice demonstrated that pannexin-1 is critical for caspase-1 activation and IL-1β secretion in LPS-stimulated macrophages pulsed with ATP (128, 129). In addition, $P2X_7R$ deficient (*P2X*$_7$*R*$^{-/-}$) mice show suppression of EAE (130). Thus we tested the hypothesis that ATP released from cuprizone-induced apoptosis within oligodendrocytes might initiate NLRP3 inflammasome activation and propagation of demyelination. However, our results with *P2X*$_7$*R*$^{-/-}$ mice showed modestly delayed microglial infiltration and astrogliosis, but no effect on demyelination or oligodendrocyte numbers. These results suggest that $P2X_7R$ contributes to neuroinflammation, but not demyelination, in a modest way. Thus activation

of $P2X_7R$ does not contribute to *in vivo* loss of oligodendrocytes in the cuprizone-induced model of demyelination.

In summary, the dual roles of NLRP3 in exacerbating neuroinflammation and inhibiting myelin debris clearance, along with a lack of its role in remyelination indicate that inhibition of NLRP3 may prove to be a valuable therapeutic approach for demyelinating diseases such as MS. The results show that the neuroinflammatory component of the disease model is mediated by an NLRP3-, caspase-1- IL-18- and $P2X_7R$-dependent pathway. However, the clearance of myelin debris is limited to NLRP3 and caspase-1. This finding has broad implications for the clearance of CNS cellular debris in other acute and chronic degenerative diseases, including amyloid-β in Alzheimer's disease, myelin in mechanical injury involving axonal transection and in Guillain-Barré syndrome, cell debris in stroke, and dead synapses plus retinal ganglion cells in glaucoma and aging (184).

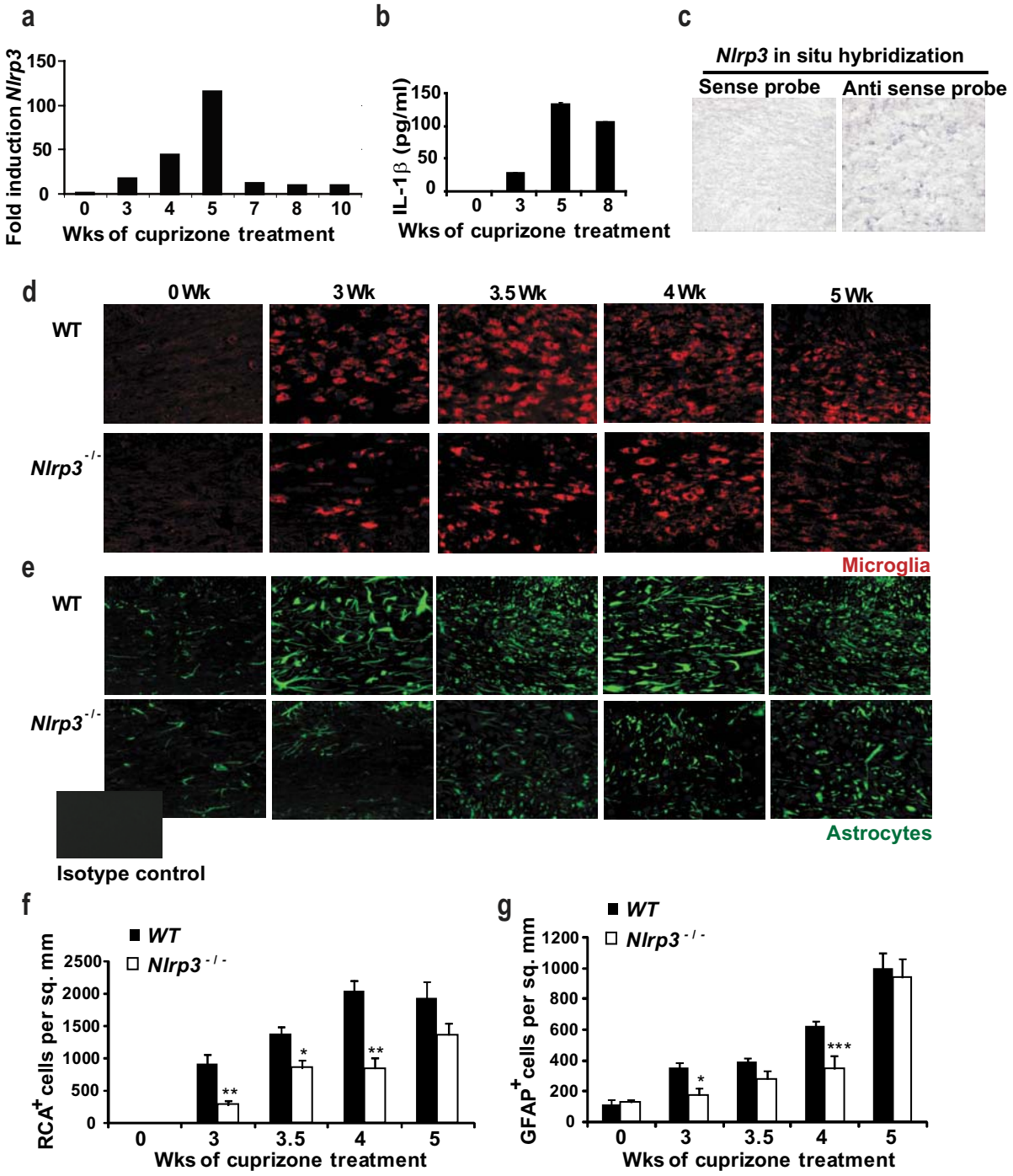
a
Fold induction Nlrp3
150
100
50
0
0 3 4 5 7 8 10
Wks of cuprizone treatment
b
IL-1β (pg/ml)
150
100
50
0
0 3 5 8
Wks of cuprizone treatment
c
Nlrp3 in situ hybridization
Sense probe
Anti sense probe
d
0 Wk
3 Wk
3.5 Wk
4 Wk
5 Wk
WT
Nlrp3 -/-
Microglia
e
WT
Nlrp3 -/-
Astrocytes
Isotype control
f
WT
Nlrp3 -/-
RCA+ cells per sq. mm
2500
2000
1500
1000
500
0
0 3 3.5 4 5
Wks of cuprizone treatment
g
WT
Nlrp3 -/-
GFAP+ cells per sq. mm
1200
1000
800
600
400
200
0
0 3 3.5 4 5
Wks of cuprizone treatment

Figure 2.1- Increases in NLRP3 expression coincide with peak disease symptoms in the cuprizone model. a. *Nlrp3* mRNA increases during cuprizone-induced demyelination. *Nlrp3* transcript was detected by real time PCR and the quantity at 0 Wk set to 1. *Nlrp3* mRNA increased progressively reaching a maximum of ~120 fold after 5 weeks of cuprizone treatment concurrent with microglia/macrophage recruitment. **b.** Increase in IL-1β release is concurrent with the increase in *Nlrp3* expression during demyelination. IL-1β release was measured by ELISA. **c.** *Nlrp3* is expressed in the adult mouse brain. *Nlrp3* RNA was detected by *in situ* hybridization. **d.** Microglial recruitment to the corpus callosum was reduced in $Nlrp3^{-/-}$ mice. Microglia were detected by RCA lectin staining (red). DAPI was used to label nuclei (blue). **e.** Astrogliosis was reduced in $Nlrp3^{-/-}$ mice. GFAP (green) was used to detect astrocyte accumulation in the corpus callosum. Inset shows isotype control for GFAP antibody**.** RCA^{+} or $GFAP^{+}$ cells with an observable DAPI stained nucleus were counted blindly twice. Cell counts are averages of between 9 and 14 mice per time point. **f.** Microglial infiltration was quantitated and found to be significantly reduced in $Nlrp3^{-/-}$ mice (white bars) during demyelination (P= 0.02 at 3 Wks, P= 0.05 at 3.5 Wks, P= 0.01 at 4 Wks). **g.** Astrocyte accumulation was quantitated and found to be significantly reduced in $Nlrp3^{-/-}$ mice during demyelination (P=0.03 at 3 Wks, P=0.001 at 4 Wks). In **f-g,** *P< 0.05, **P<0.01; n=9-14; error bars, s.e.m.

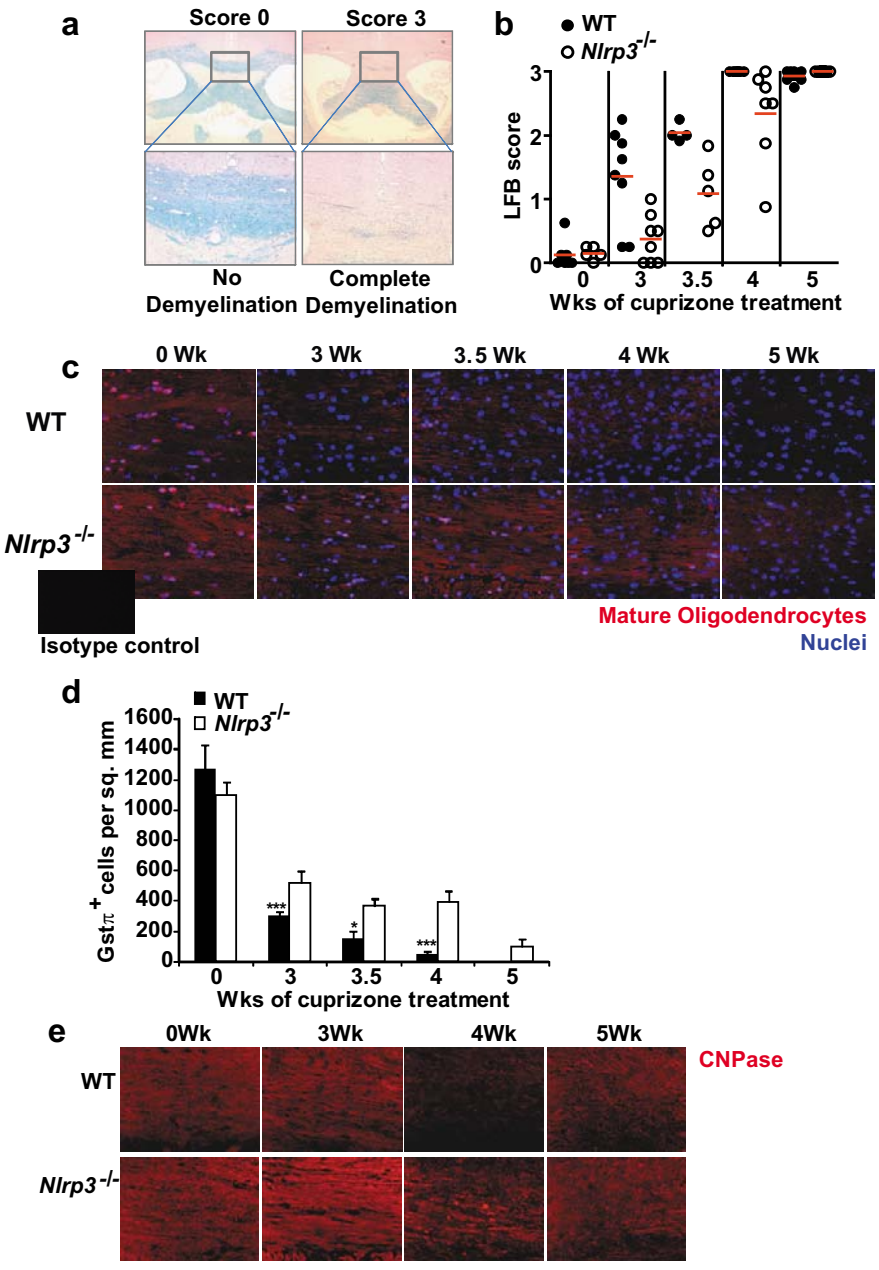
a
Score 0
Score 3
No Demyelination
Complete Demyelination
b
WT
Nlrp3-/-
LFB score
Wks of cuprizone treatment
c
0 Wk
3 Wk
3.5 Wk
4 Wk
5 Wk
WT
Nlrp3-/-
Isotype control
Mature Oligodendrocytes
Nuclei
d
WT
Nlrp3-/-
Gstπ+ cells per sq. mm
Wks of cuprizone treatment
e
0Wk
3Wk
4Wk
5Wk
WT
Nlrp3-/-
CNPase

Figure 2.2- NLRP3 exacerbates demyelination and mature oligodendrocyte death in the corpus callosum during demyelination. a. The schematic depicts the scale for scoring of demyelination. Each slide was scored by 3 independent blinded readers on a score of 0 (no demyelination) to 3 (complete demyelination). All scores are restricted to the midline corpus callosum (boxed area). **b.** *Nlrp3*$^{-/-}$ mice (open circles) show delayed demyelination as compared to WT controls (filled circles). Demyelination was quantitated by Luxol fast blue (LFB)/ periodic acid schiff's (PAS) staining. Each circle represents the averaged observed LFB score from three readers for one mouse. The mean value of each data set is depicted by a red line. **c.** Mature myelinating oligodendrocytes in the corpus callosum were increased during cuprizone treatment of WT and *Nlrp3*$^{-/-}$ mice as identified with GSTπ staining (red). DAPI was used to label nuclei (blue). Inset shows isotype control. **d.** *Nlrp3*$^{-/-}$ mice (white bar) show a significant delay in the loss of mature oligodendrocytes as compared to WT controls (black bars) (P=0.004 at 3 Wks, P=0.02 at 3.5 Wks and P=0.002 at 4 Wks). Mature oligodendrocyte depletion was quantitated by counting GSTπ^{+} cells that co-localized with a DAPI positive nucleus. Each image was scored twice in a blind manner. Average counts with standard error are depicted here. **e.** CNPase staining of paraffin-embedded 5μm brain sections from *Nlrp3*$^{-/-}$ and WT control mice during demyelination shows delayed loss of myelin in the corpus callosum of *Nlrp3*$^{-/-}$ mice. Representative images for 9 - 14 mice per time point are shown. In **d,** *P< 0.05, ***P<0.005; error bars, s.e.m.

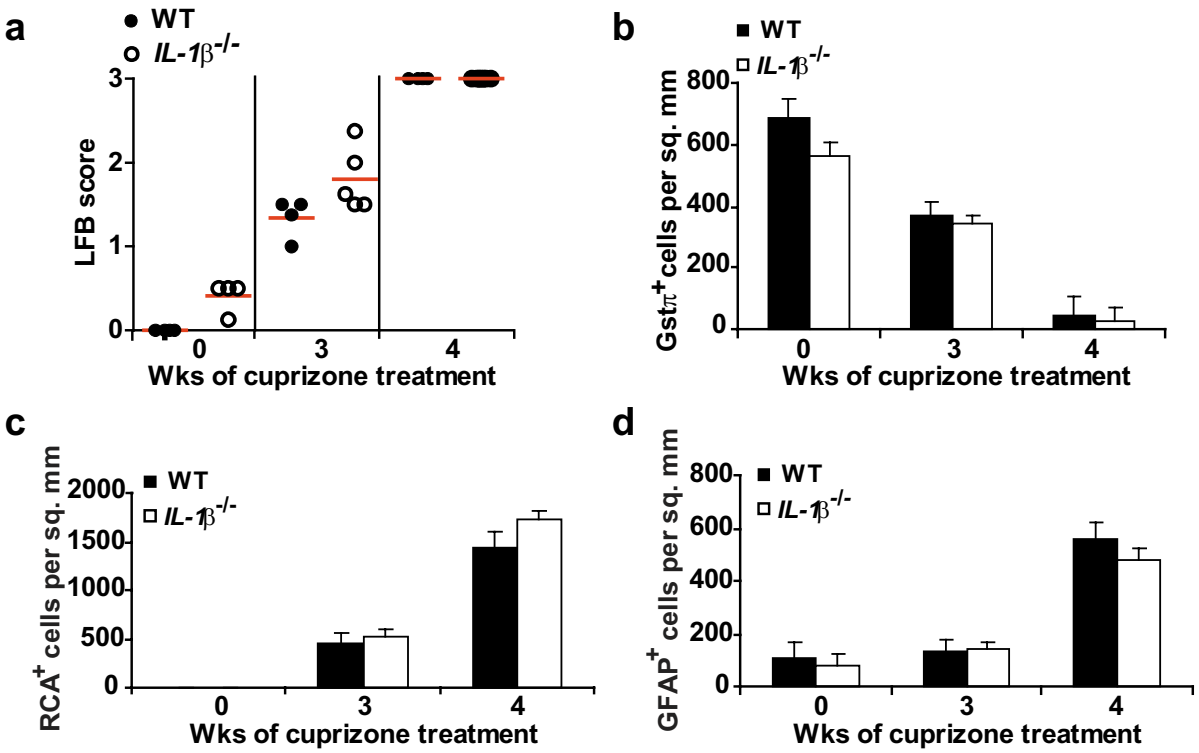
a
WT
IL-1β-/-
LFB score
Wks of cuprizone treatment
b
WT
IL-1β-/-
Gstπ+cells per sq. mm
Wks of cuprizone treatment
c
WT
IL-1β-/-
RCA+ cells per sq. mm
Wks of cuprizone treatment
d
WT
IL-1β-/-
GFAP+ cells per sq. mm
Wks of cuprizone treatment

Figure 2.3- IL-1β is not required in demyelination, astrogliosis, microglial infiltration and mature oligodendrocyte depletion. a. *IL-1β*$^{-/-}$ mice exhibit no difference in demyelination. Each circle represents the averaged observed LFB score from three readers for one mouse. Demyelination was quantitated by Luxol fast blue (LFB)/ periodic acid schiff's (PAS) staining. *IL-1β*$^{-/-}$ mice (open circles) show no difference in demyelination as compared to WT controls (filled circles). **b.** *IL-1β*$^{-/-}$ mice (white bars) exhibit no difference in mature oligodendrocyte number as compared to age-matched WT controls (black bars) (*P*=0.29 at 3 Wks, and *P*=0.16 at 4 Wks). Mature oligodendrocytes were measured by the GSTπ^+ stain at the corpus callosum. **c.** *IL-1β*$^{-/-}$ mice (white bars) exhibit no difference in microglial infiltration as compared to age-matched WT controls (black bars) (*P*=0.56 at 3 Wks, and *P*=0.15 at 4 Wks). Microglia were measured by RCA$^+$ staining at the corpus callosum after 3 and 4 wks of cuprizone treatment. **d.** *IL-1β*$^{-/-}$ mice (white bars) exhibit no difference in astrogliosis when compared to age-matched WT controls (black bars) (*P*=0.80 at 3 Wks, and *P*=0.26 at 4 Wks). Astrocytes were measured by the GFAP$^+$ stain at the corpus callosum after 3 and 4Wks of cuprizone treatment. GFAP was used to detect astrocyte accumulation in the corpus callosum. RCA$^+$ or GFAP$^+$ cells with an observable DAPI stained nucleus were counted blindly twice. Cell counts for b, c and d are averages of between 6 and 10 mice per time point.

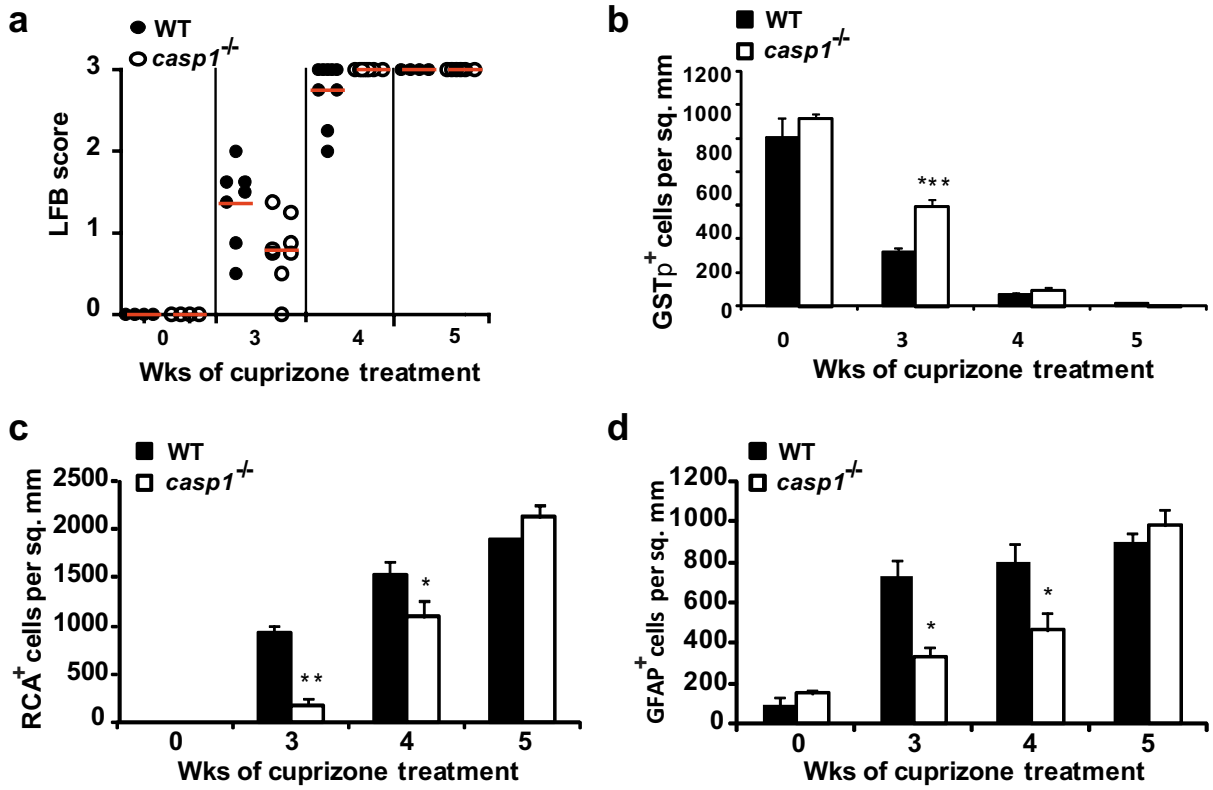
a
WT
casp1-/-
LFB score
Wks of cuprizone treatment
b
WT
casp1-/-
GSTp+ cells per sq. mm
***
Wks of cuprizone treatment
c
WT
casp1-/-
RCA+ cells per sq. mm
**
*
Wks of cuprizone treatment
d
WT
casp1-/-
GFAP+ cells per sq. mm
*
*
Wks of cuprizone treatment

Figure 2.4- Roles of caspase-1 in demyelination, mature oligodendrocyte depletion, microglial infiltration and astrogliosis. a. *casp1*$^{-/-}$ (open circles) and age-matched WT mice (filled circles) exhibit a difference in the extent of demyelination. **b.** *casp1*$^{-/-}$ mice (white bars) and age-matched WT controls (black bars) exhibit a difference in mature oligodendrocyte number (P=0.001 at 3 Wks, P=0.45 at 4 Wks and P=0.39 at 5 Wks). **c.** *casp1*$^{-/-}$ mice (white bars) exhibit reduced microglial infiltration at the corpus callosum when compared to age-matched WT controls (black bars) (P=0.008 at 3 Wks, P=0.05 at 4 Wks and P=0.19 at 5 Wks). **d.** *casp1*$^{-/-}$ mice (white bars) exhibit reduced astrogliosis at the corpus callosum when compared to age-matched WT controls (black bars) (P=0.02 at 3 Wks, P=0.01 at 4 Wks and P=0.37 at 5 Wks). Demyelination was quantitated by Luxol fast blue (LFB)/ periodic acid schiff's (PAS) staining, mature oligodendrocyte by GSTπ, microglia by RCA and astrocytes by GFAP staining as described in Fig. 3. *P< 0.05, **P<0.01, ***P<0.005; error bars, s.e.m. Cell counts for b-d are averages of between 6 and 12 mice per time point.

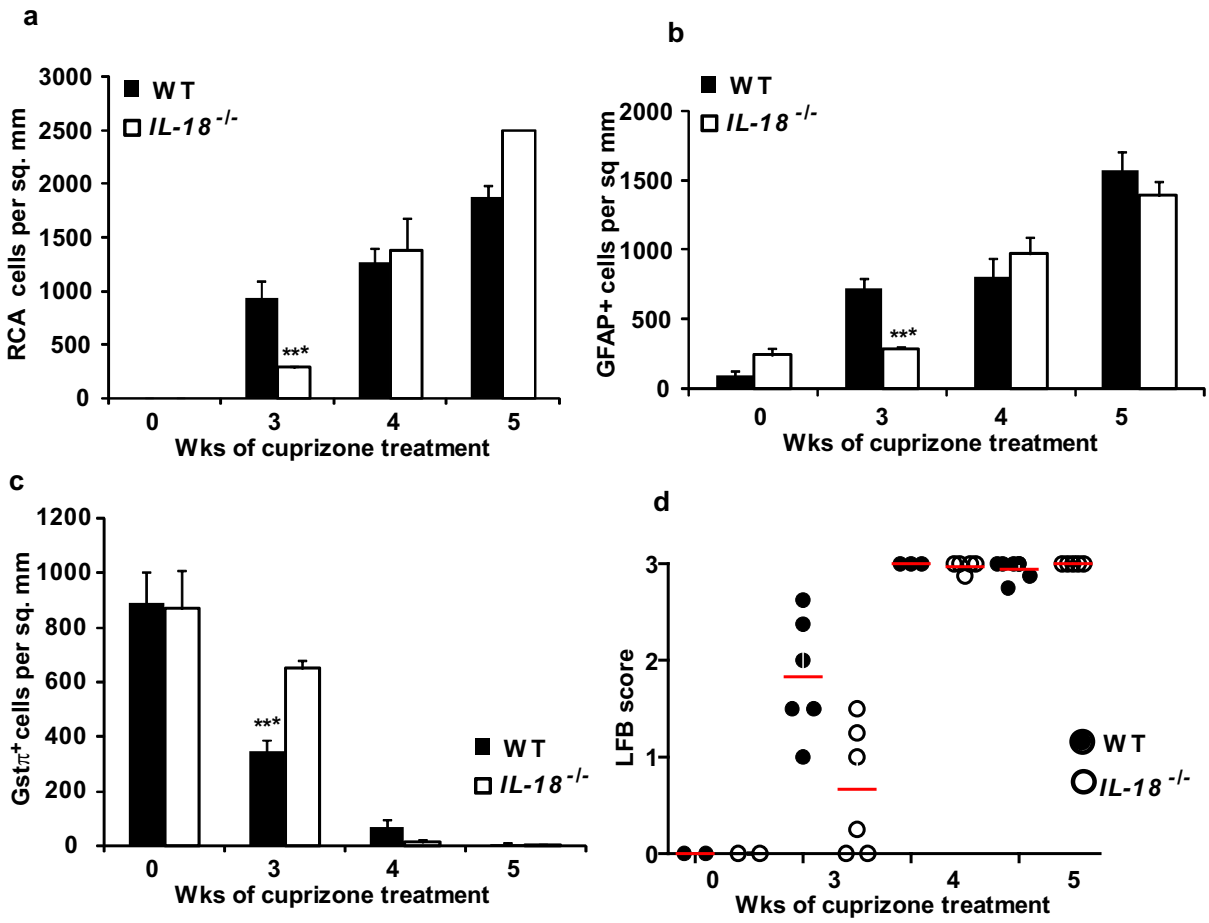
a
RCA cells per sq. mm
3000
2500
2000
1500
1000
500
0
WT
IL-18 -/-
***
0
3
4
5
Wks of cuprizone treatment
b
GFAP+ cells per sq mm
2000
1500
1000
500
0
WT
IL-18 -/-
***
0
3
4
5
Wks of cuprizone treatment
c
GstΠ+cells per sq. mm
1200
1000
800
600
400
200
0
***
WT
IL-18 -/-
0
3
4
5
Wks of cuprizone treatment
d
LFB score
3
2
1
0
WT
IL-18 -/-
0
3
4
5
Wks of cuprizone treatment

Figure 2.5- Roles of IL-18 in demyelination, mature oligodendrocyte depletion, microglial infiltration and astrogliosis. a. *IL-18*$^{-/-}$ mice (white bars) exhibit reduced microglial infiltration at the corpus callosum when compared to age-matched WT controls (black bars) (P=0.008 at 3 Wks). **b.** *IL-18*$^{-/-}$ mice (white bars) exhibit reduced astrogliosis at the corpus callosum when compared to age-matched WT controls (black bars) (P=0.02 at 3 Wks). **c.** *IL-18*$^{-/-}$ mice (white bars) and age-matched WT controls (black bars) exhibit a difference in mature oligodendrocyte number (P=0.001 at 3 Wks). **d.** *IL-18*$^{-/-}$ (open circles) and age-matched WT mice (filled circles) exhibit a difference in the extent of demyelination. Demyelination was quantitated by Luxol fast blue (LFB)/ periodic acid schiff's (PAS) staining, mature oligodendrocyte by GSTπ, microglia by RCA and astrocytes by GFAP staining as described in Fig. 3. *P< 0.05, **P<0.01, ***P<0.005; error bars, s.e.m. Cell counts for b-d are averages of between 6 and 8 mice per time point.

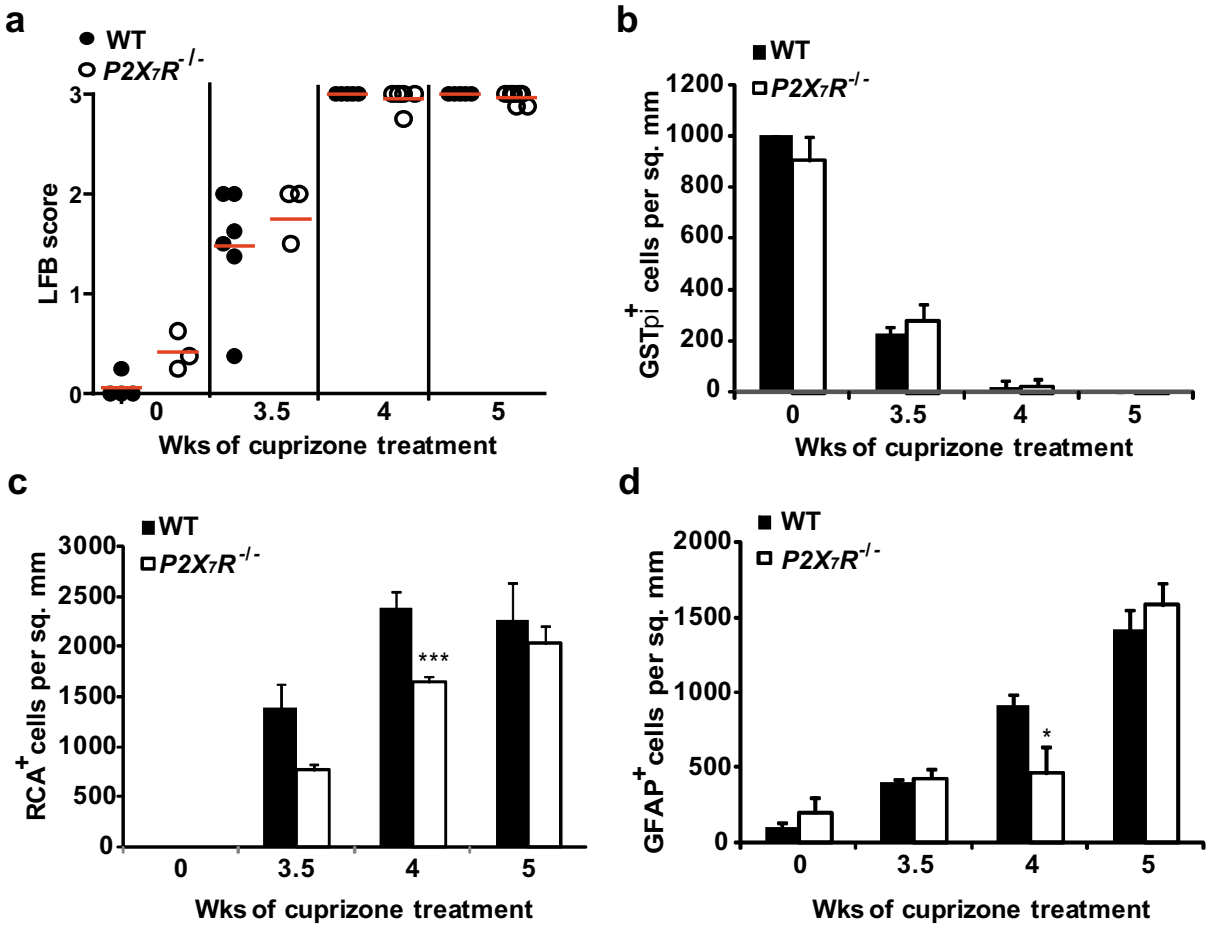
a
WT
P2X7R-/-
LFB score
0
1
2
3
0
3.5
4
5
Wks of cuprizone treatment
b
WT
P2X7R-/-
GSTpi+ cells per sq. mm
0
200
400
600
800
1000
1200
0
3.5
4
5
Wks of cuprizone treatment
c
WT
P2X7R-/-
RCA+ cells per sq. mm
0
500
1000
1500
2000
2500
3000
***
0
3.5
4
5
Wks of cuprizone treatment
d
WT
P2X7R-/-
GFAP+ cells per sq. mm
0
500
1000
1500
2000
*
0
3.5
4
5
Wks of cuprizone treatment

Figure 2.6- Roles of $P2X_7R$ in demyelination, mature oligodendrocyte depletion, microglial infiltration and astrogliosis. **a.** $P2X_7R^{-/-}$ (open circles) and WT mice (filled circles) show no difference in demyelination during the course of cuprizone treatment. **b.** $P2X_7R^{-/-}$ (white bars) and WT (black bars) mice show no difference in mature oligodendrocyte depletion during cuprizone treatment (P=0.43 at 3.5Wk, P=0.93 at 4Wk, P=0.45 at 5Wk). **c.** $P2X_7R^{-/-}$ (white bars) mice show reduced microglial infiltration when compared to WT mice (black bars) (P=0.005 at 4Wk). **d.** $P2X_7R^{-/-}$ mice (white bars) show reduced astrogliosis when compared to WT mice (black bars). LFB/PAS (panel a), GSTπ (panel b), RCA (panel c) and GFAP (panel d) were used to detect myelination, mature oligodendrocyte, microglia and astrocytes in the corpus callosum, respectively as described in Fig. 3. *P< 0.05, **P<0.01, ***P<0.005; error bars, s.e.m. Cell counts for b-d are averages of between 4 and 8 mice per time point.

Ex vivo Phagocytosis Assay Experimental Design

a

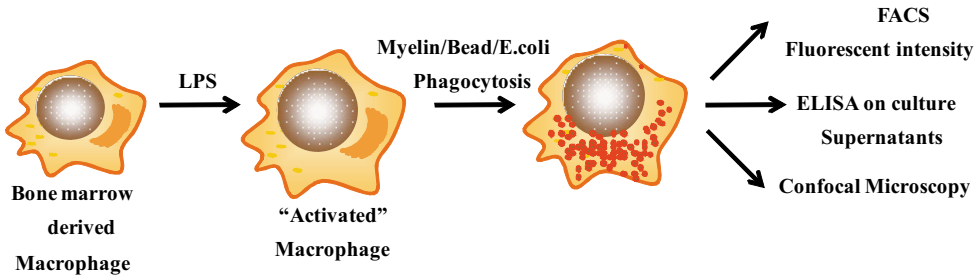

- Myelin extracted from mouse brain and labeled with DiI (20ug/250,000 cells)
- Blue-green Fluorescent latex beads (100:1, beads:cells)
- GFP expressing *E.coli* (100:1, *E.coli*:cells)

Myelin extraction from mouse brain

b

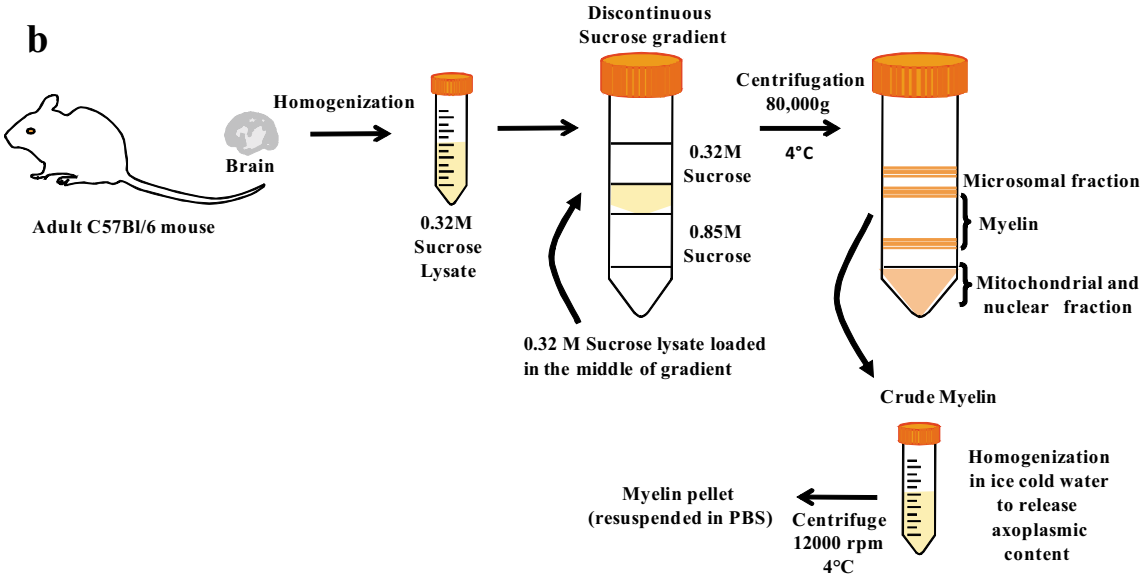

Figure 2.7- Schematic for experimental design of phagocytosis assays and myelin extraction from mouse brain a. *Ex vivo* phagocytosis assay experimental design. Bone marrow derived Macrophages were activated by overnight incubation with LPS. These macrophages were then incubated with fluorescent beads, *E.coli* or myelin. Fluorescent bead, GFP-*E.coli,* and DiI -labeled myelin ingestion was quantitated by FACS and visualized by confocal microscopy. Culture supernatants were used for ELISA. **b.** Schematic for myelin extraction from adult mouse brain. Adult C57Bl/6 mouse brain was homogenized in 0.32M sucrose. This homogenate was loaded in the middle of a discontinuous sucrose density gradient and separated by ultracentrifugation at 80,000g. The resulting crude myelin fraction was homogenized in cold water to release any axoplasmic content. A final centrifugation step resulted in isolation of myelin as a pellet that was resuspended in PBS and labeled with the lipophilic dye DiI.

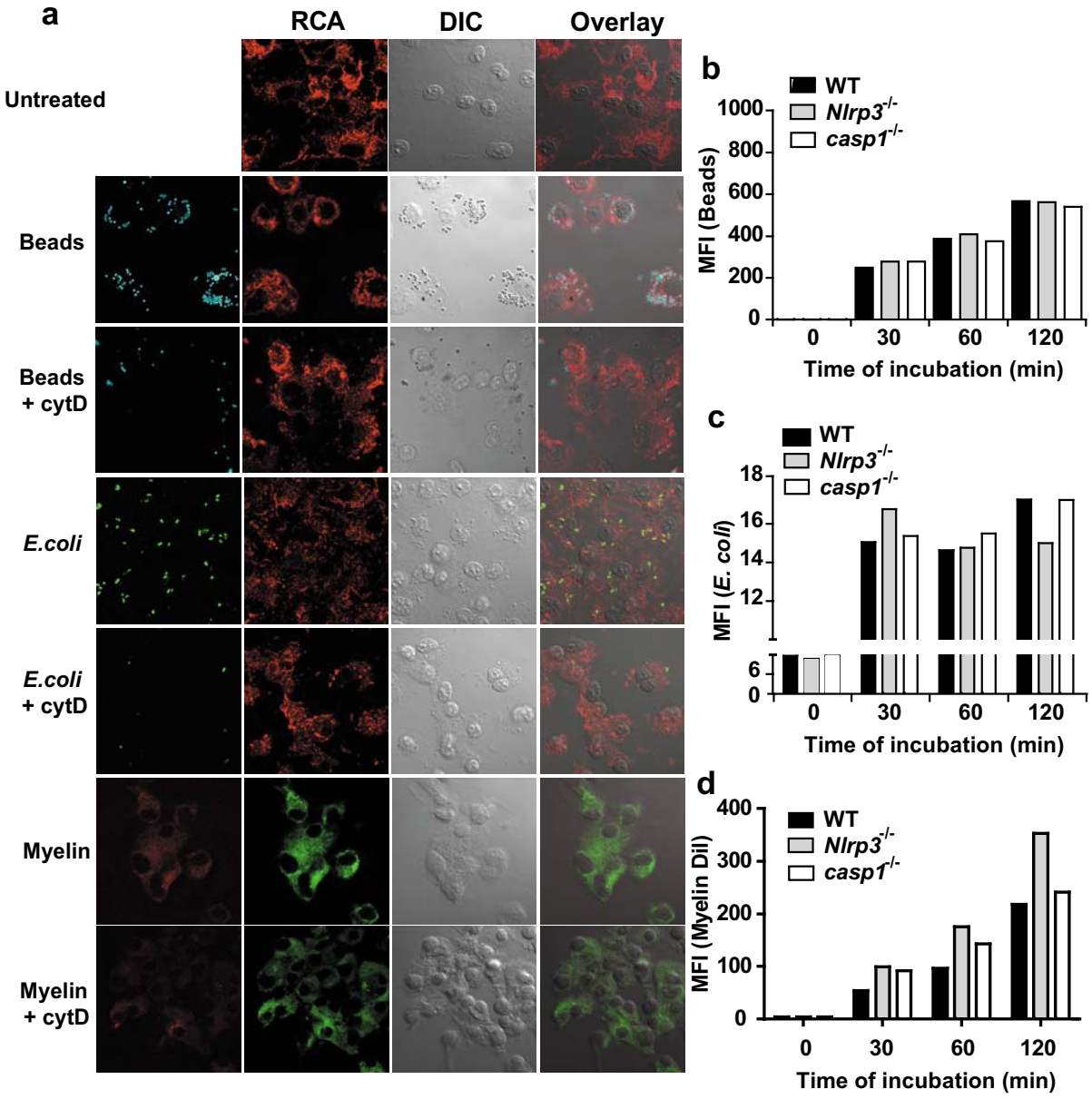
a
RCA
DIC
Overlay
Untreated
Beads
Beads + cytD
E.coli
E.coli + cytD
Myelin
Myelin + cytD
b
WT
Nlrp3-/-
casp1-/-
MFI (Beads)
1000
800
600
400
200
0
0
30
60
120
Time of incubation (min)
c
WT
Nlrp3-/-
casp1-/-
MFI (E. coli)
18
16
14
12
6
0
0
30
60
120
Time of incubation (min)
d
WT
Nlrp3-/-
casp1-/-
MFI (Myelin DiI)
400
300
200
100
0
0
30
60
120
Time of incubation (min)

Figure 2.8- *Nlrp3*$^{-/-}$ and *casp1*$^{-/-}$ macrophages show enhanced myelin phagocytosis. **a.** Macrophages readily phagocytose beads, *E.coli*, and myelin. Fluorescent latex bead, GFP-*E.coli,* and DiI -labeled myelin ingestion was visualized by confocal microscopy. Macrophages were stained with RCA lectin (green in all panels except in *E.coli* where RCA is red). Myelin (red), bead (blue) and *E.coli* (green) phagocytosis is blocked by cytD in the medium, compatible with the process of phagocytosis. **b**. *Nlrp3*$^{-/-}$, *casp1*$^{-/-}$ and WT macrophages exhibit no difference in the phagocytosis of fluorescent latex beads. Primary BMDM were incubated with fluorescent-labeled latex beads for 0, 30, 60 and 120 min. The Mean fluorescent intensity (MFI) of latex beads was measured by flow cytometry. **c.** Phagocytosis of GFP-E.coli by *Nlrp3*$^{-/-}$, *casp1*$^{-/-}$ and WT BMDMs is not different**.** BMDM were analyzed by flow cytometry as described in panel b, except cells were incubated with *E. coli* expressing GFP. **d.** Phagocytosis of fluorescently-labeled myelin is enhanced in *Nlrp3*$^{-/-}$ and *casp1*$^{-/-}$ BMDM when compared to WT BMDMs. BMDM were isolated and analyzed by flow cytometry as described in panel b, except cells were incubated with DiI-labeled myelin. Mean fluorescent intensity (MFI) of DiI-Myelin was measured by flow cytometry. Representative graphs based on 3 experiments each for *E.coli* and beads, and 5 experiments for myelin are shown here.

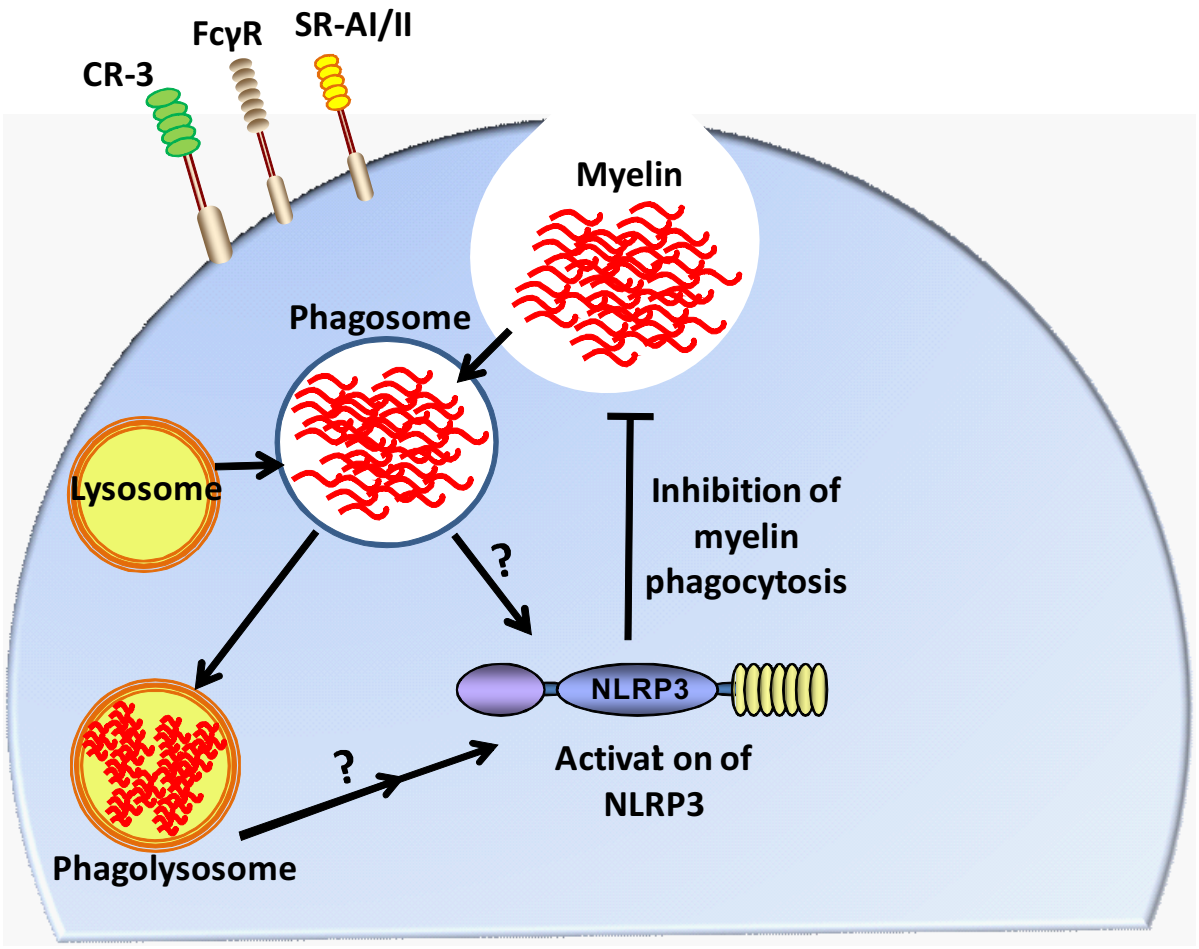
CR-3
FcγR
SR-AI/II
Myelin
Phagosome
Lysosome
Inhibition of
myelin
phagocytosis
?
NLRP3
Activat on of
NLRP3
?
Phagolysosome

Figure 2.9- Hypothetical model for the role of the Nlrp3 inflammasome in myelin phagocytosis. Myelin is phagocytosed by macrophages by multiple surface receptors including the complement receptor (CR-3), Scavenger receptors (SR-A I/II) and the Fc gamma receptor (FcγR). Once internalized via the phagosome, lysosomal enzymes degrade the myelin in the phagolysosme. By an unknown mechanism myelin phagocytosis activates the cytosolic Nlrp3 which inhibits myelin phagocytosis thus exacerbating inflammation (microglial recruitment and astrogliosis) and delaying recruitment of ODG progenitor cells.

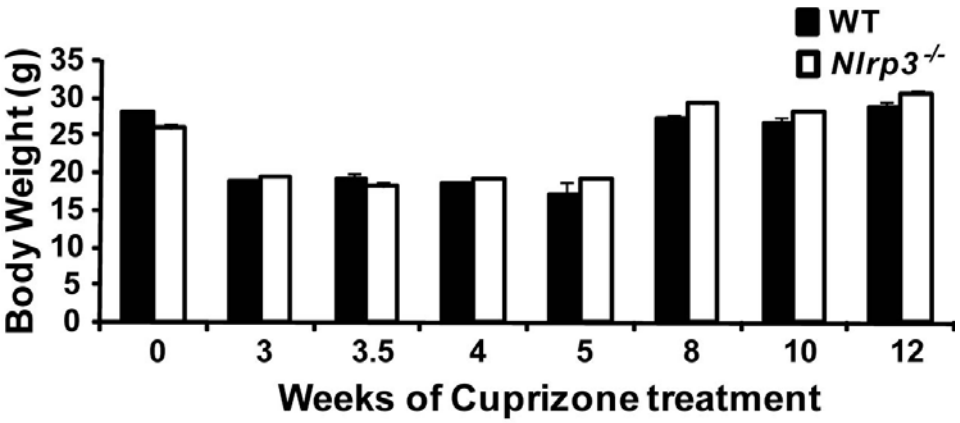
WT
Nlrp3 -/-
Body Weight (g)
35
30
25
20
15
10
5
0
0
3
3.5
4
5
8
10
12
Weeks of Cuprizone treatment

Figure 2.10- No difference in weight of *Nlrp3*$^{-/-}$ and control WT mice during cuprizone induced demyelination. 8-10 weeks old, male, *Nlrp3*$^{-/-}$ and control WT mice were fed 0.2% cuprizone mixed into ground chow *ad libidum* for 6 weeks to induce progressive demyelination. Untreated control mice were maintained on a diet of normal pellet chow. *Nlrp3*$^{-/-}$ and control WT mice showed no difference in weight during cuprizone treatment. Weights (in grams on y axis) are averages of at least 9 and up to 14 mice per time point.

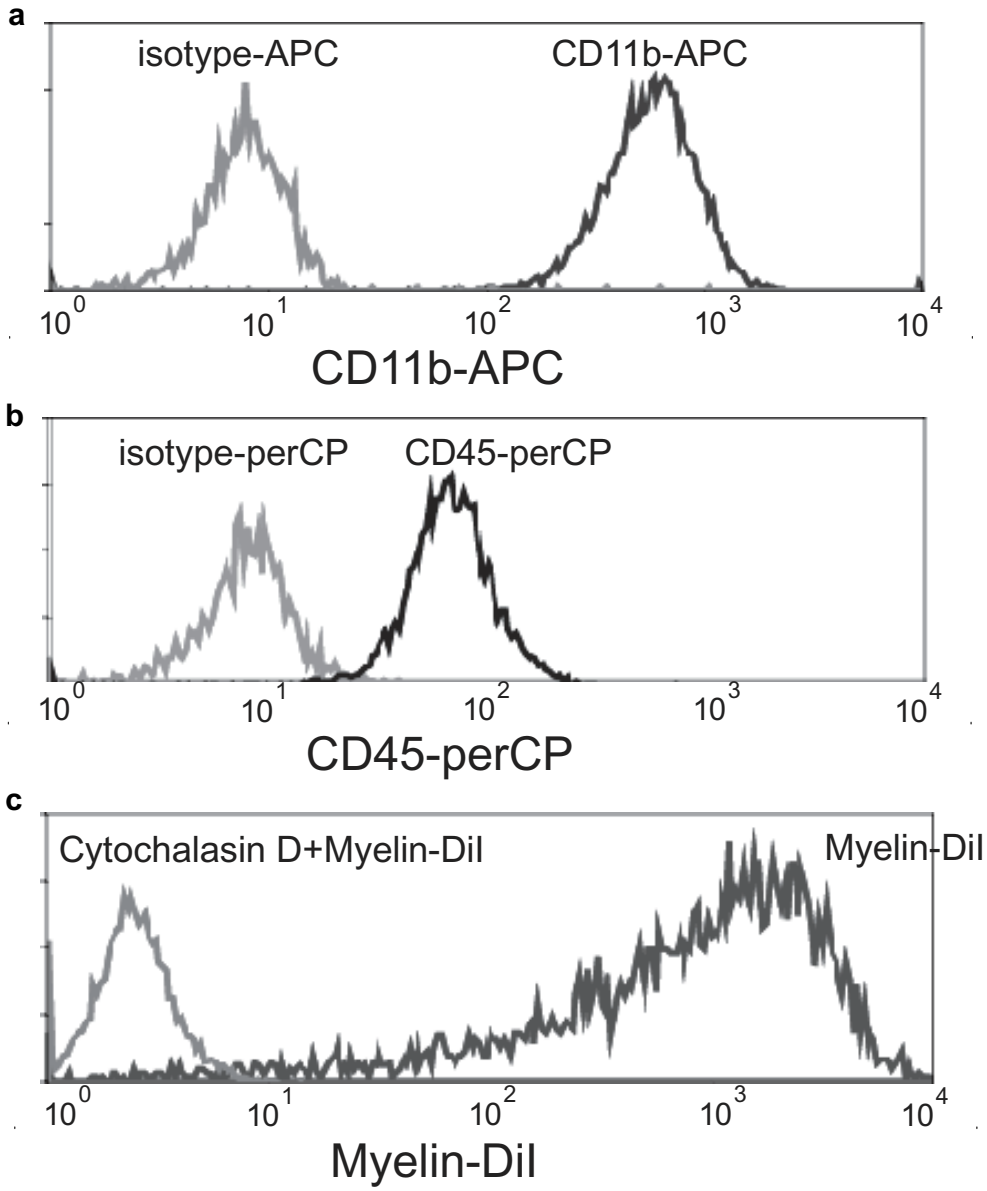
a
isotype-APC
CD11b-APC
10^0
10^1
10^2
10^3
10^4
CD11b-APC
b
isotype-perCP
CD45-perCP
10^0
10^1
10^2
10^3
10^4
CD45-perCP
c
Cytochalasin D+Myelin-DiI
Myelin-DiI
10^0
10^1
10^2
10^3
10^4
Myelin-DiI

Figure 2.11 -Quantitation of macrophage staining with CD11b-APC and CD45-perCP antibodies and myelin phagocytosis by flow cytometry. a. Macrophages stained with CD11b-APC show significantly higher fluorescent staining intensity compared to staining with isotype control antibody conjugated with APC. **b.** Macrophages stained with CD45-perCP show significantly higher fluorescent staining intensity compared to staining with isotype control antibody conjugated with perCP. **c.** Treatment with cytochalasin D inhibited myelin phagocytosis by macrophages leading to significantly decreased fluorescent intensity compared to macrophages that phagocytosed myelin in the absence of cytochalasin D.

a

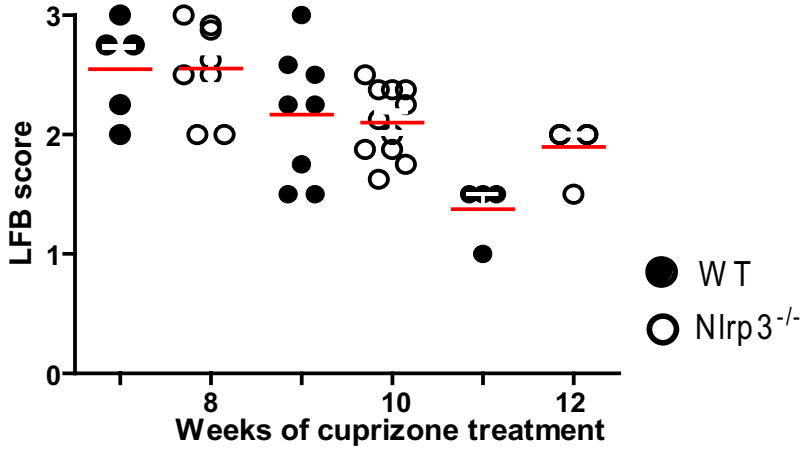
LFB score
3
2
1
0
8
10
12
Weeks of cuprizone treatment
WT
Nlrp3 -/-

b

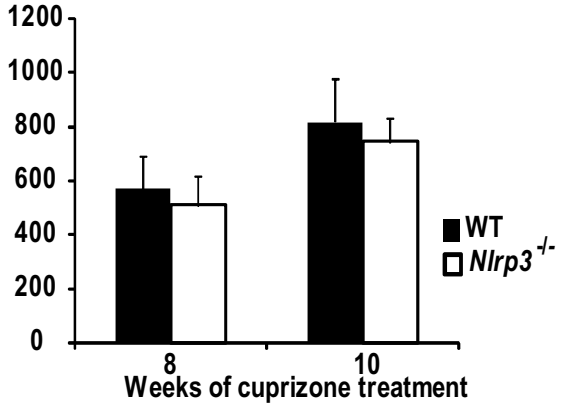
1200
1000
800
600
400
200
0
8
10
Weeks of cuprizone treatment
WT
Nlrp3 -/-

c

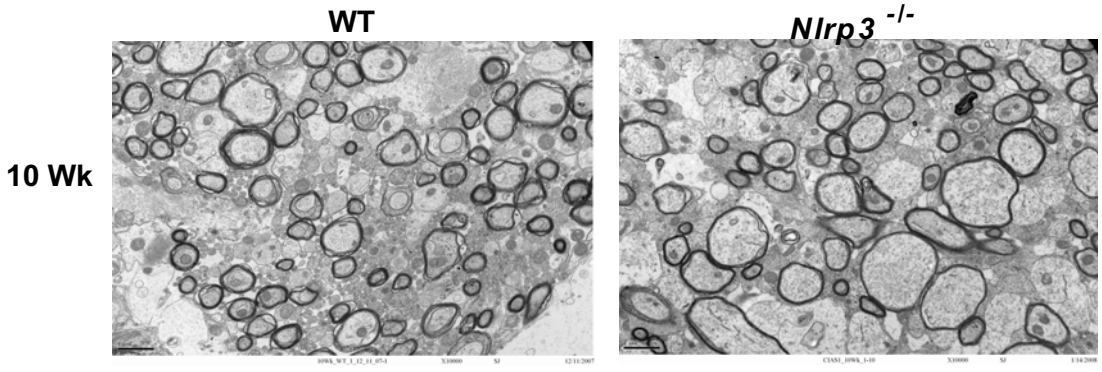
WT
Nlrp3 -/-
10 Wk

Figure 2.13 Remyelination in *Nlrp3*$^{-/-}$ mice remains unchanged

a. *Nlrp3*$^{-/-}$ (open circles) and age-matched WT mice (filled circles) exhibit no difference in the extent of remyelination at the 8, 10 and 12 week time points**. b.** *Nlrp3*$^{-/-}$ (white bars) and age-matched WT mice (filled bars) exhibit no difference in the extent of remyelination at the 8 and 10 week time points**. c.**TEM analysis in *Nlrp3*$^{-/-}$ mice during remyelination indicates that remyelination remains unchanged relative to C57Bl/6 controls at the 10 week time point of remyelination. Remyelination was quantitated by Luxol fast blue (LFB)/ periodic acid schiff's (PAS) staining and mature oligodendrocyte by GSTπ as described earlier.

CHAPTER III

A NOVEL ROLE FOR NLRC4 IN THE REGULATION OF INFLAMMATION, DEMYELINATION AND MYELIN DEBRIS CLEARANCE IN THE CNS

Parts of this chapter have been adapted from Sushmita Jha, Leslie Freeman, Siddharth Y. Srivastava and Jenny P.-Y. Ting, A novel role for the NLR family member NLRC4 in regulation of neuroinflammation and demyelination, Glia, 2009, Manuscript in preparation.

3.1 ABSTRACT

As a continuation of our studies to identify NLR family members involved in neuroinflammation we chose to analyze mice with a genetic deletion of Nlrc4 (*Nlrc4*$^{-/-}$). The NLRC4 protein has a well documented role as a cytosolic sensor of flagellin, flagellated and some non-flagellated pathogens however, it's role in inflammation remains unknown. NLRC4 can associate with procaspase-1 and cause its autocatalytic cleavage to active caspase-1. Caspase-1 in turn can cause cleavage induced maturation of over seventy substrates including the proinflammatory cytokines IL-1β and IL-18.

In this study we demonstrate a previously unknown role of NLRC4 in inflammation, demyelination and myelin debris clearance in a mouse model of cuprizone-induced demyelination. *Nlrc4*$^{-/-}$ mice showed delayed astrogliosis, microglial infiltration, mature oligodendrocyte death and demyelination during cuprizone treatment. These results along with our previous study that showed a role for NLRP3 and caspase-1 in demyelination, neuroinflammation and myelin debris clearance raises the possibility for the existence of multiple pathways upstream of caspase-1 activation in the CNS.

3.2 INTRODUCTION

Neuroinflammation is a component of several diseases including, multiple sclerosis, Parkinson's disease and Alzheimer's disease. NLR family, Caspase Recruitment domain containing 4 (*NLRC4*, also IPAF, CLAN, CARD12) protein is a cytosolic sensor of flagellin, flagellated pathogens such as *Salmonella typhimurium* (4, 5, 26),and *Legionella pneumophila* (3) and non-flagellated pathogens such as *Shigella flexneri* (7) and *Pseudomonas aeruginosa* (32). NLRC4 forms a homo-oligomeric inflammasome with caspase-1 (26). Initial characterization of NLRC4 in human tissues and cell lines demonstrated its direct association with the CARD domain of procaspase-1 through CARD-CARD interactions (40, 41). This interaction can cause autocatalytic processing of procaspase-1 to caspase-1 (40). A constitutively active NLRC4 could cause autocatalytic processing of procaspase-1 leading to caspase-1 dependent apoptosis in transfected cells (40). In macrophages, caspase-1 activation and IL-1β release by cytoplasmic flagellin requires NLRC4 (4, 5, 26).

The role of NLRC4 in inflammation remains unknown. In this study we utilized the cuprizone-induced mouse model of demyelination to evaluate the role of NLRC4 in neuroinflammation. The cuprizone model is an ideal model to study the role of the innate immune system of the CNS in neuroinflammation and demyelination. It exhibits type III and IV MS neuropathology characterized by microglial infiltration and astrogliosis in the absence of T cell infiltrates (147). Demyelination and neuroinflammation are easily induced by administering cuprizone through the chow. The disease follows a predictable time course along with a reproducible pathology involving major nerve tracts such as the corpus callosum and cerebellar peduncles (156). This model also allows for the study of factors that affect inflammation in the CNS that accompany demyelination. Using the cuprizone model, we

studied mice deficient in the gene encoding NLRC4 (*Nlrc4*$^{-/-}$), as a way to examine the role of the NLRC4 in neuroinflammation and demyelination *in vivo*. We found a significant role for the NLRC4 inflammasome pathway in the activation of neuroinflammation, but we also found an additional function for this gene in the clearance of myelin debris.

3.3 MATERIALS AND METHODS

Mice.

Nlrc4 $^{-/-}$ mice were provided by Dr Vishwa Dixit (Genentech), which were further backcrossed to C57BL/6 mice for over nine generations. C57BL/6 mice were purchased from the National Cancer Institute (Bethesda, MD) and Jackson Research Labs (Bar Harbor, ME). All mice were 8-10 weeks old prior to the start of treatment. All animal procedures conducted were approved by the Institutional Animal Care and Use Committee of UNC at Chapel Hill.

Cuprizone treatment.

8-10 weeks old male mice were fed 0.2% cuprizone [oxalic bis (cyclohexylidenehydrazide)] (Aldrich, St. Louis, MI) mixed into ground chow *ad libidum* for 6 weeks to induce progressive demyelination. Untreated control mice were maintained on a diet of normal pellet chow. During cuprizone treatment mice showed lethargic movement, weight loss (Fig. 3.7), ruffled hair and altered gait as described earlier (158, 159).

Tissue preparation.

Mice were deeply anesthetized and intra-cardially perfused with phosphate-buffered saline (PBS) followed by 4% paraformaldehyde (PFA). Brains were removed, post-fixed in PFA, and embedded in paraffin. 5-µm coronal sections were cut at the fornix region of the corpus callosum. 5µm coronal sections were cut at the fornix region of the corpus callosum for immunohistochemistry (IHC). All analyses were restricted to the mid-line corpus callosum as described previously (158, 180, 181).

Staining.

To examine demyelination, paraffin sections were rehydrated through a graded series of alcohol washes and stained with Luxol fast blue-periodic acid-Schiff's base (LFB-PAS; Sigma, St. Louis, MI) as described previously(158, 180, 181). Sections were read by three double-blinded readers and graded on a scale from 0 (complete myelination) to 3 (complete demyelination). Higher scores indicate greater pathology. For the detection of microglia/macrophages, tissue sections were rehydrated and permeabilized with 0.1% Triton/PBS for 20 min at room temperature and then incubated with *Ricinus communis* agglutinin-1 (RCA-1) lectin (1:500, Vector) at 37 °C for 1hr. Only RCA-1^{+} cells with observable 4', 6'-diamidino-2-phenylindole (DAPI) stained nucleus were included in the quantification.

Immunohistochemistry(IHC).

IHC was performed on 5-μm paraffin embedded sections that were deparaffinized and rehydrated through alcohols as described earlier. For the detection of mature oligodendrocytes, the sections were processed by boiling in antigen unmasking solution (1:100, Vector) for 13 min in a microwave. These sections were permeabilized with 0.1% Triton/PBS for 20 min and incubated with 2% normal goat serum in 0.1% triton-PBS for 20 min at room temperature. Subsequently, the sections were incubated with rabbit anti mouse polyclonal antibody anti- GSTπ (1:500, Stressgen) at 4°C overnight. Sections were then washed in PBS and incubated with the appropriate biotinylated antibody against primary antibody (1:100, Vector) and texas red-conjugated avidin (1:500, Vector). The sections were washed and incubated with Alexa Fluor conjugated 594. To detect astrocytes, sections were incubated with 5% normal goat serum in 0.1% triton-PBS for 20 min at room temperature. Subsequently, the sections were washed and incubated with rabbit anti-cow monoclonal

antibody (1:100, DAKO) and goat-anti-rabbit-fluorescein conjugated secondary antibody (1:100, Vector). Immunopositive cells with an observable DAPI stained nucleus were counted blindly twice. Cell counts are averages of at least 9 and up to 14 mice per time point.

Imaging.

All cell counts are within the mid line of the corpus callosum, confined to an area of 0.033 mm^2. An Olympus BX-40 microscope with camera (optronics engineering) and Scion image acquisition software was used for taking images.

Reverse transcription-PCR and quantitative real-time reverse transcription-PCR.

Total RNA was isolated from a dissected region of the brain containing the corpus callosum of wild-type and *Nlrc4* $^{-/-}$ mice at several points during and after cuprizone treatment. RNA isolation was performed using Trizol reagent (Ambion) under RNase-free conditions. The primers used were Nlrc4 forward, AATTCAGATGGGCAGACAGG, Nlrc4 reverse, GAGCCCTATTGTCACCAGGA, GAPDH forward, CTTCACCACCATGGAGAAGGC, GAPDH reverse, GGCATGGACTGTGGTCATGAG.

Primary cell culture.

Bone marrow derived macrophages were extracted from femurs of WT, *Nlrc4* $^{-/-}$, *casp1* $^{-/-}$ and *Nlrp3* $^{-/-}$ mice. Cells were cultured as described previously (182).

Phagocytosis Assays.

For myelin phagocytosis experiments, myelin was extracted from adult C57BL/6 mouse brains as described previously (207). Myelin was labeled with the lipophilic dye 1, 1'-dioctadecyl-3, 3, 3', 3'-tetramethylindocarbocyanine perchlorate (DiI; Molecular probes: SKU# D-282) as described previously (208). 0.25×10^6 cells/well in 24-well culture dish was incubated with 20µg labeled myelin for 0, 30, 60 and 120 minutes at 37°C. After

phagocytosis non- ingested myelin was removed by washing the cells twice with media and once with PBS. The internalization of myelin was quantified by measuring the mean cellular fluorescent intensity by flow cytometry. A Beckman coulter (Dako) CyAn ADP flow cytometer was used for all the above mentioned experiments. Experiments were repeated at least four times and the significance was determined by using student's t-test. Differences were considered statistically significant if $p < 0.05$.

Confocal microscopy was used to visualize myelin phagocytosis by macrophages. For this, 0.25×10^6 cells were plated on 24 well glass bottom plates and after 2 hours of phagocytosis, the cells were washed thrice with PBS and fixed with 2% paraformaldehyde for 10 minutes. Subsequently, cells in the wells were stained with RCA as described in the staining section. A Zeiss LSM5 Pascal confocal laser scanning microscope was used for all the confocal microscopy.

Statistical Analysis.

Data are expressed as mean ±s.e.m. Unpaired Student's *t* tests were used to statistically evaluate significant differences. Differences were considered statistically significant if $p < 0.05$.

3.4 RESULTS

NLRC4 expression is increased in the cuprizone model of demyelination

Nlrc4 mRNA was examined by reverse transcriptase PCR (Fig 3.1b). Previous reports have shown that NLRC4 protein is highly expressed in mouse brain (40). The CNS of 4 week cuprizone treated C57BL/6 mice and *Nlrc4*$^{-/-}$ mice was examined for NLRC4 expression by IHC using an antibody against mouse NLRC4. NLRC4 expression was detected after 4 weeks of cuprizone induced demyelination in WT C57BL/6 but not in *Nlrc4*$^{-/-}$ mice (Fig. 3.1a). This time point coincides with peak inflammatory cell infiltration, demyelination and mature ODG death.

Recruitment of microglia is delayed in Nlrc4$^{-/-}$ *mice*

To explore if NLRC4 has a role during cuprizone-induced neuroinflammation, we examined microglial accumulation in mice lacking NLRC4 (*Nlrc4*$^{-/-}$) (Fig. 3.2a-b). Microglia are resident immune cells of the CNS that can phagocytose myelin debris, present antigens to T cells, and release cytokines and chemokines. The microglia populations at the corpus callosum were studied by *Ricinus communis* agglutinin-1 (RCA-1) lectin staining (Fig. 3.2a). Age-matched untreated (0 Wk) *Nlrc4* $^{-/-}$ mice and C57BL/6 WT controls showed no difference in numbers of microglia at the corpus callosum (Fig 3.2b). At 3 and 4 weeks of cuprizone treatment there was progressive and significant reduction in microglial infiltration in *Nlrc4* $^{-/-}$ mice relative to WT controls (Fig. 3.2b, P=0.03 at 3 Wks and P=0.002 at 4 Wks). After 5 weeks of cuprizone treatment there was no difference in microglial accumulation between *Nlrc4* $^{-/-}$ and C57BL/6 controls (Fig.3.2b). This is consistent with other studies of the cuprizone model wherein the removal of an inflammatory gene did not affect pathology past

this time point (158, 180, 181). These results indicate that NLRC4 contributes to microglia accumulation at the corpus callosum during demyelination .

Astrogliosis is delayed in Nlrc4$^{-/-}$ mice

Astrocytes are the other cell population that contributes to cuprizone-induced neuroinflammation. We examined astrogliosis in mice lacking NLRC4 (*Nlrc4$^{-/-}$)* (Fig. 3.3 a-b). Activated astrocytes perform several overlapping roles with microglia with respect to neuroinflammation. The astrocyte populations at the corpus callosum was studied by glial fibrillary acidic protein (GFAP) staining (Fig. 3.3 a). Age-matched untreated (0 Wk) *Nlrc4 $^{-/-}$* mice and C57BL/6 WT controls showed no difference in numbers of astrocytes at the corpus callosum (Fig 3.3b). At 3 and 4 weeks of cuprizone treatment there was progressive and significant reduction in astrogliosis in the *Nlrc4$^{-/-}$* mice at week 3 and 4, (Fig. 3.3b, P=0.002 at 3 Wks and P=0.009 at 4 Wks). After 5 weeks of cuprizone treatment there was no difference in astrogliosis between *Nlrc4 $^{-/-}$* and C57BL/6 controls (Fig. 3.3b). These results indicate that NLRC4 contributes to astrogliosis in the CNS during demyelination.

Demyelination is delayed in cuprizone-treated Nlrc4$^{-/-}$ mice

Another component of the cuprizone model that is relevant to human disease is the demyelination process. To assess if NLRC4 plays a role in demyelination and the loss of mature oligodendrocytes (ODG), *Nlrc4$^{-/-}$* mice along with age matched C57BL/6 control (WT) mice were treated with cuprizone for 3, 4 and 5 weeks. Representative scoring of the extent of demyelination as measured by Luxol fast blue-periodic acid Schiff (LFB-PAS) staining is shown in Fig. 3.5a. Slides were read by three blinded readers on a scale of 0 (no demyelination) to 3 (complete demyelination). WT mice showed significant demyelination initiating at the 3 week time point and continuing to the end of the study at the 5 week time

point (Fig 3.5b). *Nlrc4* $^{-/-}$ mice showed a significant delay in demyelination at the 3 week time point when compared to WT controls (Fig 3.5b). LFB is a screening assay for myelin which requires further verification with more specific stains such as glutathione S transferase pi subunit (GSTπ), a marker of mature ODG population. Prior to cuprizone treatment (0 Wk) *Nlrc4* $^{-/-}$ mice and C57BL/6 controls showed no difference in mature ODG populations at the corpus callosum as shown in Fig. 3.4b. At 4 weeks of cuprizone treatment, the depletion of mature ODGs was attenuated in *Nlrc4* $^{-/-}$ mice relative to C57BL/6 controls. A quantitation of the composite data is shown in Fig. 3.4 b (P=0.019 at 4 Wks). After 5 weeks of cuprizone treatment, there was no difference in demyelination and mature ODG death between *Nlrc4* $^{-/-}$ and C57BL/6 control mice (Fig. 3.4b) indicating that NLRC4 delayed demyelination but did not obviate this process. This is consistent with studies of other inflammatory genes in the cuprizone model (180, 181, 209).

Myelin phagocytosis is enhanced in Nlrc4 $^{-/-}$ ***macrophages***

Our data thus far suggests that NLRC4 exacerbates neuroinflammation as measured by microglial accumulation and astrogliosis and also affects demyelination and mature ODG depletion. As described previously microglia/macrophages and astrocytes actively sample their environment. Microglia sense their environments via surface receptors and intracellular sensors such as TLRs and NLRs respectively (183). One of the several roles performed by microglia is clearance of cellular debris including but not restricted to myelin. Removal of myelin debris is critical for resolution of inflammation, prevention of further death of ODGs and recruitment of ODG progenitors for remyelination. To investigate the role of NLRC4 in myelin phagocytosis we isolated macrophages from WT and *Nlrc4*$^{-/-}$ mice along with *Nlrp3*$^{-/-}$ and *casp1*$^{-/-}$ mice as positive controls for enhanced myelin phagocytosis. *Nlrc4*$^{-/-}$

macrophages showed significantly increased phagocytosis of myelin as compared to WT controls and similar levels as compared to *Nlrp3*$^{-/-}$ and *casp1*$^{-/-}$ macrophages (Fig. 3.6b). Myelin phagocytosis was studied by incubating macrophages with myelin that was labeled with the fluorescent carbocyanine, lipophilic dye, 1, 1'-dioctadecyl-3, 3, 3', 3'-tetramethylindocarbocyanine perchlorate (DiI) for 120 minutes. Myelin internalization was measured over time by flow cytometry. Myelin internalization was also visualized by confocal microscopy. 0.25 X10^6 macrophages were plated in glass bottom 24 well plates (Fig. 3.6a, panel i). Internalization was detectable at 120 minutes (Fig. 3.6a, panel ii). Treatment with cytochalasin D, a known inhibitor of phagocytosis, was used as a negative control (Fig. 3.6a, panel iii). These findings suggest that NLRC4 might negatively affect myelin phagocytosis which is important for myelin clearance.

3.5 DISCUSSION

NLRC4 protein is abundant in the adult mouse brain (40) and can associate with procaspase-1 to form the NLRC4 inflammasome. Caspase-1 has been shown to be important for the processing of over 70 substrates including the cytokines IL-1β and IL-18(18, 19). Several studies have demonstrated the role of caspase-1 and its target proteins IL-1β and IL-18 in neuroinflammation however, the role of NLRC4 or its endogenous triggers in the CNS remain undescribed. Our studies with NLRP3 deficient (*Nlrp3*$^{-/-}$) mice in the cuprizone model showed a NLRP3/caspase-1/IL-18-dependent but IL-1β independent mechanism which leads to demyelination and the loss of mature oligodendrocytes. Moreover, our results in *Nlrp3*$^{-/-}$ mice showed that NLRP3 deficiency delayed but did not obviate demyelination and neuroinflammation. These results raised the possibility of the involvement of other NLR proteins possibly capable of processing caspase-1 in neuroinflammation and demyelination.

Here, we provide evidence that *Nlrc4*$^{-/-}$ mice exhibit delayed demyelination and neuroinflammation in the cuprizone induced mouse model of demyelination. Moreover stimulated by our earlier finding that *Nlrp3*$^{-/-}$ and *casp1*$^{-/-}$ macrophages show an increased ability to phagocytose myelin debris we investigated myelin phagocytosis in macrophages from *Nlrc4*$^{-/-}$ mice. Bone marrow derived macrophages from *Nlrc4*$^{-/-}$ mice have increased capacity for myelin phagocytosis as compared to WT macrophages, this enhanced phagocytosis was similar to that observed with *Nlrp3*$^{-/-}$ and *casp1*$^{-/-}$ macrophages.

Myelin phagocytosis is an important component of MS pathology. Macrophage and microglial clearance of myelin debris is critical to repair mechanisms following demyelination in both central and peripheral nervous system diseases (136, 138, 177, 203, 204). Myelin debris has dual proinflammatory and anti-regenerative functions, firstly, myelin

debris can activate the complement system to form membrane attack complexes that disintegrate intact myelin (139) and secondly, myelin debris inhibits oligodendrocyte precursor cell differentiation in the adult rat CNS thus impairing remyelination (135). Therefore, myelin debris removal is critical for both resolution of demyelination and for creating an environment conducive for remyelination. This corroborates our *in vivo* data that showed delayed demyelination in *Nlrc4*$^{-/-}$ mice.

It remains unclear how NLRC4 exerts its effects on phagocytosis. Myelin consists of protein and lipid components. One possible mechanism for the involvement of NLRC4 in myelin phagocytosis is the known structural homology between myelin basic protein (MBP) and flagellin (210). The structural homology between the flagellin of *Borrelia burgdorferi* and myelin basic protein led to the "mistaken-self" hypothesis for the autoimmune attack against myelin leading to demyelination observed during neuroborreliosis. Myelin differs in composition from other plasma membranes in its unusually high lipid content. Lipids constitute 70-75% dry weight of myelin (211). The molar ratio of lipids is 2:2:1:1 for cholesterol/ phospholipid/ galactolipid/ plasmalogen. Another possible mechanism could be that after phagocytosis phospholipids in myelin are degraded by phospholipase A2 causing release of lysophosphatidylcholine (LPC) (212). LPC can suppress maturation and release of IL-1β in mouse microglial cells (213).

In addition there are several receptor complexes that are involved in myelin phagocytosis including scavenger receptors I and II (SR-AI/II) (143, 145), complement receptor 3 (CR-3), galectin-3 (144), Fc gamma receptor (FcγR) (205), and the low-density lipoprotein receptor-related protein 1(LRP-1) (214). It is possible that NLRC4 affects any,

some or all of these receptors by affecting their expression or signal transduction pathways required for myelin phagocytosis.

In summary, the dual roles of NLRC4 in exacerbating neuroinflammation and inhibiting myelin debris clearance indicate that inhibition of NLRC4 may prove to be a valuable therapeutic approach for demyelinating diseases such as MS. These results show that neuroinflammation, demyelination and myelin debris clearance in this disease model are mediated by an NLRC4-dependent pathway.

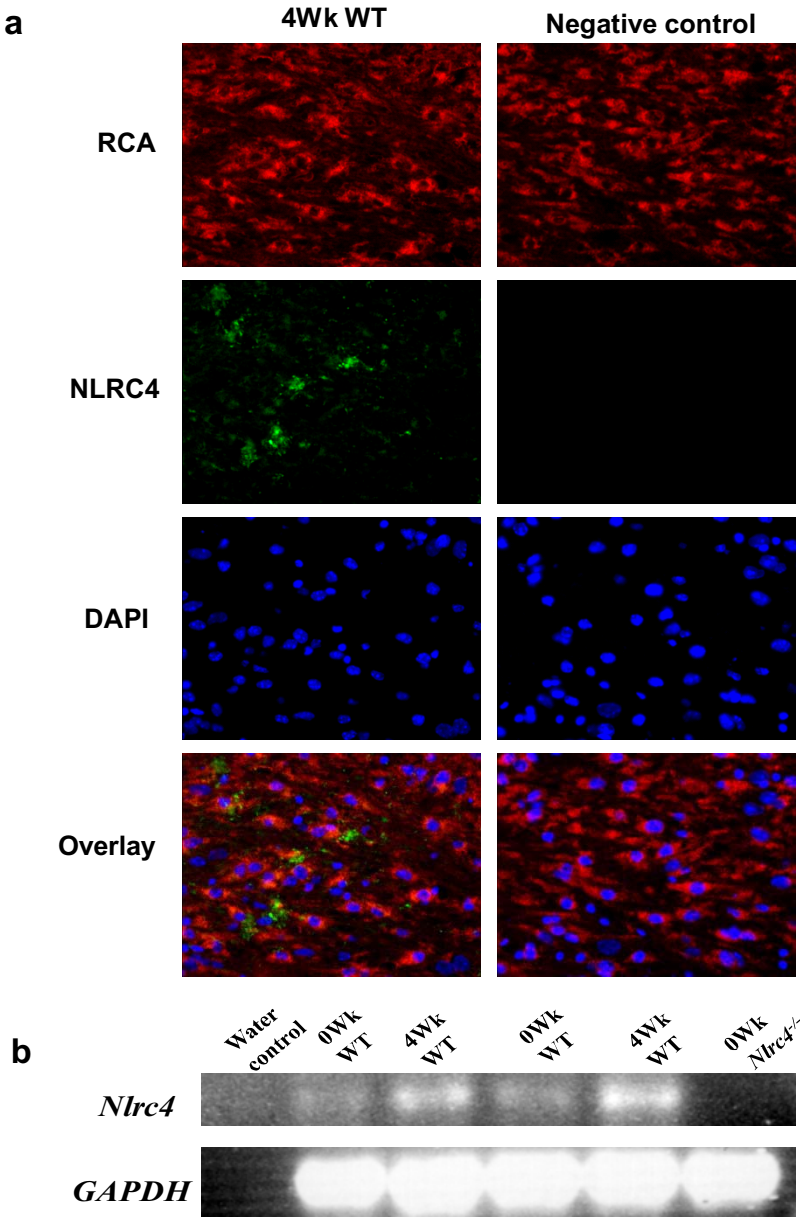
a
4Wk WT
Negative control
RCA
NLRC4
DAPI
Overlay
b
Water control
0Wk WT
4Wk WT
0Wk WT
4Wk WT
0Wk Nlrc4-/-
Nlrc4
GAPDH

Figure 3.1- Expression of NLRC4 in the CNS a. 4 week cuprizone treated WT mice brains were examined for NLRC4 expression by IHC using an antibody against mouse NLRC4. NLRC4 expression (green) was detected after 4 weeks of cuprizone induced demyelination in WT but not in *Nlrc4*$^{-/-}$ mice (Fig. 3.1a). RCA (red) was used to detect microglia at the corpus callosum. DAPI was used to label nuclei (blue). **b.** RT-PCR was used to detect Nlrc4 mRNA levels in total RNA from brains of cuprizone treated and untreated WT and *Nlrc4*$^{-/-}$ mice. GAPDH was used as a positive control and water control was included as a negative control for the PCR reaction.

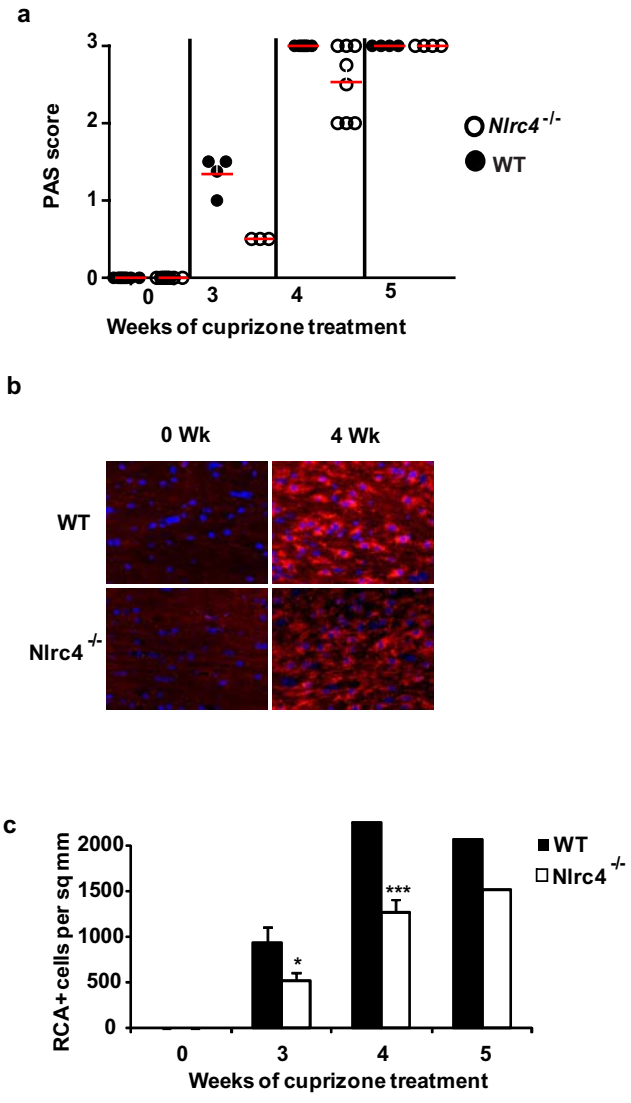
a
PAS score
3
2
1
0
0
3
4
5
Weeks of cuprizone treatment
Nlrc4 -/-
WT
b
0 Wk
4 Wk
WT
Nlrc4 -/-
c
RCA+ cells per sq mm
2000
1500
1000
500
0
*
***
0
3
4
5
Weeks of cuprizone treatment
WT
Nlrc4 -/-

Figure 3.2- Role of NLRC4 in immune cell infiltration. a. *Nlrc4*$^{-/-}$ mice (open circles) show reduced cellularity as compared to WT controls (filled circles). Cellularity was quantitated by periodic acid schiff's (PAS) staining. Each circle represents the averaged observed PAS score from three readers for one mouse. The mean value of each data set is depicted by a red line. **b.** *Nlrc4*$^{-/-}$ mice exhibit reduced microglial accumulation as compared to age-matched WT controls. Microglial cells were measured by RCA^{+} staining at the corpus callosum after 3 and 4Wks of cuprizone treatment. RCA (red) was used to detect microglial accumulation in the corpus callosum. DAPI was used to label nuclei (blue). **c.** Quantitation of microglial accumulation showed reduced microglia at the midline corpus callosum in *Nlrc4*$^{-/-}$ mice (open bars) after 3 and 4 weeks of cuprizone treatment (P=0.03 at 3 Wks and P=0.002 at 4 Wks). *P< 0.05, **P<0.01, ***P<0.005; error bars, s.e.m. Cell counts are averages of between 4 and 11 mice per time point.

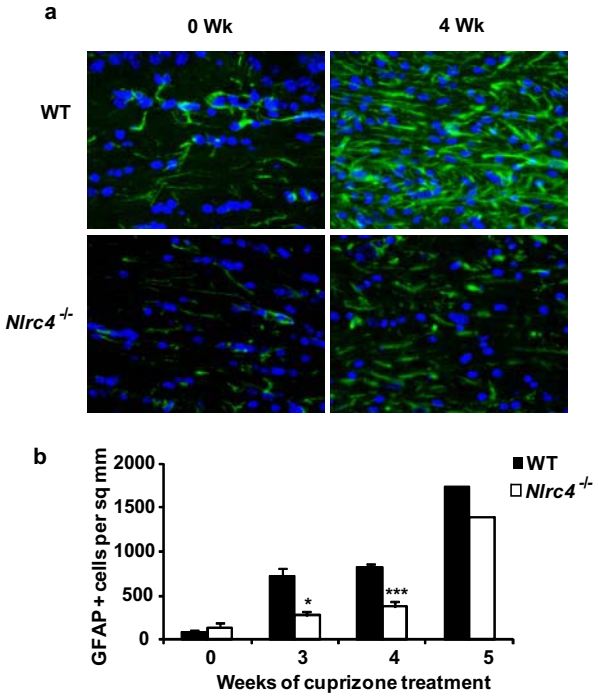
a
0 Wk
4 Wk
WT
Nlrc4 -/-
b
GFAP+ cells per sq mm
2000
1500
1000
500
0
WT
Nlrc4 -/-
*
***
0
3
4
5
Weeks of cuprizone treatment

Figure 3.3- Role of NLRC4 in astrogliosis. *Nlrc4*$^{-/-}$ mice exhibit reduced astrogliosis when compared to age-matched WT controls as measured by GFAP^{+} cell population at the corpus callosum after 3 and 4Wks of cuprizone treatment. **a.** GFAP (green) was used to detect astrocyte accumulation in the corpus callosum. DAPI was used to label nuclei (blue). **b.** Quantitation of astrogliosis showed significantly reduced astrocytes at the midline corpus callosum in *Nlrc4*$^{-/-}$ mice (open bars) after 3 and 4 weeks of cuprizone treatment (P=0.002 at 3 Wks and P=0.009 at 4 Wks). *P< 0.05, **P<0.01, ***P<0.005; error bars, s.e.m. Cell counts are averages of between 4 and 11 mice per time point.

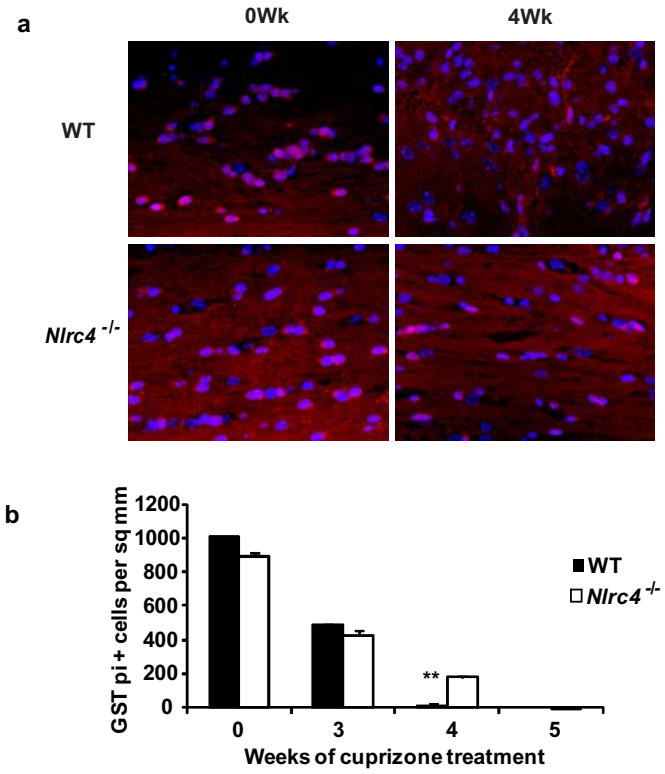
a
0Wk
4Wk
WT
Nlrc4 -/-
b
GST pi + cells per sq mm
1200
1000
800
600
400
200
0
**
0
3
4
5
Weeks of cuprizone treatment
WT
Nlrc4 -/-

Figure 3.4- Role of NLRC4 in mature ODG depletion. *Nlrc4*$^{-/-}$ mice show a significant decrease in oligodendrocyte death during demyelination. **a.** GSTπ (red) was used as a marker to detect mature myelinating oligodendrocyte accumulation. DAPI was used to label nuclei (blue). **b.** Quantitation of GSTπ^{+} cells showed significantly more oligodendrocytes at the midline corpus callosum in *Nlrc4*$^{-/-}$ mice (open bars) after 4 weeks of cuprizone treatment (P=0.019 at 4 Wks). *P< 0.05, **P<0.01, ***P<0.005; error bars, s.e.m. Cell counts are averages of between 4 and 11 mice per time point.

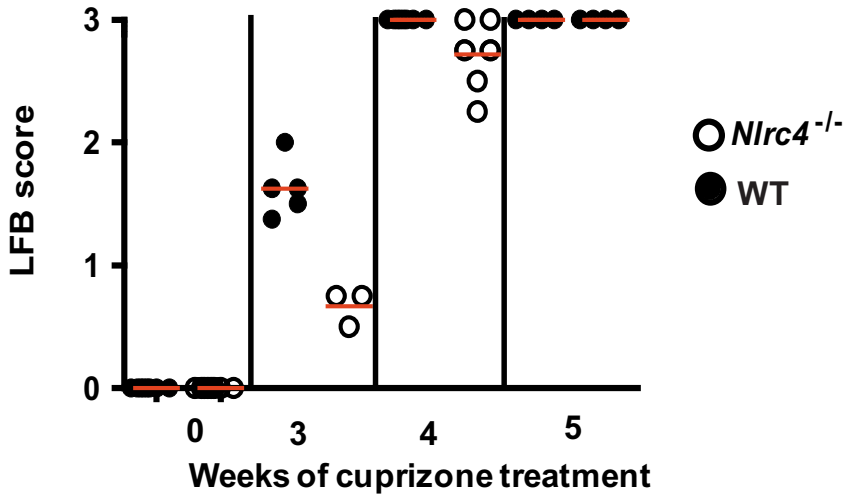
LFB score
3
2
1
0
0
3
4
5
Weeks of cuprizone treatment
Nlrc4 -/-
WT

Figure 3.5- Role of NLRC4 in demyelination. *Nlrc4*$^{-/-}$ mice (open circles) show delayed demyelination as compared to WT controls (filled circles). Each slide was scored by 3 independent blinded readers on a score of 0 (no demyelination) to 3 (complete demyelination). All scores are restricted to the midline corpus callosum (boxed area). Demyelination was quantitated by Luxol fast blue (LFB)/ periodic acid schiff's (PAS) staining. Each circle represents the averaged observed LFB score from three readers for one mouse. The mean value of each data set is depicted by a red line.

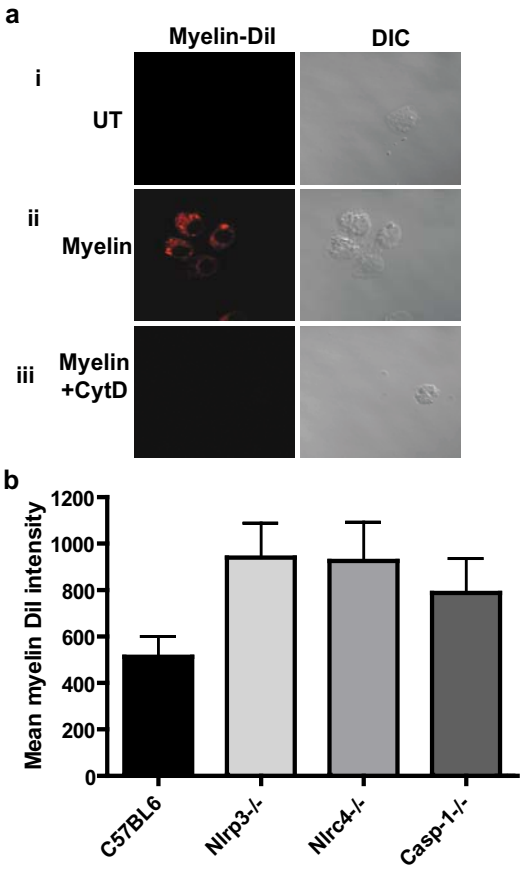
a
Myelin-DiI
DIC
i
UT
ii
Myelin
iii
Myelin
+CytD
b
Mean myelin DiI intensity
1200
1000
800
600
400
200
0
C57BL6
Nlrp3-/-
Nlrc4-/-
Casp-1-/-

Figure 3.6- Role of NLRC4 in myelin phagocytosis. a. Macrophages readily phagocytose DiI-labeled myelin. 0.25 X10^6 macrophages were plated in 24 well plates. These macrophages were incubated with DiI-labeled myelin (red) for 2 hours. Myelin phagocytosis was visualized by confocal microscopy (panel ii). As negative control samples were treated with cytochalasin D a known inhibitor of phagocytosis, in the medium (panel iii). Cytochalasin D blocked myelin phagocytosis. **b.** Phagocytosis of fluorescently-labeled myelin was enhanced in *Nlrc4*$^{-/-}$ macrophages when compared to WT macrophages. Macrophages were isolated and analyzed by flow cytometry as described previously in the methods section. Mean fluorescent intensity (MFI) of DiI-Myelin was measured by flow cytometry. *Nlrp3*$^{-/-}$and *casp1*$^{-/-}$ BMDMs were used as positive controls of myelin phagocytosis. Data from 4 experiments are shown here.

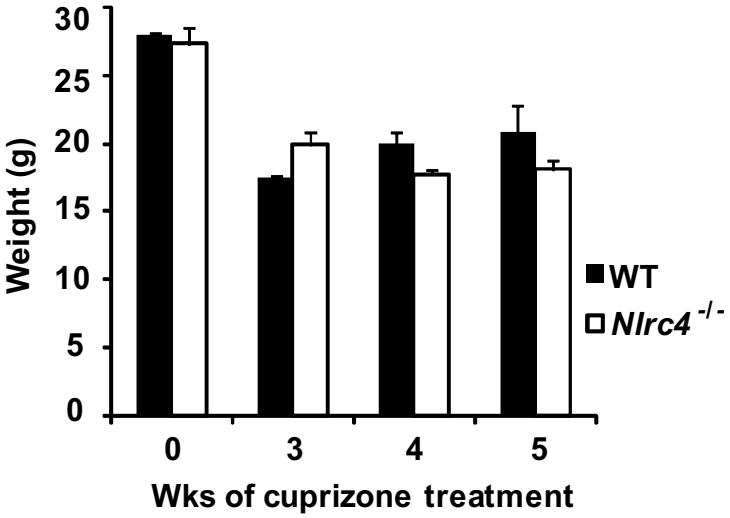
30
25
20
15
10
5
0
Weight (g)
0
3
4
5
Wks of cuprizone treatment
WT
Nlrc4 -/-

Figure 3.7 Weight of *Nlrc4*$^{-/-}$ and control WT mice was similar during cuprizone induced demyelination. 8-10 weeks old, male, *Nlrc4*$^{-/-}$ and control WT mice were fed 0.2% cuprizone mixed into ground chow *ad libidum* for 5 weeks to induce progressive demyelination. Untreated control mice were maintained on a diet of normal pellet chow. *Nlrc4*$^{-/-}$ and control WT mice showed no difference in weight during cuprizone treatment. Weights (in grams on y axis) are averages of at least 4 and up to 11 mice per time point.

CHAPTER IV

CONCLUSIONS AND FUTURE DIRECTIONS

The role of the NLR family members as sensors of PAMPs and DAMPs is a field of extensive study however their role in neuroinflammation and demyelination remains largely unexplored. As discussed in detail in chapter 1, mutations in *NLRP3* in humans leads to three autoinflammatory syndromes - FCAS, MWS and CINCA that are collectively referred to as CAPS(52-56). CINCA patients often display chronic aseptic meningitis which is reversed after treatment with the IL-1β receptor antagonist Anakinra (164). This is indicative of a role for NLRP3 in neuroinflammation. The aim of this dissertation was to firstly; elucidate the possible contribution of NLRP3 to neuroinflammation, demyelination and remyelination, secondly to determine the molecular mediators and mechanisms of NLRP3 dependent regulation of neuroinflammation and demyelination and lastly to identify other NLRs that could play pro- or anti-inflammatory roles in demyelination. To address these questions we utilized a two pronged approach utilizing an *in vivo* cuprizone-induced mouse model of neuroinflammation, demyelination and remyelination and *ex vivo* macrophage based assays. Our studies utilized an extensive panel of mice deficient in genes encoding either NLRs or their signaling/effector components including, *Nlrp3*$^{-/-}$, *casp-1*$^{-/-}$, *P2X*$_7$*R*$^{-/-}$, *IL-1β*$^{-/-}$, *IL-18*$^{-/-}$ and *Nlrc4*$^{-/-}$ mice. Table 4.1 summarizes the findings from these studies.

1. **Neuroinflammation, demyelination and myelin debris clearance in the cuprizone model is NLRP3 inflammasome dependent.** As described in detail in chapter 2 mice lacking *Nlrp3 and caspase-1* exhibited reduced neuroinflammation, demyelination and mature oligodendrocyte loss in the cuprizone-induced demyelination and neuroinflammation model. The absence of IL-1β did not affect disease outcome, while the absence of P2X$_7$R reduced neuroinflammation but not demyelination. Macrophages from *Nlrp3*$^{-/-}$ and *casp-1*$^{-/-}$ but not WT mice exhibited augmented capacity to phagocytize

and clear myelin debris. This ability was specific to myelin phagocytosis and did not extend to phagocytosis of latex beads or bacteria.

Several new research opportunities and questions arise as a result of these studies; firstly what are the DAMPs that might activate the inflammasome pathways in the CNS, in complex immune diseases such as multiple sclerosis? Secondly, what are the surface receptors on microglia/macrophages and potentially astrocytes that could sense myelin and activate downstream signaling pathways leading to the activation of the inflammasome related or other NLRs?

Is the expression of the receptors involved in myelin phagocytosis regulated by expression of NLRP3?

Several surface molecules are important for myelin phagocytosis, including complement-receptor-3 (CR-3), scavenger-receptor-AI/II (SR-AI/II) and Fc gamma receptor (FcγR) (138, 143, 145, 215, 216). Recent data also implicate the Mac-3 molecule (also known as galectin-3) (144) and the low-density lipoprotein receptor-related protein 1(LRP-1) in myelin phagocytosis (214). Downstream signaling pathways necessary for myelin phagocytosis include Ras, PI3K, and PLCγ.

Our preliminary studies have shown that myelin phagocytosis by CD11b and SRAI/II is independent of NLRP3 expression. Suggesting that, further studies investigating the expression of other receptors such as Mac-3, LRP-1 and FcγR during myelin phagocytosis in WT and *Nlrp3*$^{-/-}$ macrophages are required. Additional experiments could include blocking myelin phagocytosis by antibodies against these receptors to establish if one or more receptors are responsible for the increased myelin phagocytosis that is observed in *Nlrp3*$^{-/-}$

macrophages. Anti-CR3 (216), anti-FcγR (141), anti-SRA-I/II (143) and anti-Mac3 blocking antibodies (144) have been successfully used previously to reduce myelin phagocytosis.

Does NLRP3-regulated myelin phagocytosis rely on conventional myelin phagocytosis signaling pathways?

The Ras, PI3K, and PLCγ signaling pathways have been shown to be necessary for myelin phagocytosis pharmacological inhibitors against specific components of these pathways could be used to elucidate their relative contribution to myelin phagocytosis in WT and *Nlrp3*$^{-/-}$ macrophages. The PI3K pathway inhibitors, Ly294002 and wortmannin and the PLCγ inhibitors, 3-nitrocoumarin (3-NC) and U-73122 have been extensively studied and can be used for these studies (141-144).

How does the increased myelin phagocytosis in *Nlrp3*$^{-/-}$ macrophages correlate with *in vivo* delay in demyelination in *Nlrp3*$^{-/-}$ mice?

Macrophage and microglia mediated myelin debris phagocytosis has been reported in multiple sclerosis plaques as well as mouse models of CNS and PNS neuroinflammatory disorders (217, 218). To study myelin phagocytosis *in vivo* Oil red O (ORO) staining is performed. ORO is a lipophilic dye that stains myelin degradation products such as triglycerides and lipoproteins. ORO staining and/or antibody mediated detection of MBP along with a microglial markers (such as RCA or CD11b) can be used to study microglial myelin phagocytosis. A recent study of mice deficient in the Axl gene *(Axl*$^{-/-}$*)* showed that cuprizone-treated *Axl*$^{-/-}$ mice exhibit delayed myelin debris clearance (219). While WT mice showed robust ORO staining after 4 weeks of cuprizone treatment *Axl*$^{-/-}$ did not show ORO staining until 6 weeks. Our preliminary studies with *Nlrp3*$^{-/-}$ mice show strong ORO staining after 5 weeks of cuprizone treatment. Since our *ex vivo* data utilizing mouse macrophages

showed increased phagocytosis in *Nlrp3*$^{-/-}$ macrophages as compared to WT macrophages a comprehensive study utilizing ORO staining to examine myelin phagocytosis *in vivo* in mice from 2 to 5 weeks after start of cuprizone treatment will allow for a better understanding of the role of NLRP3 in myelin phagocytosis *in vivo*.

2. **Remyelination in the cuprizone model is NLRP3 independent.** Regulation of remyelination is a potential therapeutic intervention for MS. Previous studies in the cuprizone model have shown that remyelination is dramatically reduced in *IL-1β*$^{-/-}$ mice (165). IL-1β regulates remyelination via its regulation of IGF-1 which is critical for conversion of ODG progenitors to mature ODGs (165, 188). Moreover, transgenic mice constitutively expressing IGF1 have reduced mature ODG death by apoptosis (166, 167). Thus, we hypothesized that NLRP3 via its regulation of IL-1β processing and consequently IGF-1 may regulate oligodendrogenesis and remyelination. However our data with *Nlrp3*$^{-/-}$ mice during remyelination (8, 10 and 12 week time points) indicated that remyelination remains unchanged relative to C57Bl/6 controls by GST pi and LFB/PAS staining, and TEM analysis. Interestingly our preliminary data with remyelination utilizing *IL-18*$^{-/-}$ mice showed that these animals have more rapid remyelination as compared to WT controls at the same time point, indicating that IL-18 may be detrimental to remyelination *in vivo*. These findings are novel in that they provide inhibition of a NLRP3 as a novel therapeutic intervention for MS. Earlier studies with other mediators of neuroinflammation and demyelination have been inconsequential in terms of clinical translation due to the dual role of these mediators in demyelination and remyelination. Thus, compromising their therapeutic use. Moreover, this is the first report

documenting the role of IL-18 during remyelination. A detailed analysis of ODG progenitor cell population and their proliferation as compared to WT controls during remyelination in the cuprizone model may yield interesting insight into the mechanistic role of IL-18 in remyelination. In addition a study of *casp-1*$^{-/-}$ and *IL-1β*$^{-/-}$/*IL-18*$^{-/-}$ mice during remyelination may also provide a better understanding of the relative contribution of these molecules towards remyelination in this model. To establish the role of caspase-1 and IL-18 in ODG progenitor proliferation BrdU incorporation in NG2^{+} ODG progenitor cell population can be studied as described previously (158). NG2^{+} BrdU^{+} cells can be detected by immunofluorescence for NG2 and quantitated. Moreover, IGF-1 expression in *casp-1*$^{-/-}$ and *IL-1β*$^{-/-}$/*IL-18*$^{-/-}$ mice versus WT control mice can be studied by IGF-1 ELISA.

3. **Neuroinflammation, demyelination and myelin debris clearance in the cuprizone model is NLRC4 dependent.** Considering the delay but not complete abolition of demyelination and neuroinflammation in the cuprizone model our final question explored the existence of other NLRs that could compensate for the loss of NLRP3. Since NLRP3 dependent caspase-1 cleavage is required for neuroinflammation and demyelination in our model we explored other NLR proteins that could cleave caspase-1. NLRC4 can associate with procaspase-1 and cause its autocatalytic cleavage to active caspase-1. However, NLRC4 is a cytosolic sensor for flagellin, flagellated and some non-flagellated pathogens so we expected that NLRC4 would not contribute to inflammation in the cuprizone model. Interestingly, our data with *Nlrc4*$^{-/-}$ mice showed delayed astrogliosis, microglial infiltration, mature oligodendrocyte death and demyelination. *Nlrc4*$^{-/-}$ mice

also showed a similarity to *Nlrp3*$^{-/-}$ mice in terms enhanced ability to clear myelin debris. These results raise the possibility of the existence of multiple contributing pathways upstream of caspase-1 activation that could lead to demyelination and neuroinflammation. The known structural homology between myelin basic protein (MBP) and flagellin or regulation of NLRC4 by myelin lipid mediators could provide a possible explanation. As in the case of NLRP3 regulated myelin debris clearance the identity of surface receptors involved in myelin phagocytosis and mechanism of delivery to the cytosolic NLR sensor remains unexplored. Future studies investigating the role of lipid and protein components of myelin such as by utilizing purified myelin basic protein or inhibitors of phospholipase A2 in phagocytosis experiments with macrophages from WT and *Nlrc4*$^{-/-}$ mice could provide much insight into the mechanism and mediators of myelin phagocytosis.

Features	WT	*Nlrp3*$^{-/-}$	*Casp-1*$^{-/-}$	*IL-1β*$^{-/-}$	*IL-18*$^{-/-}$	*P2X$_7$R*$^{-/-}$	*Nlrc4*$^{-/-}$
Demyelination		Delayed	Delayed	No effect	Delayed	No effect	Delayed
•Microglial accumulation		Delayed	Delayed	No effect	Delayed	Delayed	Delayed
•Astrogliosis		Delayed	Delayed	No effect	Delayed	Delayed	Delayed
•Mature ODG cell depletion		Delayed	Delayed	No effect	Delayed	No effect	Delayed
•Myelin Phagocytosis		Enhanced	Enhanced	ND	ND	ND	Enhanced
•E.coli Phagocytosis		No effect	No effect	ND	ND	ND	No effect
•Bead Phagocytosis		No effect	No effect	ND	ND	ND	No effect
Interpretation		NLRP3 exacerbates demyelination	Caspase-1 partially exacerbates demyelination	IL-1β does not affect demyelination	IL-18 partially exacerbates demyelination	P2X$_7$R signaling does not affect demyelination	NLRC4 exacerbates demyelination

Table 4.1. Summary of cuprizone studies

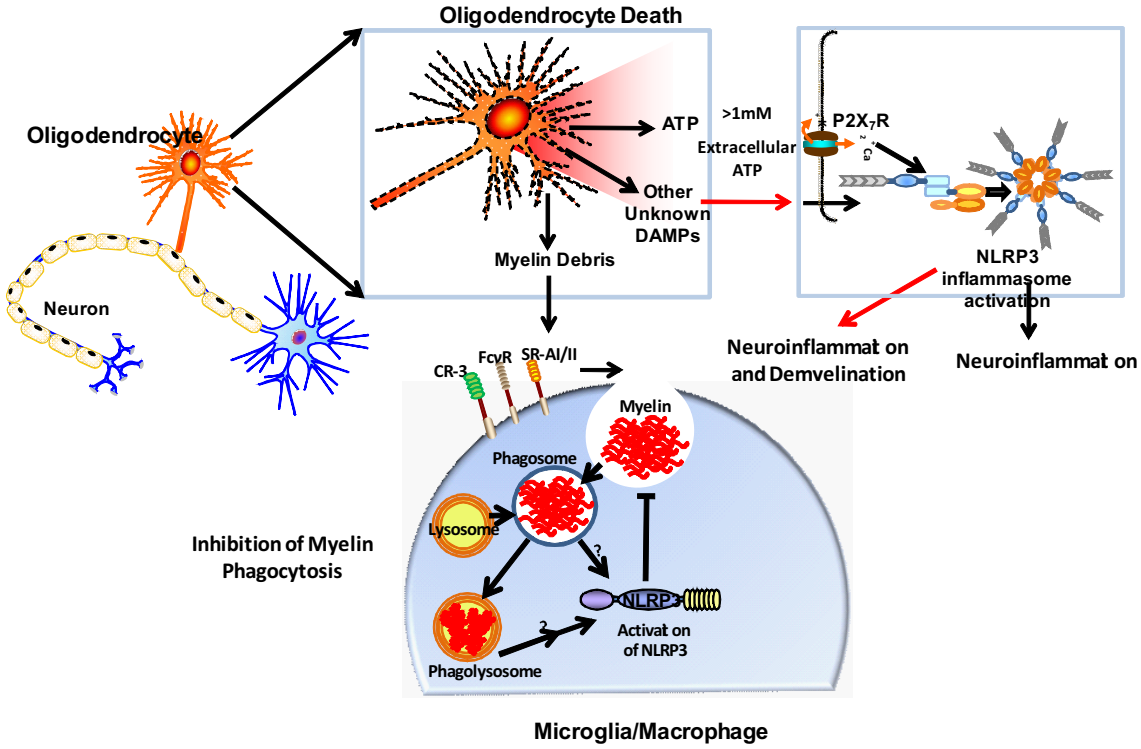

Figure 4.1 Summary of possible moleculat mechanisms. Mature ODG cell death leads to release of ATP, myelin and other unknown DAMPs that may contribute to neuroinflammation and/or demyelination. ATP signaling via $P2X_7R$ contributes to microglial accumulation. Other unknown DAMPs are sensed via the NLRP3 inflammasome complex and lead to neuroinflammation and demyelination. Myelin phagocytosis is inhibited by the NLRP3 inflammasome by unknown mechanisms.

References

1. Ting, J. P., D. L. Kastner, and H. M. Hoffman. 2006. CATERPILLERs, pyrin and hereditary immunological disorders. *Nature reviews.Immunology* 6:183-195.

2. Harton, J. A., M. W. Linhoff, J. Zhang, and J. P. Ting. 2002. Cutting edge: CATERPILLER: a large family of mammalian genes containing CARD, pyrin, nucleotide-binding, and leucine-rich repeat domains. *Journal of immunology (Baltimore, Md.: 1950)* 169:4088-4093.

3. Amer, A., L. Franchi, T. D. Kanneganti, M. Body-Malapel, N. Ozoren, G. Brady, S. Meshinchi, R. Jagirdar, A. Gewirtz, S. Akira, and G. Nunez. 2006. Regulation of Legionella phagosome maturation and infection through flagellin and host Ipaf. *The Journal of biological chemistry* 281:35217-35223.

4. Franchi, L., A. Amer, M. Body-Malapel, T. D. Kanneganti, N. Ozoren, R. Jagirdar, N. Inohara, P. Vandenabeele, J. Bertin, A. Coyle, E. P. Grant, and G. Nunez. 2006. Cytosolic flagellin requires Ipaf for activation of caspase-1 and interleukin 1beta in salmonella-infected macrophages. *Nature immunology* 7:576-582.

5. Miao, E. A., C. M. Alpuche-Aranda, M. Dors, A. E. Clark, M. W. Bader, S. I. Miller, and A. Aderem. 2006. Cytoplasmic flagellin activates caspase-1 and secretion of interleukin 1beta via Ipaf. *Nature immunology* 7:569-575.

6. Miao, E. A., R. K. Ernst, M. Dors, D. P. Mao, and A. Aderem. 2008. Pseudomonas aeruginosa activates caspase 1 through Ipaf. *Proceedings of the National Academy of Sciences of the United States of America* 105:2562-2567.

7. Suzuki, T., L. Franchi, C. Toma, H. Ashida, M. Ogawa, Y. Yoshikawa, H. Mimuro, N. Inohara, C. Sasakawa, and G. Nunez. 2007. Differential regulation of caspase-1 activation, pyroptosis, and autophagy via Ipaf and ASC in Shigella-infected macrophages. *PLoS pathogens* 3:e111.

8. Kanneganti, T. D., N. Ozoren, M. Body-Malapel, A. Amer, J. H. Park, L. Franchi, J. Whitfield, W. Barchet, M. Colonna, P. Vandenabeele, J. Bertin, A. Coyle, E. P. Grant, S. Akira, and G. Nunez. 2006. Bacterial RNA and small antiviral compounds activate caspase-1 through cryopyrin/Nalp3. *Nature* 440:233-236.

9. Mariathasan, S., D. S. Weiss, K. Newton, J. McBride, K. O'Rourke, M. Roose-Girma, W. P. Lee, Y. Weinrauch, D. M. Monack, and V. M. Dixit. 2006. Cryopyrin activates the inflammasome in response to toxins and ATP. *Nature* 440:228-232.

10. Martinon, F., V. Petrilli, A. Mayor, A. Tardivel, and J. Tschopp. 2006. Gout-associated uric acid crystals activate the NALP3 inflammasome. *Nature* 440:237-241.

11. Shi, Y., J. E. Evans, and K. L. Rock. 2003. Molecular identification of a danger signal that alerts the immune system to dying cells. *Nature* 425:516-521.

12. Halle, A., V. Hornung, G. C. Petzold, C. R. Stewart, B. G. Monks, T. Reinheckel, K. A. Fitzgerald, E. Latz, K. J. Moore, and D. T. Golenbock. 2008. The NALP3 inflammasome is involved in the innate immune response to amyloid-beta. *Nat Immunol* 9:857-865.

13. Scheibner, K. A., M. A. Lutz, S. Boodoo, M. J. Fenton, J. D. Powell, and M. R. Horton. 2006. Hyaluronan fragments act as an endogenous danger signal by engaging TLR2. *J Immunol* 177:1272-1281.

14. Ogura, Y., F. S. Sutterwala, and R. A. Flavell. 2006. The inflammasome: first line of the immune response to cell stress. *Cell* 126:659-662.

15. Cain, K., S. B. Bratton, C. Langlais, G. Walker, D. G. Brown, X. M. Sun, and G. M. Cohen. 2000. Apaf-1 oligomerizes into biologically active approximately 700-kDa and inactive approximately 1.4-MDa apoptosome complexes. *J Biol Chem* 275:6067-6070.

16. Zou, H., Y. Li, X. Liu, and X. Wang. 1999. An APAF-1.cytochrome c multimeric complex is a functional apoptosome that activates procaspase-9. *J Biol Chem* 274:11549-11556.

17. Muzio, M., A. M. Chinnaiyan, F. C. Kischkel, K. O'Rourke, A. Shevchenko, J. Ni, C. Scaffidi, J. D. Bretz, M. Zhang, R. Gentz, M. Mann, P. H. Krammer, M. E. Peter, and V. M. Dixit. 1996. FLICE, a novel FADD-homologous ICE/CED-3-like protease, is recruited to the CD95 (Fas/APO-1) death--inducing signaling complex. *Cell* 85:817-827.

18. Shao, W., G. Yeretssian, K. Doiron, S. N. Hussain, and M. Saleh. 2007. The caspase-1 digestome identifies the glycolysis pathway as a target during infection and septic shock. *The Journal of biological chemistry* 282:36321-36329.

19. Keller, M., A. Ruegg, S. Werner, and H. D. Beer. 2008. Active caspase-1 is a regulator of unconventional protein secretion. *Cell* 132:818-831.

20. Sutterwala, F. S., Y. Ogura, M. Szczepanik, M. Lara-Tejero, G. S. Lichtenberger, E. P. Grant, J. Bertin, A. J. Coyle, J. E. Galan, P. W. Askenase, and R. A. Flavell. 2006. Critical role for NALP3/CIAS1/Cryopyrin in innate and adaptive immunity through its regulation of caspase-1. *Immunity* 24:317-327.

21. Kanneganti, T. D., M. Body-Malapel, A. Amer, J. H. Park, J. Whitfield, L. Franchi, Z. F. Taraporewala, D. Miller, J. T. Patton, N. Inohara, and G. Nunez. 2006. Critical role for Cryopyrin/Nalp3 in activation of caspase-1 in response to viral infection and double-stranded RNA. *J Biol Chem* 281:36560-36568.

22. Yamasaki, K., J. Muto, K. R. Taylor, A. L. Cogen, D. Audish, J. Bertin, E. P. Grant, A. J. Coyle, A. Misaghi, H. M. Hoffman, and R. L. Gallo. 2009. NLRP3/Cryopyrin Is Necessary for Interleukin-1{beta} (IL-1{beta}) Release in Response to Hyaluronan, an Endogenous Trigger of Inflammation in Response to Injury. *J Biol Chem* 284:12762-12771.

23. Hornung, V., F. Bauernfeind, A. Halle, E. O. Samstad, H. Kono, K. L. Rock, K. A. Fitzgerald, and E. Latz. 2008. Silica crystals and aluminum salts activate the NALP3 inflammasome through phagosomal destabilization. *Nat Immunol* 9:847-856.

24. Dostert, C., V. Petrilli, R. Van Bruggen, C. Steele, B. T. Mossman, and J. Tschopp. 2008. Innate immune activation through Nalp3 inflammasome sensing of asbestos and silica. *Science (New York, N.Y* 320:674-677.

25. Li, H., S. B. Willingham, J. P. Ting, and F. Re. 2008. Cutting edge: inflammasome activation by alum and alum's adjuvant effect are mediated by NLRP3. *J Immunol* 181:17-21.

26. Mariathasan, S., K. Newton, D. M. Monack, D. Vucic, D. M. French, W. P. Lee, M. Roose-Girma, S. Erickson, and V. M. Dixit. 2004. Differential activation of the inflammasome by caspase-1 adaptors ASC and Ipaf. *Nature* 430:213-218.

27. Li, P., H. Allen, S. Banerjee, and T. Seshadri. 1997. Characterization of mice deficient in interleukin-1 beta converting enzyme. *Journal of cellular biochemistry* 64:27-32.

28. Muruve, D. A., V. Petrilli, A. K. Zaiss, L. R. White, S. A. Clark, P. J. Ross, R. J. Parks, and J. Tschopp. 2008. The inflammasome recognizes cytosolic microbial and host DNA and triggers an innate immune response. *Nature* 452:103-107.

29. Di Paolo, N. C., E. A. Miao, Y. Iwakura, K. Murali-Krishna, A. Aderem, R. A. Flavell, T. Papayannopoulou, and D. M. Shayakhmetov. 2009. Virus binding to a plasma membrane receptor triggers interleukin-1 alpha-mediated proinflammatory macrophage response in vivo. *Immunity* 31:110-121.

30. Duncan, J. A., X. Gao, M. T. Huang, B. P. O'Connor, C. E. Thomas, S. B. Willingham, D. T. Bergstralh, G. A. Jarvis, P. F. Sparling, and J. P. Ting. 2009. Neisseria gonorrhoeae activates the proteinase cathepsin B to mediate the signaling activities of the NLRP3 and ASC-containing inflammasome. *J Immunol* 182:6460-6469.

31. Marina-Garcia, N., L. Franchi, Y. G. Kim, D. Miller, C. McDonald, G. J. Boons, and G. Nunez. 2008. Pannexin-1-mediated intracellular delivery of muramyl dipeptide induces caspase-1 activation via cryopyrin/NLRP3 independently of Nod2. *J Immunol* 180:4050-4057.

32. Sutterwala, F. S., L. A. Mijares, L. Li, Y. Ogura, B. I. Kazmierczak, and R. A. Flavell. 2007. Immune recognition of Pseudomonas aeruginosa mediated by the IPAF/NLRC4 inflammasome. *The Journal of experimental medicine* 204:3235-3245.

33. Lightfield, K. L., J. Persson, S. W. Brubaker, C. E. Witte, J. von Moltke, E. A. Dunipace, T. Henry, Y. H. Sun, D. Cado, W. F. Dietrich, D. M. Monack, R. M. Tsolis, and R. E. Vance. 2008. Critical function for Naip5 in inflammasome activation by a conserved carboxy-terminal domain of flagellin. *Nat Immunol* 9:1171-1178.

34. Martinon, F., K. Burns, and J. Tschopp. 2002. The inflammasome: a molecular platform triggering activation of inflammatory caspases and processing of proIL-beta. *Molecular cell* 10:417-426.

35. Ting, J. P., R. C. Lovering, E. S. Alnemri, J. Bertin, J. M. Boss, B. K. Davis, R. A. Flavell, S. E. Girardin, A. Godzik, J. A. Harton, H. M. Hoffman, J. P. Hugot, N. Inohara, A. Mackenzie, L. J. Maltais, G. Nunez, Y. Ogura, L. A. Otten, D. Philpott, J. C. Reed, W. Reith, S. Schreiber, V. Steimle, and P. A. Ward. 2008. The NLR gene family: a standard nomenclature. *Immunity* 28:285-287.

36. Chu, Z. L., F. Pio, Z. Xie, K. Welsh, M. Krajewska, S. Krajewski, A. Godzik, and J. C. Reed. 2001. A novel enhancer of the Apaf1 apoptosome involved in cytochrome c-dependent caspase activation and apoptosis. *J Biol Chem* 276:9239-9245.

37. Hlaing, T., R. F. Guo, K. A. Dilley, J. M. Loussia, T. A. Morrish, M. M. Shi, C. Vincenz, and P. A. Ward. 2001. Molecular cloning and characterization of DEFCAP-L and -S, two isoforms of a novel member of the mammalian Ced-4 family of apoptosis proteins. *J Biol Chem* 276:9230-9238.

38. Faustin, B., L. Lartigue, J. M. Bruey, F. Luciano, E. Sergienko, B. Bailly-Maitre, N. Volkmann, D. Hanein, I. Rouiller, and J. C. Reed. 2007. Reconstituted NALP1 inflammasome reveals two-step mechanism of caspase-1 activation. *Molecular cell* 25:713-724.

39. Hsu, L. C., S. R. Ali, S. McGillivray, P. H. Tseng, S. Mariathasan, E. W. Humke, L. Eckmann, J. J. Powell, V. Nizet, V. M. Dixit, and M. Karin. 2008. A NOD2-NALP1 complex mediates caspase-1-dependent IL-1beta secretion in response to Bacillus anthracis infection and muramyl dipeptide. *Proc Natl Acad Sci U S A* 105:7803-7808.

40. Poyet, J. L., S. M. Srinivasula, M. Tnani, M. Razmara, T. Fernandes-Alnemri, and E. S. Alnemri. 2001. Identification of Ipaf, a human caspase-1-activating protein related to Apaf-1. *The Journal of biological chemistry* 276:28309-28313.

41. Geddes, B. J., L. Wang, W. J. Huang, M. Lavellee, G. A. Manji, M. Brown, M. Jurman, J. Cao, J. Morgenstern, S. Merriam, M. A. Glucksmann, P. S. DiStefano, and J. Bertin. 2001. Human CARD12 is a novel CED4/Apaf-1 family member that induces apoptosis. *Biochem Biophys Res Commun* 284:77-82.

42. Endrizzi, M. G., V. Hadinoto, J. D. Growney, W. Miller, and W. F. Dietrich. 2000. Genomic sequence analysis of the mouse Naip gene array. *Genome research* 10:1095-1102.

43. Zamboni, D. S., K. S. Kobayashi, T. Kohlsdorf, Y. Ogura, E. M. Long, R. E. Vance, K. Kuida, S. Mariathasan, V. M. Dixit, R. A. Flavell, W. F. Dietrich, and C. R. Roy. 2006. The Birc1e cytosolic pattern-recognition receptor contributes to the detection and control of Legionella pneumophila infection. *Nat Immunol* 7:318-325.

44. Huang, W. X., P. Huang, and J. Hillert. 2004. Increased expression of caspase-1 and interleukin-18 in peripheral blood mononuclear cells in patients with multiple sclerosis. *Multiple sclerosis (Houndmills, Basingstoke, England)* 10:482-487.

45. Furlan, R., G. Martino, F. Galbiati, P. L. Poliani, S. Smiroldo, A. Bergami, G. Desina, G. Comi, R. Flavell, M. S. Su, and L. Adorini. 1999. Caspase-1 regulates the inflammatory process leading to autoimmune demyelination. *Journal of immunology (Baltimore, Md.: 1950)* 163:2403-2409.

46. Ahmed, Z., A. I. Doward, G. Pryce, D. L. Taylor, J. M. Pocock, J. P. Leonard, D. Baker, and M. L. Cuzner. 2002. A role for caspase-1 and -3 in the pathology of experimental allergic encephalomyelitis : inflammation versus degeneration. *Am J Pathol* 161:1577-1586.

47. Conti, B., L. C. Park, N. Y. Calingasan, Y. Kim, H. Kim, Y. Bae, G. E. Gibson, and T. H. Joh. 1999. Cultures of astrocytes and microglia express interleukin 18. *Brain Res Mol Brain Res* 67:46-52.

48. Prinz, M., and U. K. Hanisch. 1999. Murine microglial cells produce and respond to interleukin-18. *J Neurochem* 72:2215-2218.

49. Sugama, S., B. P. Cho, H. Baker, T. H. Joh, J. Lucero, and B. Conti. 2002. Neurons of the superior nucleus of the medial habenula and ependymal cells express IL-18 in rat CNS. *Brain Res* 958:1-9.

50. Masters, S. L., A. A. Lobito, J. Chae, and D. L. Kastner. 2006. Recent advances in the molecular pathogenesis of hereditary recurrent fevers. *Current opinion in allergy and clinical immunology* 6:428-433.

51. Ryan, J. G., and D. L. Kastner. 2008. Fevers, genes, and innate immunity. *Curr Top Microbiol Immunol* 321:169-184.

52. Boschan, C., O. Witt, P. Lohse, I. Foeldvari, H. Zappel, and L. Schweigerer. 2006. Neonatal-onset multisystem inflammatory disease (NOMID) due to a novel S331R mutation of the CIAS1 gene and response to interleukin-1 receptor antagonist treatment. *American journal of medical genetics.Part A* 140:883-886.

53. Lequerre, T., O. Vittecoq, P. Saugier-Veber, A. Goldenberg, P. Patoz, T. Frebourg, and X. L. Loet. 2006. A cryopyrin-associated periodic syndrome with joint destruction. *Rheumatology (Oxford, England)*.

54. Kone-Paut, I., E. Sanchez, A. Le Quellec, R. Manna, and I. Touitou. 2007. Autoinflammatory gene mutations in Behcet's disease. *Annals of the Rheumatic Diseases*.

55. Appels, C. W., and M. Kloppenburg. 2006. Muckle-Wells syndrome: a rare periodic fever syndrome. *Nederlands tijdschrift voor geneeskunde* 150:1628-1631.

56. Neven, B., I. Callebaut, A. M. Prieur, J. Feldmann, C. Bodemer, L. Lepore, B. Derfalvi, S. Benjaponpitak, R. Vesely, M. J. Sauvain, S. Oertle, R. Allen, G. Morgan, A. Borkhardt, C. Hill, J. Gardner-Medwin, A. Fischer, and G. de Saint Basile. 2004. Molecular basis of the spectral expression of CIAS1 mutations associated with phagocytic cell-mediated autoinflammatory disorders CINCA/NOMID, MWS, and FCU. *Blood* 103:2809-2815.

57. Agostini, L., F. Martinon, K. Burns, M. F. McDermott, P. N. Hawkins, and J. Tschopp. 2004. NALP3 forms an IL-1beta-processing inflammasome with increased activity in Muckle-Wells autoinflammatory disorder. *Immunity* 20:319-325.

58. Dode, C., N. Le Du, L. Cuisset, F. Letourneur, J. M. Berthelot, G. Vaudour, A. Meyrier, R. A. Watts, D. G. Scott, A. Nicholls, B. Granel, C. Frances, F. Garcier, P. Edery, S. Boulinguez, J. P. Domergues, M. Delpech, and G. Grateau. 2002. New mutations of CIAS1 that are responsible for Muckle-Wells syndrome and familial cold urticaria: a novel mutation underlies both syndromes. *Am J Hum Genet* 70:1498-1506.

59. Aksentijevich, I., M. Nowak, M. Mallah, J. J. Chae, W. T. Watford, S. R. Hofmann, L. Stein, R. Russo, D. Goldsmith, P. Dent, H. F. Rosenberg, F. Austin, E. F. Remmers, J. E. Balow, Jr., S. Rosenzweig, H. Komarow, N. G. Shoham, G. Wood, J. Jones, N. Mangra, H. Carrero, B. S. Adams, T. L. Moore, K. Schikler, H. Hoffman, D. J. Lovell, R. Lipnick, K. Barron, J. J. O'Shea, D. L. Kastner, and R. Goldbach-Mansky. 2002. De novo CIAS1 mutations, cytokine activation, and evidence for genetic heterogeneity in patients with neonatal-onset multisystem inflammatory disease (NOMID): a new member of the expanding family of pyrin-associated autoinflammatory diseases. *Arthritis Rheum* 46:3340-3348.

60. Hoffman, H. M., S. G. Gregory, J. L. Mueller, M. Tresierras, D. H. Broide, A. A. Wanderer, and R. D. Kolodner. 2003. Fine structure mapping of CIAS1: identification of an ancestral haplotype and a common FCAS mutation, L353P. *Human genetics* 112:209-216.

61. Hoffman, H. M., J. L. Mueller, D. H. Broide, A. A. Wanderer, and R. D. Kolodner. 2001. Mutation of a new gene encoding a putative pyrin-like protein causes familial cold autoinflammatory syndrome and Muckle-Wells syndrome. *Nature genetics* 29:301-305.

62. Feldmann, J., A. M. Prieur, P. Quartier, P. Berquin, S. Certain, E. Cortis, D. Teillac-Hamel, A. Fischer, and G. de Saint Basile. 2002. Chronic infantile neurological cutaneous and articular syndrome is caused by mutations in CIAS1, a gene highly expressed in polymorphonuclear cells and chondrocytes. *Am J Hum Genet* 71:198-203.

63. Manji, G. A., L. Wang, B. J. Geddes, M. Brown, S. Merriam, A. Al-Garawi, S. Mak, J. M. Lora, M. Briskin, M. Jurman, J. Cao, P. S. DiStefano, and J. Bertin. 2002. PYPAF1, a PYRIN-containing Apaf1-like protein that assembles with ASC and regulates activation of NF-kappa B. *J Biol Chem* 277:11570-11575.

64. Milhavet, F., L. Cuisset, H. M. Hoffman, R. Slim, H. El-Shanti, I. Aksentijevich, S. Lesage, H. Waterham, C. Wise, C. Sarrauste de Menthiere, and I. Touitou. 2008. The infevers autoinflammatory mutation online registry: update with new genes and functions. *Human mutation* 29:803-808.

65. Brydges, S. D., J. L. Mueller, M. D. McGeough, C. A. Pena, A. Misaghi, C. Gandhi, C. D. Putnam, D. L. Boyle, G. S. Firestein, A. A. Horner, P. Soroosh, W. T. Watford, J. J. O'Shea, D. L. Kastner, and H. M. Hoffman. 2009. Inflammasome-mediated disease animal models reveal roles for innate but not adaptive immunity. *Immunity* 30:875-887.

66. Meng, G., F. Zhang, I. Fuss, A. Kitani, and W. Strober. 2009. A mutation in the Nlrp3 gene causing inflammasome hyperactivation potentiates Th17 cell-dominant immune responses. *Immunity* 30:860-874.

67. Jin, Y., C. M. Mailloux, K. Gowan, S. L. Riccardi, G. LaBerge, D. C. Bennett, P. R. Fain, and R. A. Spritz. 2007. NALP1 in vitiligo-associated multiple autoimmune disease. *N Engl J Med* 356:1216-1225.

68. Jeru, I., P. Duquesnoy, T. Fernandes-Alnemri, E. Cochet, J. W. Yu, M. Lackmy-Port-Lis, E. Grimprel, J. Landman-Parker, V. Hentgen, S. Marlin, K. McElreavey, T. Sarkisian, G. Grateau, E. S. Alnemri, and S. Amselem. 2008. Mutations in NALP12 cause hereditary periodic fever syndromes. *Proc Natl Acad Sci U S A* 105:1614-1619.

69. Aksentijevich, I., Y. Torosyan, J. Samuels, M. Centola, E. Pras, J. J. Chae, C. Oddoux, G. Wood, M. P. Azzaro, G. Palumbo, R. Giustolisi, M. Pras, H. Ostrer, and D. L. Kastner. 1999. Mutation and haplotype studies of familial Mediterranean fever reveal new ancestral relationships and evidence for a high carrier frequency with reduced penetrance in the Ashkenazi Jewish population. *Am J Hum Genet* 64:949-962.

70. Bhat, A., S. M. Naguwa, and M. E. Gershwin. 2007. Genetics and new treatment modalities for familial Mediterranean fever. *Annals of the New York Academy of Sciences* 1110:201-208.

71. Matzner, Y., S. Abedat, E. Shapiro, S. Eisenberg, A. Bar-Gil-Shitrit, P. Stepensky, S. Calco, Y. Azar, and S. Urieli-Shoval. 2000. Expression of the familial Mediterranean fever gene and activity of the C5a inhibitor in human primary fibroblast cultures. *Blood* 96:727-731.

72. Diaz, A., C. Hu, D. L. Kastner, P. Schaner, A. M. Reginato, N. Richards, and D. L. Gumucio. 2004. Lipopolysaccharide-induced expression of multiple alternatively spliced MEFV transcripts in human synovial fibroblasts: a prominent splice isoform lacks the C-terminal domain that is highly mutated in familial Mediterranean fever. *Arthritis Rheum* 50:3679-3689.

73. Shoham, N. G., M. Centola, E. Mansfield, K. M. Hull, G. Wood, C. A. Wise, and D. L. Kastner. 2003. Pyrin binds the PSTPIP1/CD2BP1 protein, defining familial Mediterranean fever and PAPA syndrome as disorders in the same pathway. *Proc Natl Acad Sci U S A* 100:13501-13506.

74. Yu, J. W., T. Fernandes-Alnemri, P. Datta, J. Wu, C. Juliana, L. Solorzano, M. McCormick, Z. Zhang, and E. S. Alnemri. 2007. Pyrin activates the ASC pyroptosome in response to engagement by autoinflammatory PSTPIP1 mutants. *Molecular cell* 28:214-227.

75. Papin, S., S. Cuenin, L. Agostini, F. Martinon, S. Werner, H. D. Beer, C. Grutter, M. Grutter, and J. Tschopp. 2007. The SPRY domain of Pyrin, mutated in familial Mediterranean fever patients, interacts with inflammasome components and inhibits proIL-1beta processing. *Cell Death Differ* 14:1457-1466.

76. Chae, J. J., G. Wood, S. L. Masters, K. Richard, G. Park, B. J. Smith, and D. L. Kastner. 2006. The B30.2 domain of pyrin, the familial Mediterranean fever protein, interacts directly with caspase-1 to modulate IL-1beta production. *Proc Natl Acad Sci U S A* 103:9982-9987.

77. Chae, J. J., H. D. Komarow, J. Cheng, G. Wood, N. Raben, P. P. Liu, and D. L. Kastner. 2003. Targeted disruption of pyrin, the FMF protein, causes heightened sensitivity to endotoxin and a defect in macrophage apoptosis. *Molecular cell* 11:591-604.

78. Yu, J. W., J. Wu, Z. Zhang, P. Datta, I. Ibrahimi, S. Taniguchi, J. Sagara, T. Fernandes-Alnemri, and E. S. Alnemri. 2006. Cryopyrin and pyrin activate caspase-1, but not NF-kappaB, via ASC oligomerization. *Cell Death Differ* 13:236-249.

79. Satsangi, J., M. Parkes, E. Louis, L. Hashimoto, N. Kato, K. Welsh, J. D. Terwilliger, G. M. Lathrop, J. I. Bell, and D. P. Jewell. 1996. Two stage genome-wide search in inflammatory bowel disease provides evidence for susceptibility loci on chromosomes 3, 7 and 12. *Nature genetics* 14:199-202.

80. Reinecker, H. C., M. Steffen, T. Witthoeft, I. Pflueger, S. Schreiber, R. P. MacDermott, and A. Raedler. 1993. Enhanced secretion of tumour necrosis factor-alpha, IL-6, and IL-1 beta by isolated lamina propria mononuclear cells from patients with ulcerative colitis and Crohn's disease. *Clinical and experimental immunology* 94:174-181.

81. Hugot, J. P., M. Chamaillard, H. Zouali, S. Lesage, J. P. Cezard, J. Belaiche, S. Almer, C. Tysk, C. A. O'Morain, M. Gassull, V. Binder, Y. Finkel, A. Cortot, R. Modigliani, P. Laurent-Puig, C. Gower-Rousseau, J. Macry, J. F. Colombel, M. Sahbatou, and G. Thomas. 2001. Association of NOD2 leucine-rich repeat variants with susceptibility to Crohn's disease. *Nature* 411:599-603.

82. Ogura, Y., D. K. Bonen, N. Inohara, D. L. Nicolae, F. F. Chen, R. Ramos, H. Britton, T. Moran, R. Karaliuskas, R. H. Duerr, J. P. Achkar, S. R. Brant, T. M. Bayless, B. S. Kirschner, S. B. Hanauer, G. Nunez, and J. H. Cho. 2001. A frameshift mutation in NOD2 associated with susceptibility to Crohn's disease. *Nature* 411:603-606.

83. Chin, A. I., P. W. Dempsey, K. Bruhn, J. F. Miller, Y. Xu, and G. Cheng. 2002. Involvement of receptor-interacting protein 2 in innate and adaptive immune responses. *Nature* 416:190-194.

84. Kobayashi, K., N. Inohara, L. D. Hernandez, J. E. Galan, G. Nunez, C. A. Janeway, R. Medzhitov, and R. A. Flavell. 2002. RICK/Rip2/CARDIAK mediates signalling for receptors of the innate and adaptive immune systems. *Nature* 416:194-199.

85. Kobayashi, K. S., M. Chamaillard, Y. Ogura, O. Henegariu, N. Inohara, G. Nunez, and R. A. Flavell. 2005. Nod2-dependent regulation of innate and adaptive immunity in the intestinal tract. *Science (New York, N.Y* 307:731-734.

86. Maeda, S., L. C. Hsu, H. Liu, L. A. Bankston, M. Iimura, M. F. Kagnoff, L. Eckmann, and M. Karin. 2005. Nod2 mutation in Crohn's disease potentiates NF-kappaB activity and IL-1beta processing. *Science (New York, N.Y* 307:734-738.

87. Inohara, N., Y. Ogura, A. Fontalba, O. Gutierrez, F. Pons, J. Crespo, K. Fukase, S. Inamura, S. Kusumoto, M. Hashimoto, S. J. Foster, A. P. Moran, J. L. Fernandez-Luna, and G. Nunez. 2003. Host recognition of bacterial muramyl dipeptide mediated through NOD2. Implications for Crohn's disease. *J Biol Chem* 278:5509-5512.

88. Schreiber, S., S. Nikolaus, and J. Hampe. 1998. Activation of nuclear factor kappa B inflammatory bowel disease. *Gut* 42:477-484.

89. Li, J., T. Moran, E. Swanson, C. Julian, J. Harris, D. K. Bonen, M. Hedl, D. L. Nicolae, C. Abraham, and J. H. Cho. 2004. Regulation of IL-8 and IL-1beta expression in Crohn's disease associated NOD2/CARD15 mutations. *Human molecular genetics* 13:1715-1725.

90. van Heel, D. A., S. Ghosh, M. Butler, K. A. Hunt, A. M. Lundberg, T. Ahmad, D. P. McGovern, C. Onnie, K. Negoro, S. Goldthorpe, B. M. Foxwell, C. G. Mathew, A. Forbes, D. P. Jewell, and R. J. Playford. 2005. Muramyl dipeptide and toll-like receptor sensitivity in NOD2-associated Crohn's disease. *Lancet* 365:1794-1796.

91. Watanabe, T., N. Asano, P. J. Murray, K. Ozato, P. Tailor, I. J. Fuss, A. Kitani, and W. Strober. 2008. Muramyl dipeptide activation of nucleotide-binding oligomerization domain 2 protects mice from experimental colitis. *The Journal of clinical investigation* 118:545-559.

92. Cadwell, K., J. Y. Liu, S. L. Brown, H. Miyoshi, J. Loh, J. K. Lennerz, C. Kishi, W. Kc, J. A. Carrero, S. Hunt, C. D. Stone, E. M. Brunt, R. J. Xavier, B. P. Sleckman, E. Li, N. Mizushima, T. S. Stappenbeck, and H. W. t. Virgin. 2008. A key role for autophagy and the autophagy gene Atg16l1 in mouse and human intestinal Paneth cells. *Nature* 456:259-263.

93. Saitoh, T., N. Fujita, M. H. Jang, S. Uematsu, B. G. Yang, T. Satoh, H. Omori, T. Noda, N. Yamamoto, M. Komatsu, K. Tanaka, T. Kawai, T. Tsujimura, O. Takeuchi, T. Yoshimori, and S. Akira. 2008. Loss of the autophagy protein Atg16L1 enhances endotoxin-induced IL-1beta production. *Nature* 456:264-268.

94. Parkes, M., J. C. Barrett, N. J. Prescott, M. Tremelling, C. A. Anderson, S. A. Fisher, R. G. Roberts, E. R. Nimmo, F. R. Cummings, D. Soars, H. Drummond, C. W. Lees, S. A. Khawaja, R. Bagnall, D. A. Burke, C. E. Todhunter, T. Ahmad, C. M. Onnie, W. McArdle, D. Strachan, G. Bethel, C. Bryan, C. M. Lewis, P. Deloukas, A. Forbes, J. Sanderson, D. P. Jewell, J. Satsangi, J. C. Mansfield, L. Cardon, and C. G. Mathew. 2007. Sequence variants in the autophagy gene IRGM and multiple other replicating loci contribute to Crohn's disease susceptibility. *Nature genetics* 39:830-832.

95. Singh, S. B., A. S. Davis, G. A. Taylor, and V. Deretic. 2006. Human IRGM induces autophagy to eliminate intracellular mycobacteria. *Science (New York, N.Y* 313:1438-1441.

96. Miceli-Richard, C., S. Lesage, M. Rybojad, A. M. Prieur, S. Manouvrier-Hanu, R. Hafner, M. Chamaillard, H. Zouali, G. Thomas, and J. P. Hugot. 2001. CARD15 mutations in Blau syndrome. *Nature genetics* 29:19-20.

97. Wise, C. A., L. B. Bennett, V. Pascual, J. D. Gillum, and A. M. Bowcock. 2000. Localization of a gene for familial recurrent arthritis. *Arthritis Rheum* 43:2041-2045.

98. Chen, C. J., Y. Shi, A. Hearn, K. Fitzgerald, D. Golenbock, G. Reed, S. Akira, and K. L. Rock. 2006. MyD88-dependent IL-1 receptor signaling is essential for gouty inflammation stimulated by monosodium urate crystals. *The Journal of clinical investigation* 116:2262-2271.

99. Hebert, L. E., P. A. Scherr, J. L. Bienias, D. A. Bennett, and D. A. Evans. 2003. Alzheimer disease in the US population: prevalence estimates using the 2000 census. *Archives of neurology* 60:1119-1122.

100. Udan, M. L., D. Ajit, N. R. Crouse, and M. R. Nichols. 2008. Toll-like receptors 2 and 4 mediate Abeta(1-42) activation of the innate immune response in a human monocytic cell line. *J Neurochem* 104:524-533.

101. Tahara, K., H. D. Kim, J. J. Jin, J. A. Maxwell, L. Li, and K. Fukuchi. 2006. Role of toll-like receptor signalling in Abeta uptake and clearance. *Brain* 129:3006-3019.

102. Ojala, J., I. Alafuzoff, S. K. Herukka, T. van Groen, H. Tanila, and T. Pirttila. 2009. Expression of interleukin-18 is increased in the brains of Alzheimer's disease patients. *Neurobiology of aging* 30:198-209.

103. Zhu, S. G., J. G. Sheng, R. A. Jones, M. M. Brewer, X. Q. Zhou, R. E. Mrak, and W. S. Griffin. 1999. Increased interleukin-1beta converting enzyme expression and activity in Alzheimer disease. *J Neuropathol Exp Neurol* 58:582-587.

104. Zuliani, G., M. Ranzini, G. Guerra, L. Rossi, M. R. Munari, A. Zurlo, S. Volpato, A. R. Atti, A. Ble, and R. Fellin. 2007. Plasma cytokines profile in older subjects with late onset Alzheimer's disease or vascular dementia. *Journal of psychiatric research* 41:686-693.

105. Lue, L. F., R. Rydel, E. F. Brigham, L. B. Yang, H. Hampel, G. M. Murphy, Jr., L. Brachova, S. D. Yan, D. G. Walker, Y. Shen, and J. Rogers. 2001. Inflammatory repertoire of Alzheimer's disease and nondemented elderly microglia in vitro. *Glia* 35:72-79.

106. Perkins, R. C., R. K. Scheule, R. Hamilton, G. Gomes, G. Freidman, and A. Holian. 1993. Human alveolar macrophage cytokine release in response to in vitro and in vivo asbestos exposure. *Experimental lung research* 19:55-65.

107. Gasse, P., N. Riteau, S. Charron, S. Girre, L. Fick, V. Petrilli, J. Tschopp, V. Lagente, V. F. Quesniaux, B. Ryffel, and I. Couillin. 2009. Uric acid is a danger signal activating NALP3 inflammasome in lung injury inflammation and fibrosis. *American journal of respiratory and critical care medicine* 179:903-913.

108. Lich, J. D., K. L. Williams, C. B. Moore, J. C. Arthur, B. K. Davis, D. J. Taxman, and J. P. Ting. 2007. Monarch-1 suppresses non-canonical NF-kappaB activation and p52-dependent chemokine expression in monocytes. *Journal of immunology (Baltimore, Md.: 1950)* 178:1256-1260.

109. Williams, K. L., J. D. Lich, J. A. Duncan, W. Reed, P. Rallabhandi, C. Moore, S. Kurtz, V. M. Coffield, M. A. Accavitti-Loper, L. Su, S. N. Vogel, M. Braunstein, and J. P. Ting. 2005. The CATERPILLER protein monarch-1 is an antagonist of toll-like receptor-, tumor necrosis factor alpha-, and Mycobacterium tuberculosis-induced pro-inflammatory signals. *The Journal of biological chemistry* 280:39914-39924.

110. Kummer, J. A., R. Broekhuizen, H. Everett, L. Agostini, L. Kuijk, F. Martinon, R. van Bruggen, and J. Tschopp. 2007. Inflammasome components NALP 1 and 3 show distinct but separate expression profiles in human tissues suggesting a site-specific role in the inflammatory response. *J Histochem Cytochem* 55:443-452.

111. Kinoshita, T., Y. Wang, M. Hasegawa, R. Imamura, and T. Suda. 2005. PYPAF3, a PYRIN-containing APAF-1-like protein, is a feedback regulator of caspase-1-dependent interleukin-1beta secretion. *J Biol Chem* Chu280:21720-21725.

112. Wang, Y., M. Hasegawa, R. Imamura, T. Kinoshita, C. Kondo, K. Konaka, and T. Suda. 2004. PYNOD, a novel Apaf-1/CED4-like protein is an inhibitor of ASC and caspase-1. *Int Immunol* 16:777-786.

113. Tattoli, I., L. A. Carneiro, M. Jehanno, J. G. Magalhaes, Y. Shu, D. J. Philpott, D. Arnoult, and S. E. Girardin. 2008. NLRX1 is a mitochondrial NOD-like receptor that

amplifies NF-kappaB and JNK pathways by inducing reactive oxygen species production. *EMBO reports* 9:293-300.

114. Gotz, R., C. Karch, M. R. Digby, J. Troppmair, U. R. Rapp, and M. Sendtner. 2000. The neuronal apoptosis inhibitory protein suppresses neuronal differentiation and apoptosis in PC12 cells. *Human molecular genetics* 9:2479-2489.

115. O'Keefe, G. M., V. T. Nguyen, and E. N. Benveniste. 1999. Class II transactivator and class II MHC gene expression in microglia: modulation by the cytokines TGF-beta, IL-4, IL-13 and IL-10. *European journal of immunology* 29:1275-1285.

116. Collawn, J. F., and E. N. Benveniste. 1999. Regulation of MHC class II expression in the central nervous system. *Microbes and infection / Institut Pasteur* 1:893-902.

117. de Rivero Vaccari, J. P., G. Lotocki, A. E. Marcillo, W. D. Dietrich, and R. W. Keane. 2008. A molecular platform in neurons regulates inflammation after spinal cord injury. *J Neurosci* 28:3404-3414.

118. Stuve, O., S. Youssef, A. J. Slavin, C. L. King, J. C. Patarroyo, D. L. Hirschberg, W. J. Brickey, J. M. Soos, J. F. Piskurich, H. A. Chapman, and S. S. Zamvil. 2002. The role of the MHC class II transactivator in class II expression and antigen presentation by astrocytes and in susceptibility to central nervous system autoimmune disease. *J Immunol* 169:6720-6732.

119. Pari, G., F. Berrada, G. Verge, G. Karpati, and J. Nalbantoglu. 2000. Immunolocalization of NAIP in the human brain and spinal cord. *Neuroreport* 11:9-14.

120. Matsunaga, T., T. Ishida, M. Takekawa, S. Nishimura, M. Adachi, and K. Imai. 2002. Analysis of gene expression during maturation of immature dendritic cells derived from peripheral blood monocytes. *Scandinavian journal of immunology* 56:593-601.

121. Roy, N., M. S. Mahadevan, M. McLean, G. Shutler, Z. Yaraghi, R. Farahani, S. Baird, A. Besner-Johnston, C. Lefebvre, X. Kang, and et al. 1995. The gene for neuronal apoptosis inhibitory protein is partially deleted in individuals with spinal muscular atrophy. *Cell* 80:167-178.

122. Ting, J. P., and B. K. Davis. 2005. CATERPILLER: a novel gene family important in immunity, cell death, and diseases. *Annual Review of Immunology* 23:387-414.

123. North, R. A. 2002. Molecular physiology of P2X receptors. *Physiological reviews* 82:1013-1067.

124. Bianco, F., S. Ceruti, A. Colombo, M. Fumagalli, D. Ferrari, C. Pizzirani, M. Matteoli, F. Di Virgilio, M. P. Abbracchio, and C. Verderio. 2006. A role for P2X7 in microglial proliferation. *Journal of neurochemistry* 99:745-758.

125. Sim, J. A., M. T. Young, H. Y. Sung, R. A. North, and A. Surprenant. 2004. Reanalysis of P2X7 receptor expression in rodent brain. *The Journal of neuroscience : the official journal of the Society for Neuroscience* 24:6307-6314.

126. Sperlagh, B., E. S. Vizi, K. Wirkner, and P. Illes. 2006. P2X7 receptors in the nervous system. *Progress in neurobiology* 78:327-346.

127. Suadicani, S. O., C. F. Brosnan, and E. Scemes. 2006. P2X7 receptors mediate ATP release and amplification of astrocytic intercellular Ca2+ signaling. *The Journal of neuroscience : the official journal of the Society for Neuroscience* 26:1378-1385.

128. Pelegrin, P., and A. Surprenant. 2006. Pannexin-1 mediates large pore formation and interleukin-1beta release by the ATP-gated P2X7 receptor. *The EMBO journal* 25:5071-5082.

129. Kanneganti, T. D., M. Lamkanfi, Y. G. Kim, G. Chen, J. H. Park, L. Franchi, P. Vandenabeele, and G. Nunez. 2007. Pannexin-1-mediated recognition of bacterial molecules activates the cryopyrin inflammasome independent of Toll-like receptor signaling. *Immunity* 26:433-443.

130. Sharp, A. J., P. E. Polak, V. Simonini, S. X. Lin, J. C. Richardson, E. R. Bongarzone, and D. L. Feinstein. 2008. P2x7 deficiency suppresses development of experimental autoimmune encephalomyelitis. *Journal of neuroinflammation* 5:33.

131. Chen, L., and C. F. Brosnan. 2006. Exacerbation of experimental autoimmune encephalomyelitis in P2X7R-/- mice: evidence for loss of apoptotic activity in lymphocytes. *Journal of immunology (Baltimore, Md.: 1950)* 176:3115-3126.

132. Petrilli, V., S. Papin, C. Dostert, A. Mayor, F. Martinon, and J. Tschopp. 2007. Activation of the NALP3 inflammasome is triggered by low intracellular potassium concentration. *Cell Death Differ* 14:1583-1589.

133. Baumann, N., and D. Pham-Dinh. 2001. Biology of oligodendrocyte and myelin in the mammalian central nervous system. *Physiological reviews* 81:871-927.

134. Neumann, H., M. R. Kotter, and R. J. Franklin. 2009. Debris clearance by microglia: an essential link between degeneration and regeneration. *Brain* 132:288-295.

135. Kotter, M. R., W. W. Li, C. Zhao, and R. J. Franklin. 2006. Myelin impairs CNS remyelination by inhibiting oligodendrocyte precursor cell differentiation. *J Neurosci* 26:328-332.

136. Constantinescu, C. S., D. B. Goodman, B. Hilliard, M. Wysocka, and J. A. Cohen. 2000. Murine macrophages stimulated with central and peripheral nervous system myelin or purified myelin proteins release inflammatory products. *Neuroscience letters* 287:171-174.

137. Tzeng, S. F., G. E. Deibler, and G. H. DeVries. 1995. Exogenous myelin basic protein promotes oligodendrocyte death via increased calcium influx. *J Neurosci Res* 42:768-774.

138. Bruck, W., Y. Bruck, U. Diederich, and S. J. Piddlesden. 1995. The membrane attack complex of complement mediates peripheral nervous system demyelination in vitro. *Acta Neuropathol* 90:601-607.

139. Mead, R. J., S. K. Singhrao, J. W. Neal, H. Lassmann, and B. P. Morgan. 2002. The membrane attack complex of complement causes severe demyelination associated with acute axonal injury. *J Immunol* 168:458-465.

140. Baer, A. S., Y. A. Syed, S. U. Kang, D. Mitteregger, R. Vig, C. Ffrench-Constant, R. J. Franklin, F. Altmann, G. Lubec, and M. R. Kotter. 2009. Myelin-mediated inhibition of oligodendrocyte precursor differentiation can be overcome by pharmacological modulation of Fyn-RhoA and protein kinase C signalling. *Brain* 132:465-481.

141. Cohen, G., C. Makranz, M. Spira, T. Kodama, F. Reichert, and S. Rotshenker. 2006. Non-PKC DAG/phorbol-ester receptor(s) inhibit complement receptor-3 and nPKC inhibit scavenger receptor-AI/II-mediated myelin phagocytosis but cPKC, PI3k, and PLCgamma activate myelin phagocytosis by both. *Glia* 53:538-550.

142. Makranz, C., G. Cohen, A. Baron, L. Levidor, T. Kodama, F. Reichert, and S. Rotshenker. 2004. Phosphatidylinositol 3-kinase, phosphoinositide-specific

phospholipase-Cgamma and protein kinase-C signal myelin phagocytosis mediated by complement receptor-3 alone and combined with scavenger receptor-AI/II in macrophages. *Neurobiol Dis* 15:279-286.

143. Reichert, F., and S. Rotshenker. 2003. Complement-receptor-3 and scavenger-receptor-AI/II mediated myelin phagocytosis in microglia and macrophages. *Neurobiol Dis* 12:65-72.

144. Rotshenker, S., F. Reichert, M. Gitik, R. Haklai, G. Elad-Sfadia, and Y. Kloog. 2008. Galectin-3/MAC-2, Ras and PI3K activate complement receptor-3 and scavenger receptor-AI/II mediated myelin phagocytosis in microglia. *Glia* 56:1607-1613.

145. da Costa, C. C., L. J. van der Laan, C. D. Dijkstra, and W. Bruck. 1997. The role of the mouse macrophage scavenger receptor in myelin phagocytosis. *The European journal of neuroscience* 9:2650-2657.

146. Hauser, S. L., and J. R. Oksenberg. 2006. The neurobiology of multiple sclerosis: genes, inflammation, and neurodegeneration. *Neuron* 52:61-76.

147. Lucchinetti, C., W. Bruck, J. Parisi, B. Scheithauer, M. Rodriguez, and H. Lassmann. 2000. Heterogeneity of multiple sclerosis lesions: implications for the pathogenesis of demyelination. *Annals of Neurology* 47:707-717.

148. Pittock, S. J., and C. F. Lucchinetti. 2007. The Pathology of MS: New Insights and Potential Clinical Applications. *Neurologist* 13:45-56.

149. Sospedra, M., and R. Martin. 2005. Immunology of multiple sclerosis. *Annual Review of Immunology* 23:683-747.

150. Hemmer, B., J. J. Archelos, and H. P. Hartung. 2002. New concepts in the immunopathogenesis of multiple sclerosis. *Nature reviews.Neuroscience* 3:291-301.

151. Hemmer, B., S. Nessler, D. Zhou, B. Kieseier, and H. P. Hartung. 2006. Immunopathogenesis and immunotherapy of multiple sclerosis. *Nature clinical practice.Neurology* 2:201-211.

152. Hemmer, B., J. J. Archelos, and H. P. Hartung. 2002. New concepts in the immunopathogenesis of multiple sclerosis. *Nature reviews* 3:291-301.

153. Madsen, E., and J. D. Gitlin. 2007. Copper and iron disorders of the brain. *Annual Review of Neuroscience* 30:317-337.

154. Hartmann, H. A., and M. A. Evenson. 1992. Deficiency of copper can cause neuronal degeneration. *Medical hypotheses* 38:75-85.

155. Ludwin, S. K. 1978. Central nervous system demyelination and remyelination in the mouse: an ultrastructural study of cuprizone toxicity. *Laboratory investigation; a journal of technical methods and pathology* 39:597-612.

156. Matsushima, G. K., and P. Morell. 2001. The neurotoxicant, cuprizone, as a model to study demyelination and remyelination in the central nervous system. *Brain pathology (Zurich, Switzerland)* 11:107-116.

157. Fujita, N., H. Ishiguro, S. Sato, T. Kurihara, R. Kuwano, K. Sakimura, Y. Takahashi, and T. Miyatake. 1990. Induction of myelin-associated glycoprotein mRNA in experimental remyelination. *Brain research* 513:152-155.

158. Arnett, H. A., J. Mason, M. Marino, K. Suzuki, G. K. Matsushima, and J. P. Ting. 2001. TNF alpha promotes proliferation of oligodendrocyte progenitors and remyelination. *Nature neuroscience* 4:1116-1122.

159. Franco-Pons, N., M. Torrente, M. T. Colomina, and E. Vilella. 2007. Behavioral deficits in the cuprizone-induced murine model of demyelination/remyelination. *Toxicology letters*.

160. de Jong, B. A., T. W. Huizinga, E. L. Bollen, B. M. Uitdehaag, G. P. Bosma, M. A. van Buchem, E. J. Remarque, A. C. Burgmans, N. F. Kalkers, C. H. Polman, and R. G. Westendorp. 2002. Production of IL-1beta and IL-1Ra as risk factors for susceptibility and progression of relapse-onset multiple sclerosis. *Journal of neuroimmunology* 126:172-179.

161. Kantarci, O. H., E. J. Atkinson, D. D. Hebrink, C. T. McMurray, and B. G. Weinshenker. 2000. Association of two variants in IL-1beta and IL-1 receptor antagonist genes with multiple sclerosis. *Journal of neuroimmunology* 106:220-227.

162. Bauer, J., F. Berkenbosch, A. M. Van Dam, and C. D. Dijkstra. 1993. Demonstration of interleukin-1 beta in Lewis rat brain during experimental allergic encephalomyelitis by immunocytochemistry at the light and ultrastructural level. *J Neuroimmunol* 48:13-21.

163. Jacobs, C. A., P. E. Baker, E. R. Roux, K. S. Picha, B. Toivola, S. Waugh, and M. K. Kennedy. 1991. Experimental autoimmune encephalomyelitis is exacerbated by IL-1 alpha and suppressed by soluble IL-1 receptor. *J Immunol* 146:2983-2989.

164. Goldbach-Mansky, R., N. J. Dailey, S. W. Canna, A. Gelabert, J. Jones, B. I. Rubin, H. J. Kim, C. Brewer, C. Zalewski, E. Wiggs, S. Hill, M. L. Turner, B. I. Karp, I. Aksentijevich, F. Pucino, S. R. Penzak, M. H. Haverkamp, L. Stein, B. S. Adams, T. L. Moore, R. C. Fuhlbrigge, B. Shaham, J. N. Jarvis, K. O'Neil, R. K. Vehe, L. O. Beitz, G. Gardner, W. P. Hannan, R. W. Warren, W. Horn, J. L. Cole, S. M. Paul, P. N. Hawkins, T. H. Pham, C. Snyder, R. A. Wesley, S. C. Hoffmann, S. M. Holland, J. A. Butman, and D. L. Kastner. 2006. Neonatal-onset multisystem inflammatory disease responsive to interleukin-1beta inhibition. *The New England journal of medicine* 355:581-592.

165. Mason, J. L., K. Suzuki, D. D. Chaplin, and G. K. Matsushima. 2001. Interleukin-1beta promotes repair of the CNS. *J Neurosci* 21:7046-7052.

166. Mason, J. L., J. J. Jones, M. Taniike, P. Morell, K. Suzuki, and G. K. Matsushima. 2000. Mature oligodendrocyte apoptosis precedes IGF-1 production and oligodendrocyte progenitor accumulation and differentiation during demyelination/remyelination. *Journal of neuroscience research* 61:251-262.

167. Mason, J. L., P. Ye, K. Suzuki, A. J. D'Ercole, and G. K. Matsushima. 2000. Insulin-like growth factor-1 inhibits mature oligodendrocyte apoptosis during primary demyelination. *The Journal of neuroscience : the official journal of the Society for Neuroscience* 20:5703-5708.

168. Braddock, M., and A. Quinn. 2004. Targeting IL-1 in inflammatory disease: new opportunities for therapeutic intervention. *Nat Rev Drug Discov* 3:330-339.

169. Ichikawa, K., H. Hirai, M. Ishiguro, T. Kambara, Y. Kato, Y. J. Kim, Y. Kojima, Y. Matsunaga, H. Nishida, Y. Shiomi, N. Yoshikawa, L. H. Huang, and N. Kojima. 2001. Cytokine production inhibitors produced by a fungus, Oidiodendron griseum. *The Journal of antibiotics* 54:697-702.

170. Hoffman, H. M. 2009. Rilonacept for the treatment of cryopyrin-associated periodic syndromes (CAPS). *Expert opinion on biological therapy* 9:519-531.

171. Bartfai, T., M. M. Behrens, S. Gaidarova, J. Pemberton, A. Shivanyuk, and J. Rebek, Jr. 2003. A low molecular weight mimic of the Toll/IL-1 receptor/resistance domain inhibits IL-1 receptor-mediated responses. *Proc Natl Acad Sci U S A* 100:7971-7976.

172. Loiarro, M., F. Capolunghi, N. Fanto, G. Gallo, S. Campo, B. Arseni, R. Carsetti, P. Carminati, R. De Santis, V. Ruggiero, and C. Sette. 2007. Pivotal Advance: Inhibition of MyD88 dimerization and recruitment of IRAK1 and IRAK4 by a novel peptidomimetic compound. *Journal of leukocyte biology* 82:801-810.

173. Loiarro, M., C. Sette, G. Gallo, A. Ciacci, N. Fanto, D. Mastroianni, P. Carminati, and V. Ruggiero. 2005. Peptide-mediated interference of TIR domain dimerization in MyD88 inhibits interleukin-1-dependent activation of NF-{kappa}B. *J Biol Chem* 280:15809-15814.

174. Buckley, G. M., L. Gowers, A. P. Higueruelo, K. Jenkins, S. R. Mack, T. Morgan, D. M. Parry, W. R. Pitt, O. Rausch, M. D. Richard, V. Sabin, and J. L. Fraser. 2008. IRAK-4 inhibitors. Part 1: a series of amides. *Bioorganic & medicinal chemistry letters* 18:3211-3214.

175. Buckley, G. M., R. Fosbeary, J. L. Fraser, L. Gowers, A. P. Higueruelo, L. A. James, K. Jenkins, S. R. Mack, T. Morgan, D. M. Parry, W. R. Pitt, O. Rausch, M. D. Richard, and V. Sabin. 2008. IRAK-4 inhibitors. Part III: a series of imidazo[1,2-a]pyridines. *Bioorganic & medicinal chemistry letters* 18:3656-3660.

176. Buckley, G. M., T. A. Ceska, J. L. Fraser, L. Gowers, C. R. Groom, A. P. Higueruelo, K. Jenkins, S. R. Mack, T. Morgan, D. M. Parry, W. R. Pitt, O. Rausch, M. D. Richard, and V. Sabin. 2008. IRAK-4 inhibitors. Part II: a structure-based assessment of imidazo[1,2-a]pyridine binding. *Bioorganic & medicinal chemistry letters* 18:3291-3295.

177. Slobodov, U., F. Reichert, R. Mirski, and S. Rotshenker. 2001. Distinct inflammatory stimuli induce different patterns of myelin phagocytosis and degradation in recruited macrophages. *Exp Neurol* 167:401-409.

178. Rigante, D., V. Ansuini, M. Caldarelli, B. Bertoni, I. La Torraca, and A. Stabile. 2006. Hydrocephalus in CINCA syndrome treated with anakinra. *Child's nervous system : ChNS : official journal of the International Society for Pediatric Neurosurgery* 22:334-337.

179. Shornick, L. P., P. De Togni, S. Mariathasan, J. Goellner, J. Strauss-Schoenberger, R. W. Karr, T. A. Ferguson, and D. D. Chaplin. 1996. Mice deficient in IL-1beta manifest impaired contact hypersensitivity to trinitrochlorobenzone. *The Journal of experimental medicine* 183:1427-1436.

180. Plant, S. R., H. A. Iocca, Y. Wang, J. C. Thrash, B. P. O'Connor, H. A. Arnett, Y. X. Fu, M. J. Carson, and J. P. Ting. 2007. Lymphotoxin beta receptor (Lt betaR): dual roles in demyelination and remyelination and successful therapeutic intervention using Lt betaR-Ig protein. *J Neurosci* 27:7429-7437.

181. Arnett, H. A., R. P. Hellendall, G. K. Matsushima, K. Suzuki, V. E. Laubach, P. Sherman, and J. P. Ting. 2002. The protective role of nitric oxide in a neurotoxicant-induced demyelinating model. *J Immunol* 168:427-433.

182. Willingham, S. B., D. T. Bergstralh, W. O'Connor, A. C. Morrison, D. J. Taxman, J. A. Duncan, S. Barnoy, M. M. Venkatesan, R. A. Flavell, M. Deshmukh, H. M. Hoffman, and J. P. Ting. 2007. Microbial pathogen-induced necrotic cell death mediated by the inflammasome components CIAS1/cryopyrin/NLRP3 and ASC. *Cell host & microbe* 2:147-159.

183. Hanisch, U. K., and H. Kettenmann. 2007. Microglia: active sensor and versatile effector cells in the normal and pathologic brain. *Nat Neurosci* 10:1387-1394.

184. Napoli, I., and H. Neumann. 2009. Microglial clearance function in health and disease. *Neuroscience* 158:1030-1038.

185. Dong, Y., and E. N. Benveniste. 2001. Immune function of astrocytes. *Glia* 36:180-190.

186. Solle, M., J. Labasi, D. G. Perregaux, E. Stam, N. Petrushova, B. H. Koller, R. J. Griffiths, and C. A. Gabel. 2001. Altered cytokine production in mice lacking P2X(7) receptors. *The Journal of biological chemistry* 276:125-132.

187. Piccio, L., C. Buonsanti, M. Cella, I. Tassi, R. E. Schmidt, C. Fenoglio, J. Rinker, 2nd, R. T. Naismith, P. Panina-Bordignon, N. Passini, D. Galimberti, E. Scarpini, M. Colonna, and A. H. Cross. 2008. Identification of soluble TREM-2 in the cerebrospinal fluid and its association with multiple sclerosis and CNS inflammation. *Brain*.

188. Mason, J. L., S. Xuan, I. Dragatsis, A. Efstratiadis, and J. E. Goldman. 2003. Insulin-like growth factor (IGF) signaling through type 1 IGF receptor plays an important role in remyelination. *The Journal of neuroscience : the official journal of the Society for Neuroscience* 23:7710-7718.

189. Shaftel, S. S., T. J. Carlson, J. A. Olschowka, S. Kyrkanides, S. B. Matousek, and M. K. O'Banion. 2007. Chronic interleukin-1beta expression in mouse brain leads to leukocyte infiltration and neutrophil-independent blood brain barrier permeability without overt neurodegeneration. *J Neurosci* 27:9301-9309.

190. Badovinac, V., M. Mostarica-Stojkovic, C. A. Dinarello, and S. Stosic-Grujicic. 1998. Interleukin-1 receptor antagonist suppresses experimental autoimmune encephalomyelitis (EAE) in rats by influencing the activation and proliferation of encephalitogenic cells. *J Neuroimmunol* 85:87-95.

191. Takahashi, J. L., F. Giuliani, C. Power, Y. Imai, and V. W. Yong. 2003. Interleukin-1beta promotes oligodendrocyte death through glutamate excitotoxicity. *Ann Neurol* 53:588-595.

192. Balashov, K. E., J. B. Rottman, H. L. Weiner, and W. W. Hancock. 1999. CCR5(+) and CXCR3(+) T cells are increased in multiple sclerosis and their ligands MIP-1alpha and IP-10 are expressed in demyelinating brain lesions. *Proceedings of the National Academy of Sciences of the United States of America* 96:6873-6878.

193. Nicoletti, F., R. Di Marco, K. Mangano, F. Patti, E. Reggio, A. Nicoletti, K. Bendtzen, and A. Reggio. 2001. Increased serum levels of interleukin-18 in patients with multiple sclerosis. *Neurology* 57:342-344.

194. Losy, J., and A. Niezgoda. 2001. IL-18 in patients with multiple sclerosis. *Acta Neurologica Scandinavica* 104:171-173.

195. Cannella, B., and C. S. Raine. 2004. Multiple sclerosis: cytokine receptors on oligodendrocytes predict innate regulation. *Annals of Neurology* 55:46-57.

196. Wildbaum, G., S. Youssef, N. Grabie, and N. Karin. 1998. Neutralizing antibodies to IFN-gamma-inducing factor prevent experimental autoimmune encephalomyelitis. *Journal of immunology (Baltimore, Md.: 1950)* 161:6368-6374.

197. Jander, S., and G. Stoll. 1998. Differential induction of interleukin-12, interleukin-18, and interleukin-1beta converting enzyme mRNA in experimental autoimmune encephalomyelitis of the Lewis rat. *J Neuroimmunol* 91:93-99.

198. Shi, F. D., K. Takeda, S. Akira, N. Sarvetnick, and H. G. Ljunggren. 2000. IL-18 directs autoreactive T cells and promotes autodestruction in the central nervous

system via induction of IFN-gamma by NK cells. *Journal of immunology (Baltimore, Md.: 1950)* 165:3099-3104.

199. Gutcher, I., E. Urich, K. Wolter, M. Prinz, and B. Becher. 2006. Interleukin 18-independent engagement of interleukin 18 receptor-alpha is required for autoimmune inflammation. *Nature immunology* 7:946-953.

200. Blander, J. M., and R. Medzhitov. 2004. Regulation of phagosome maturation by signals from toll-like receptors. *Science (New York, N.Y* 304:1014-1018.

201. Shiratsuchi, A., I. Watanabe, O. Takeuchi, S. Akira, and Y. Nakanishi. 2004. Inhibitory effect of Toll-like receptor 4 on fusion between phagosomes and endosomes/lysosomes in macrophages. *J Immunol* 172:2039-2047.

202. Yates, R. M., and D. G. Russell. 2005. Phagosome maturation proceeds independently of stimulation of toll-like receptors 2 and 4. *Immunity* 23:409-417.

203. Liu, Y., W. Hao, M. Letiembre, S. Walter, M. Kulanga, H. Neumann, and K. Fassbender. 2006. Suppression of microglial inflammatory activity by myelin phagocytosis: role of p47-PHOX-mediated generation of reactive oxygen species. *J Neurosci* 26:12904-12913.

204. Reichert, F., A. Saada, and S. Rotshenker. 1994. Peripheral nerve injury induces Schwann cells to express two macrophage phenotypes: phagocytosis and the galactose-specific lectin MAC-2. *J Neurosci* 14:3231-3245.

205. Mosley, K., and M. L. Cuzner. 1996. Receptor-mediated phagocytosis of myelin by macrophages and microglia: effect of opsonization and receptor blocking agents. *Neurochem Res* 21:481-487.

206. Li, H., A. Ambade, and F. Re. 2009. Cutting edge: Necrosis activates the NLRP3 inflammasome. *J Immunol* 183:1528-1532.

207. Norton, W. T., and S. E. Poduslo. 1973. Myelination in rat brain: method of myelin isolation. *J Neurochem* 21:749-757.

208. Hendriks, J. J., H. E. de Vries, S. M. van der Pol, T. K. van den Berg, E. A. van Tol, and C. D. Dijkstra. 2003. Flavonoids inhibit myelin phagocytosis by macrophages; a structure-activity relationship study. *Biochem Pharmacol* 65:877-885.

209. McMahon, E. J., K. Suzuki, and G. K. Matsushima. 2002. Peripheral macrophage recruitment in cuprizone-induced CNS demyelination despite an intact blood-brain barrier. *Journal of neuroimmunology* 130:32-45.

210. Weigelt, W., T. Schneider, and R. Lange. 1992. Sequence homology between spirochaete flagellin and human myelin basic protein. *Immunology today* 13:279-280.

211. Jahn, O., S. Tenzer, and H. B. Werner. 2009. Myelin proteomics: molecular anatomy of an insulating sheath. *Molecular neurobiology* 40:55-72.

212. De, S., M. A. Trigueros, A. Kalyvas, and S. David. 2003. Phospholipase A2 plays an important role in myelin breakdown and phagocytosis during Wallerian degeneration. *Mol Cell Neurosci* 24:753-765.

213. Takenouchi, T., Y. Iwamaru, S. Sugama, M. Sato, M. Hashimoto, and H. Kitani. 2008. Lysophospholipids and ATP mutually suppress maturation and release of IL-1 beta in mouse microglial cells using a Rho-dependent pathway. *J Immunol* 180:7827-7839.

214. Gaultier, A., X. Wu, N. Le Moan, S. Takimoto, G. Mukandala, K. Akassoglou, W. M. Campana, and S. L. Gonias. 2009. Low-density lipoprotein receptor-related protein 1 is an essential receptor for myelin phagocytosis. *J Cell Sci* 122:1155-1162.

215. Bruck, W., Y. Bruck, and R. L. Friede. 1992. TNF-alpha suppresses CR3-mediated myelin removal by macrophages. *J Neuroimmunol* 38:9-17.

216. Bruck, W., and R. L. Friede. 1990. Anti-macrophage CR3 antibody blocks myelin phagocytosis by macrophages in vitro. *Acta Neuropathol* 80:415-418.

217. Li, H., J. Newcombe, N. P. Groome, and M. L. Cuzner. 1993. Characterization and distribution of phagocytic macrophages in multiple sclerosis plaques. *Neuropathol Appl Neurobiol* 19:214-223.

218. Vallieres, L., and P. E. Sawchenko. 2003. Bone marrow-derived cells that populate the adult mouse brain preserve their hematopoietic identity. *The Journal of neuroscience : the official journal of the Society for Neuroscience* 23:5197-5207.

219. Hoehn, H. J., Y. Kress, A. Sohn, C. F. Brosnan, S. Bourdon, and B. Shafit-Zagardo. 2008. Axl-/- mice have delayed recovery and prolonged axonal damage following cuprizone toxicity. *Brain Res* 1240:1-11.